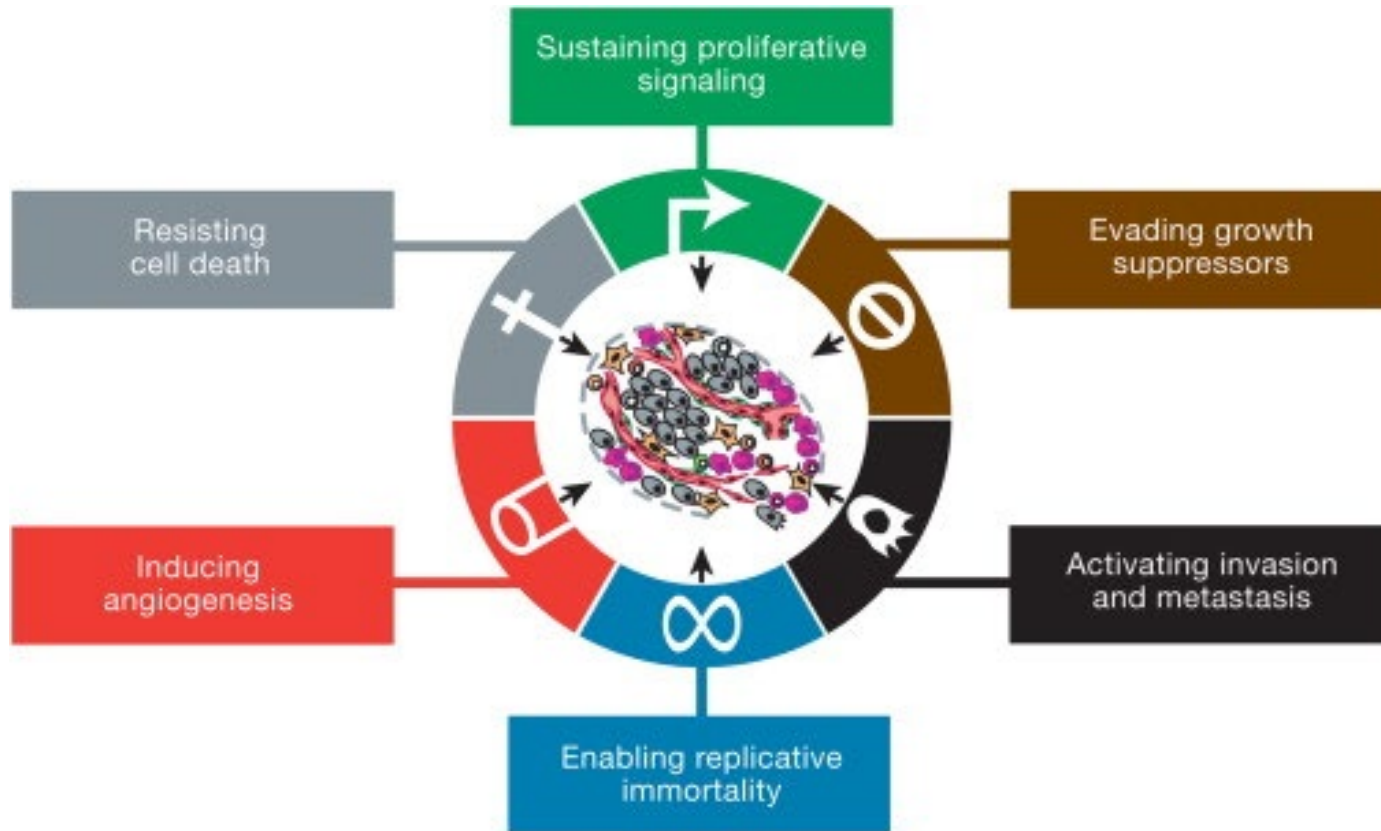
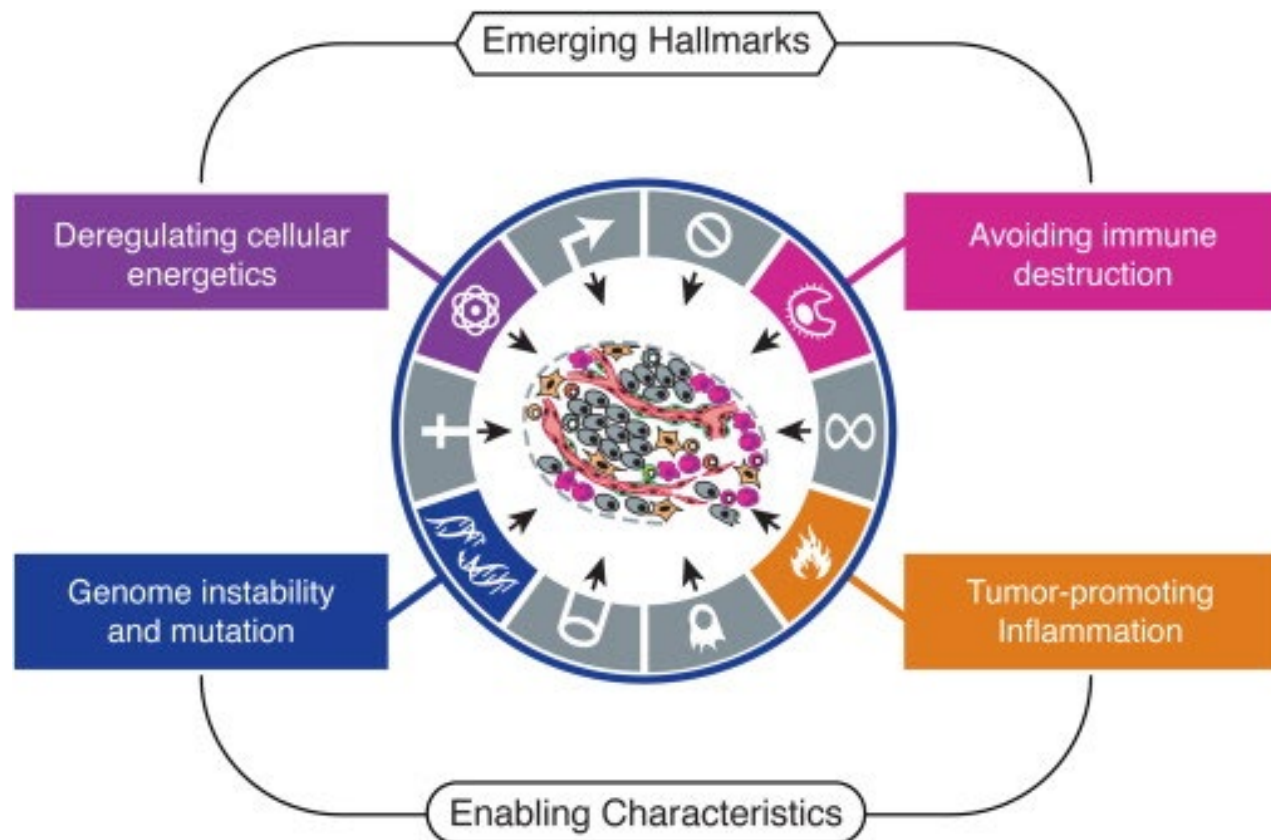


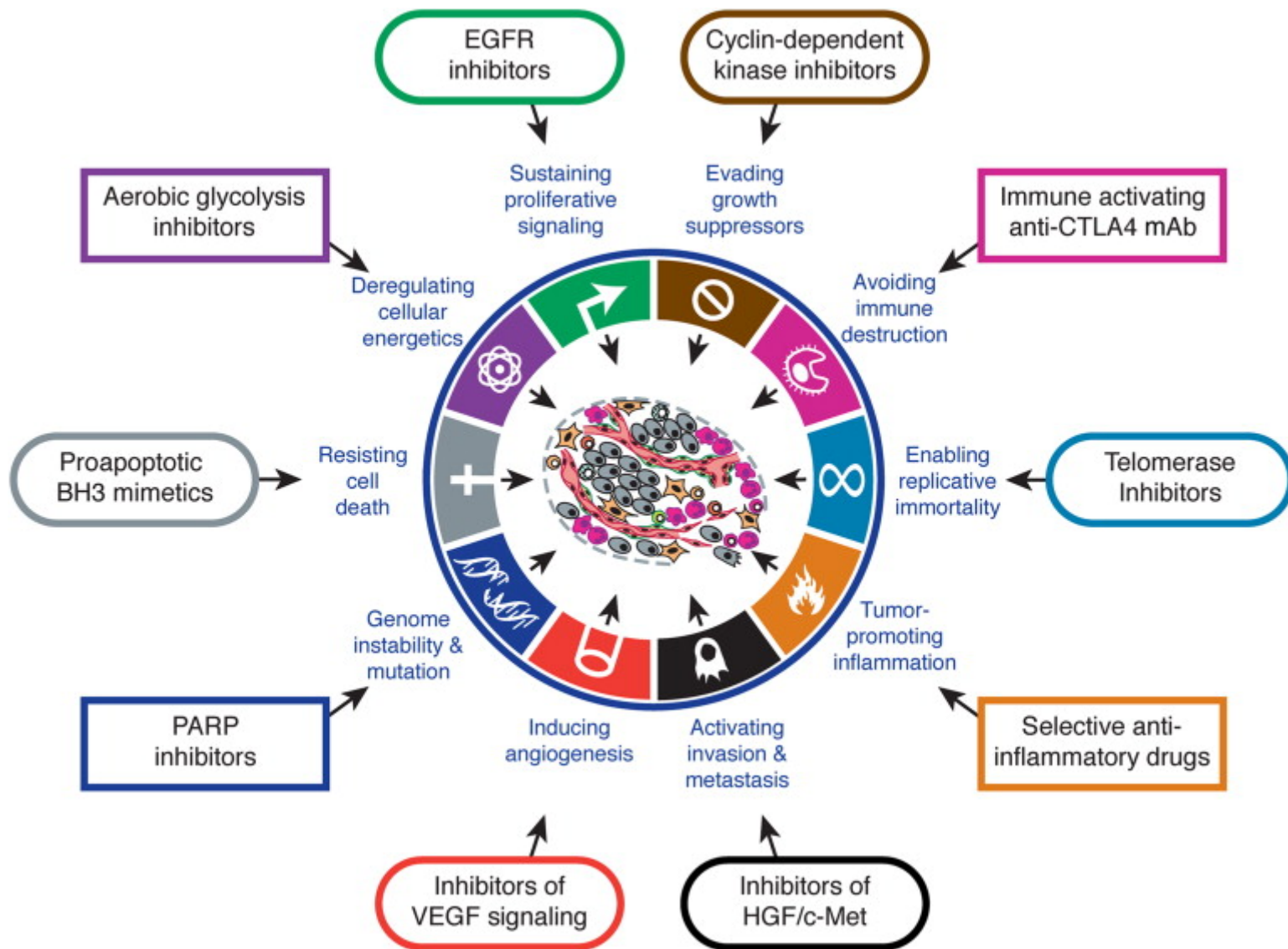
Nanomedicine

Cancer Hallmark

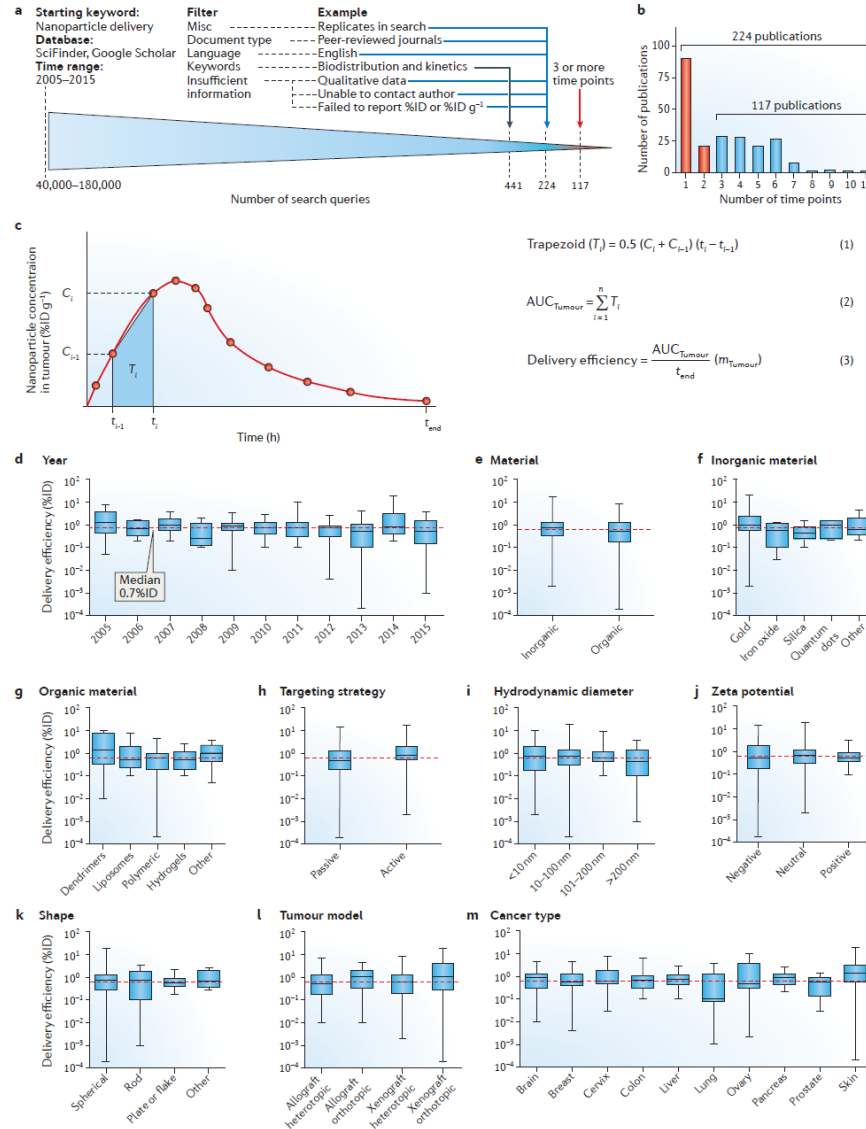




An increasing body of research suggests that two additional hallmarks of cancer are involved in the pathogenesis of some and perhaps all cancers. One involves the capability to modify, or reprogram, cellular metabolism in order to most effectively support neoplastic proliferation. The second allows cancer cells to evade immunological destruction, in particular by T and B lymphocytes, macrophages, and natural killer cells. Because neither capability is yet generalized and fully validated, they are labeled as emerging hallmarks. Additionally, two consequential characteristics of neoplasia facilitate acquisition of both core and emerging hallmarks. Genomic instability and thus mutability endow cancer cells with genetic alterations that drive tumor progression. Inflammation by innate immune cells designed to fight infections and heal wounds can instead result in their inadvertent support of multiple hallmark capabilities, thereby manifesting the now widely appreciated tumor-promoting consequences of inflammatory responses.

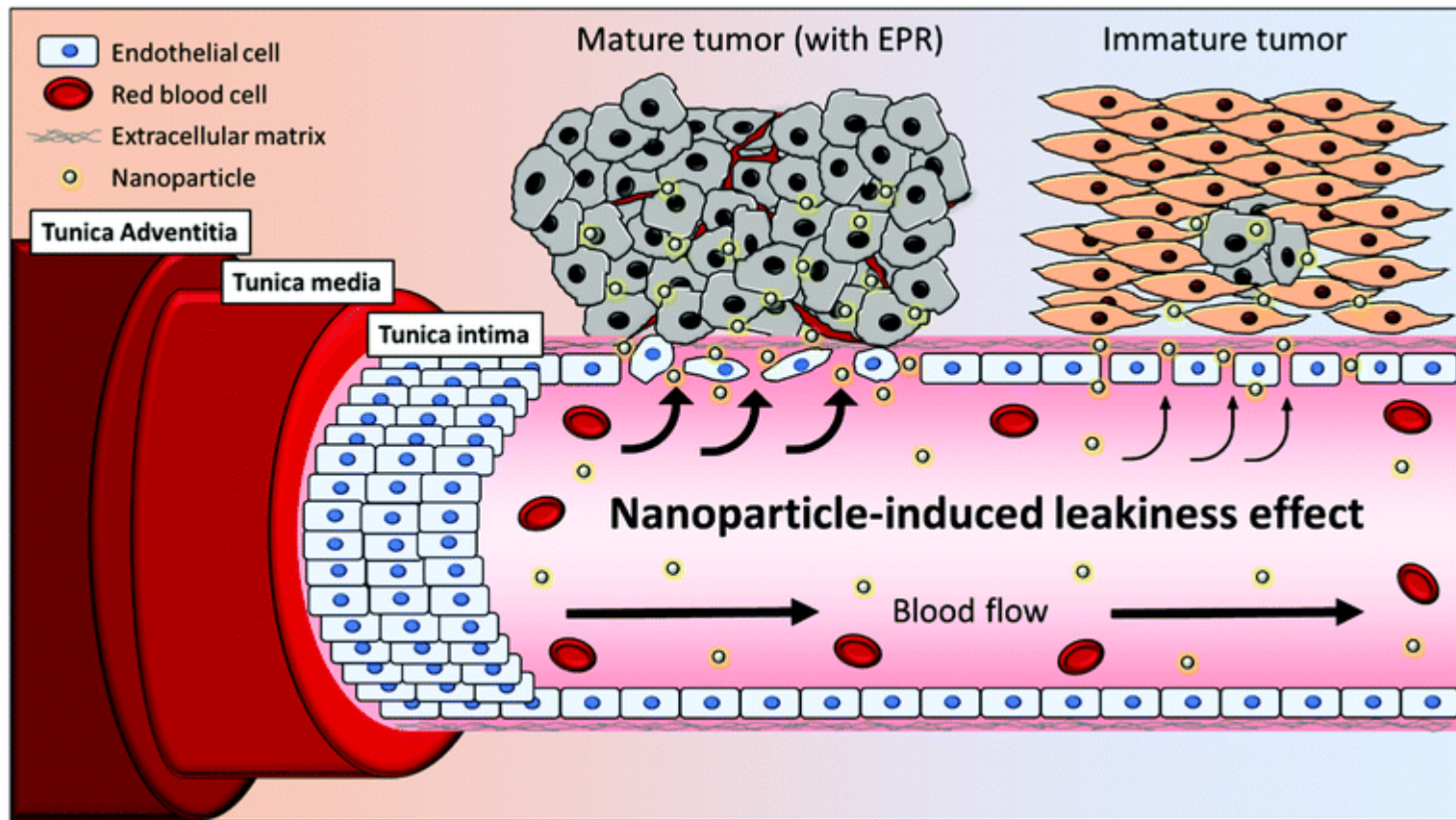


Delivery Efficiency



< 1%ID

EPR Effect

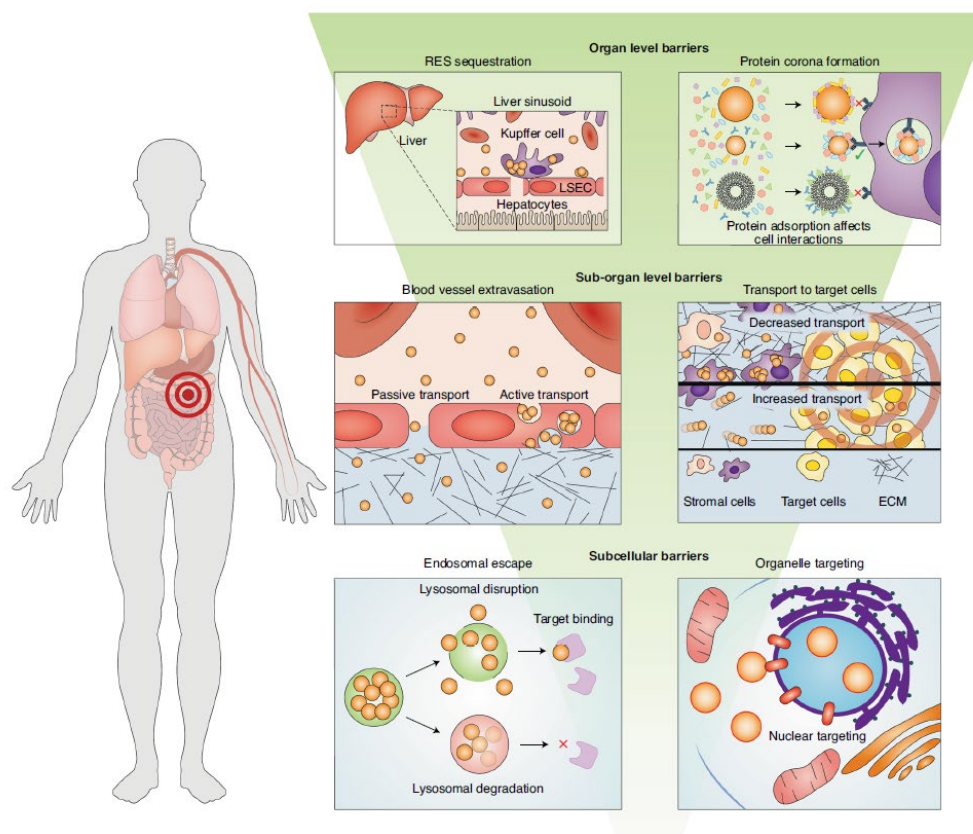




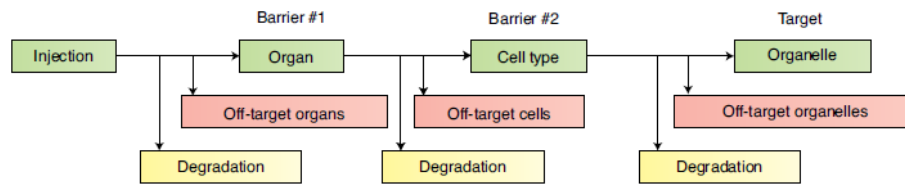
A framework for designing delivery systems

Wilson Poon^{1,2,7}, Benjamin R. Kingston^{1,2,7}, Ben Ouyang^{1,2,3}, Wayne Ngo^{1,2} and Warren C. W. Chan^{1,2,4,5,6} ✉

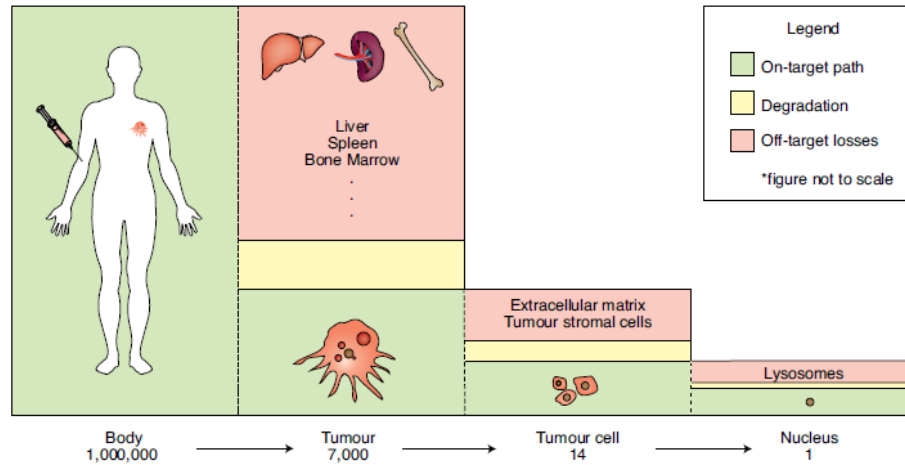
NATURE NANOTECHNOLOGY | VOL 15 | OCTOBER 2020 | 819–829



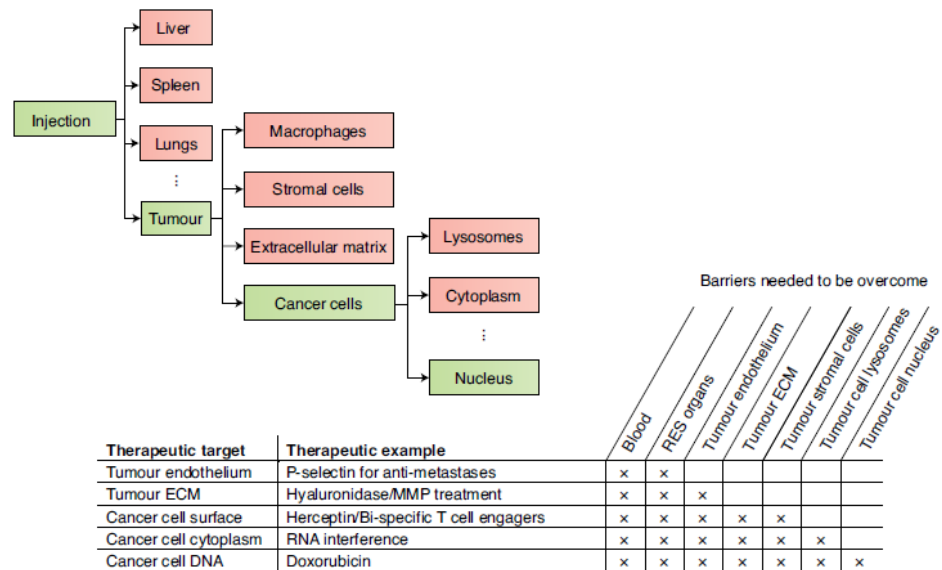
a



b



c



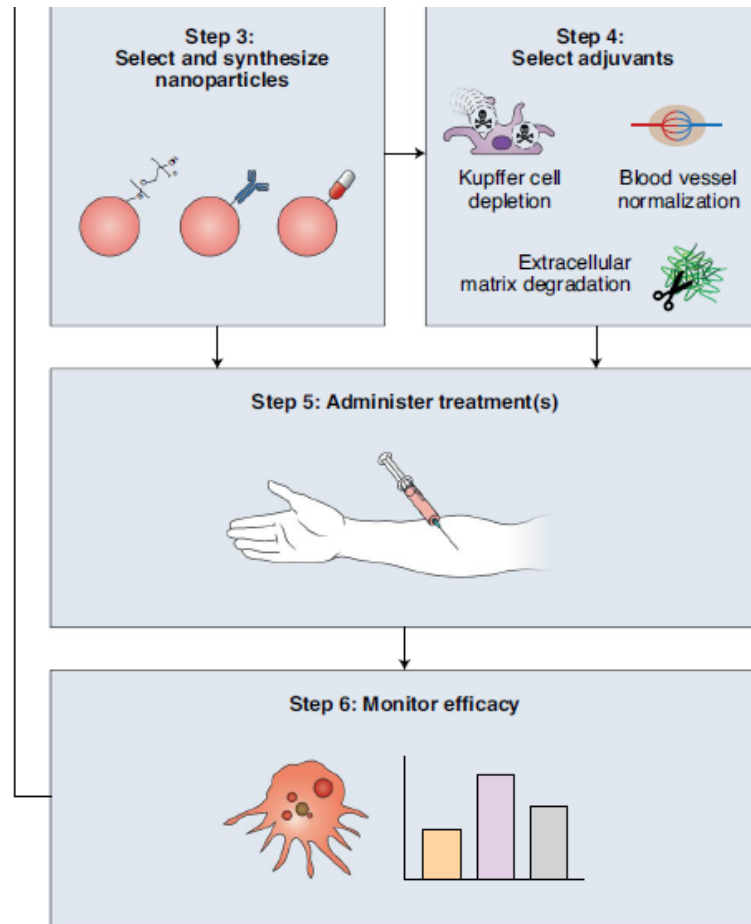
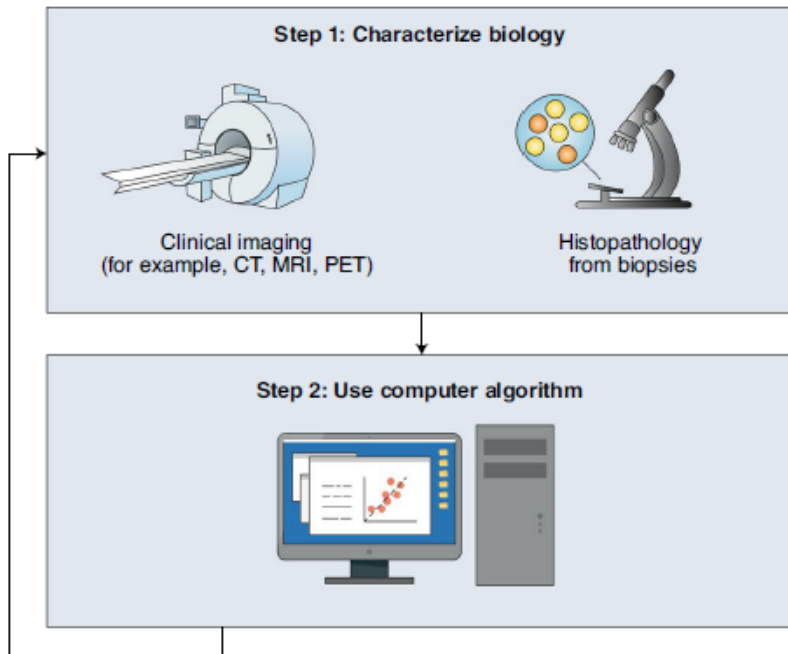
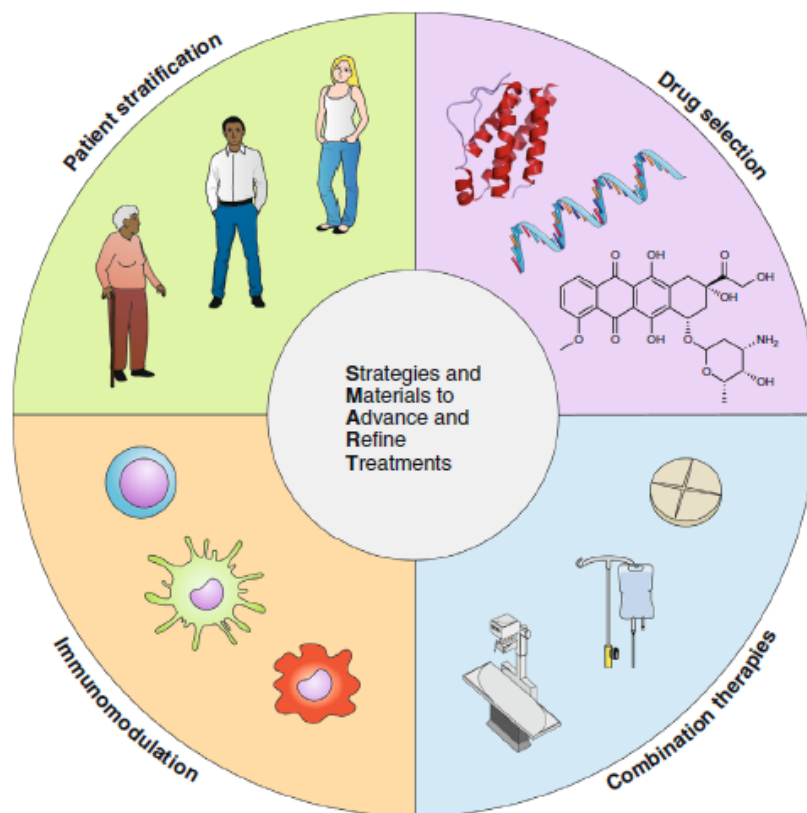


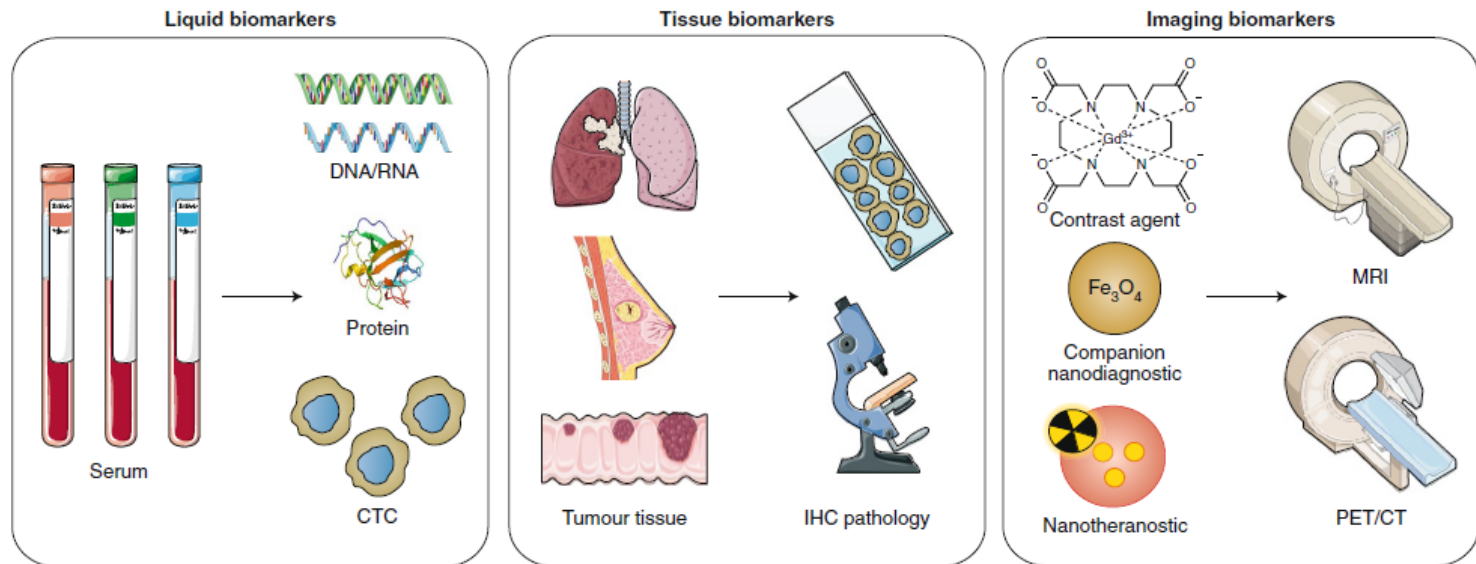
Table 1 | Critical questions for designing nanoparticle delivery systems

| Question | Rationale for the question |
|--|---|
| (1) Where is the delivery target? | The specific biological target (organ or tissue, cell type and subcellular location) defines design of the nanoparticle strategy. |
| (2) What is the cargo or active agent that needs to be delivered to the target location? | This defines the chemistry for incorporating the agents into the nanoparticle for delivery. |
| (3) Where is the site of administration? | The location of administration and the delivery target location define the delivery pathway. |
| (4) What are the specific organs, tissues and cells encountered along the delivery pathway? | This defines the barriers that the nanoparticle will encounter. |
| (5) What are the interactions between the nanoparticle carrier and the body in each of these biological environments along the delivery pathway? | These interactions will determine if the formulation is degraded or sequestered before it can reach its intended target location. |
| (6) What strategies are available to overcome the barriers at each step in the delivery pathway? | This allows the development of specific strategies to overcome the barriers. |
| (7) How will any administered components leave the disease site and be excreted from the body? | This helps to define locations of toxicity and elimination routes. |

Smart cancer nanomedicine

NATURE NANOTECHNOLOGY | VOL 14 | NOVEMBER 2019 | 1007-1017 |



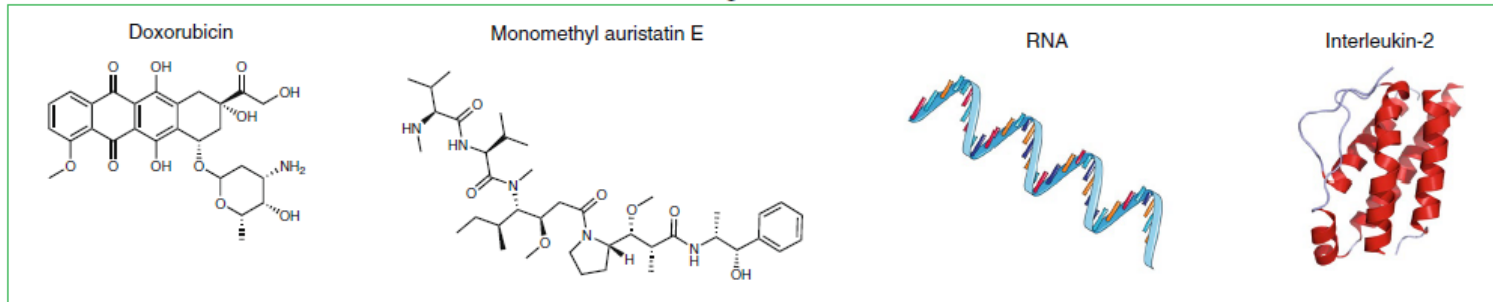


Simplicity

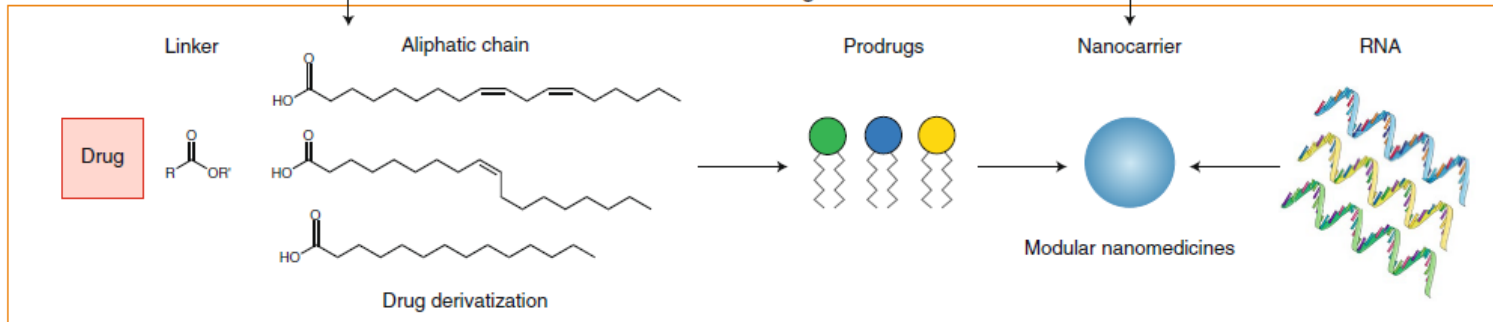
Specificity

Figure 1. Biomarkers and their detection methods. The diagram illustrates the detection of biomarkers in liquid, tissue, and imaging forms, showing the progression from sample collection to analysis and imaging.

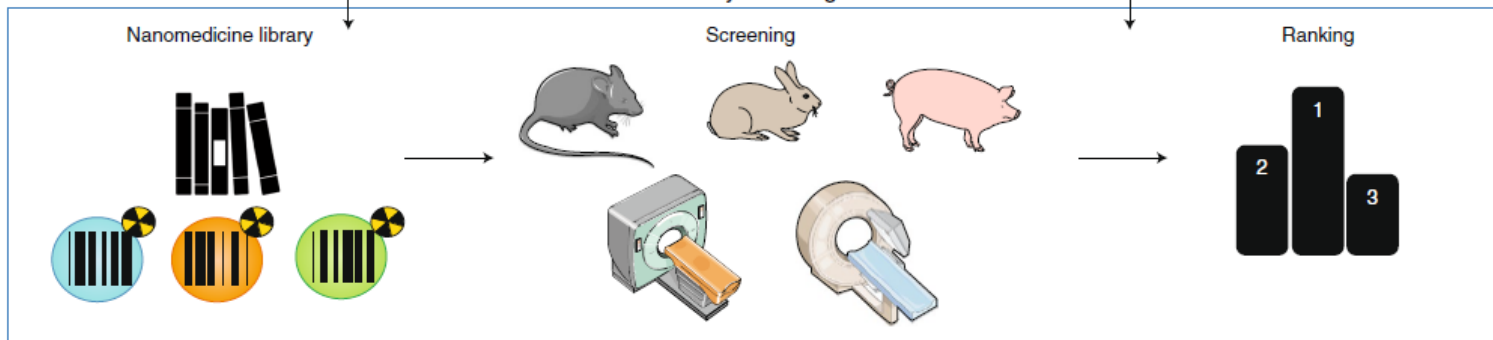
Drug classes

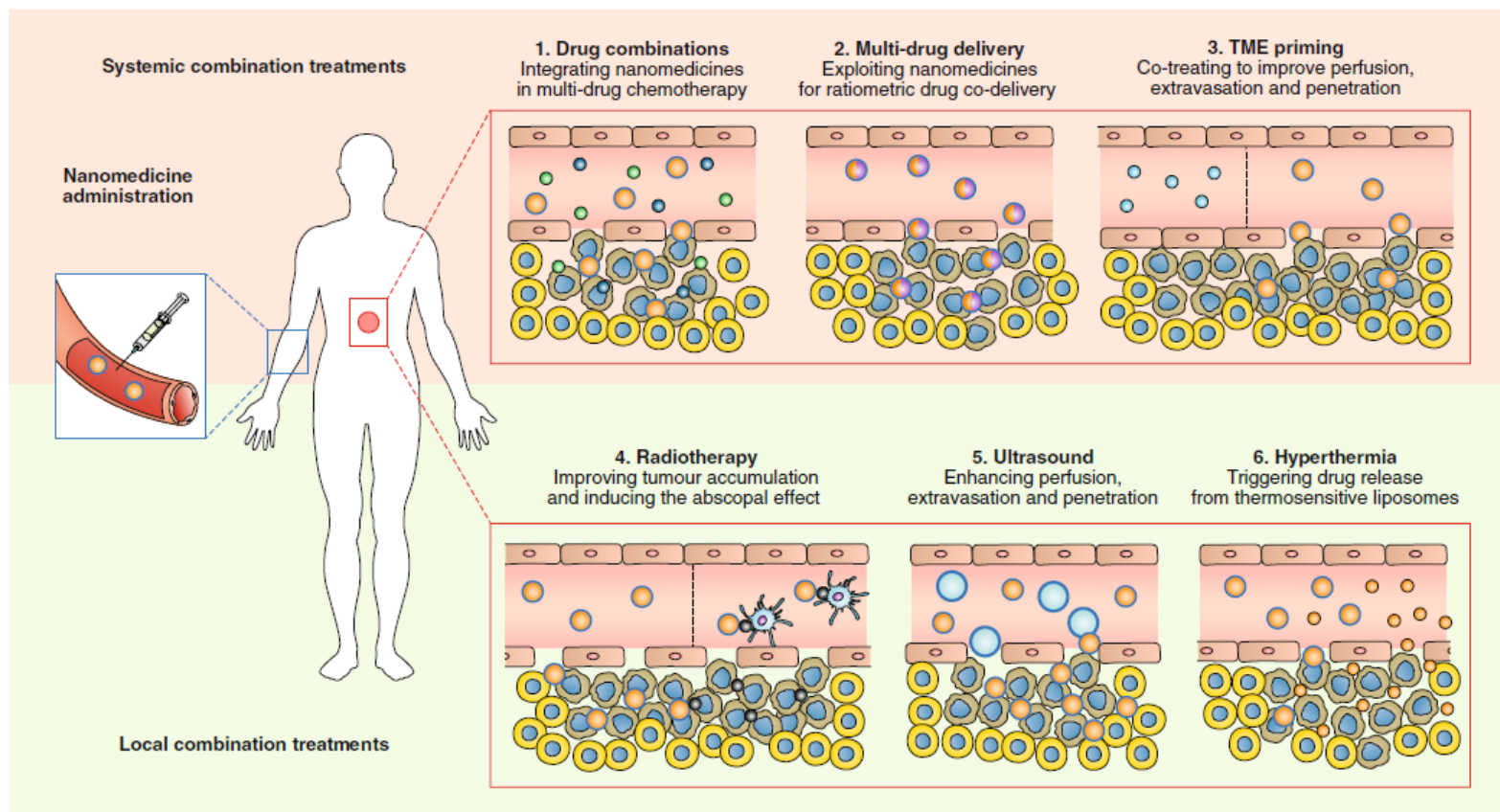


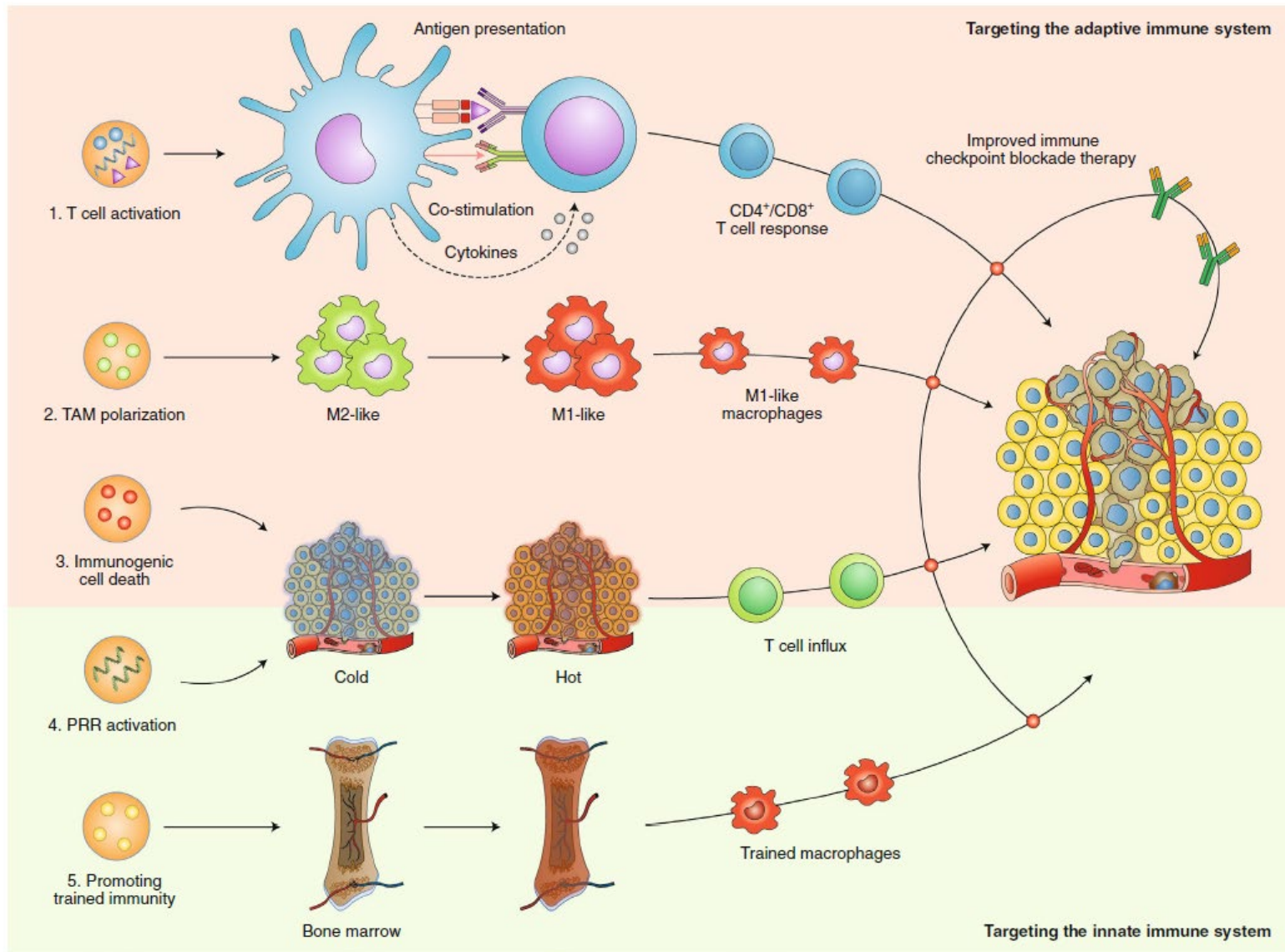
Modular design



Library screening







Cancer nanomedicine: progress, challenges and opportunities

Jinjun Shi¹, Philip W. Kantoff², Richard Wooster³ and Omid C. Farokhzad^{1,4}

Box 1 | Distinctive features of nanotechnology in oncological applications

- Improvement of the drug therapeutic index by increasing efficacy and/or reducing toxicities
- Targeted delivery of drugs in a tissue-, cell- or organelle-specific manner
- Enhancement of the pharmaceutical properties (for example, stability, solubility, circulating half-life and tumour accumulation) of therapeutic molecules
- Enabling of sustained or stimulus-triggered drug release
- Facilitation of the delivery of biomacromolecular drugs (for example, DNA, small interfering RNA (siRNA), mRNA and protein) to intracellular sites of action
- Co-delivery of multiple drugs to improve therapeutic efficacy and overcome drug resistance, by providing more precise control of the spatiotemporal exposure of each drug and the delivery of appropriate drug ratio to the target of interest
- Transcytosis of drugs across tight epithelial and endothelial barriers (for example, gastrointestinal tract and the blood–brain barrier)
- More sensitive cancer diagnosis and imaging
- Visualization of sites of drug delivery by combining therapeutic agents with imaging modalities, and/or real-time feedback on the *in vivo* efficacy of a therapeutic agent
- Provision of new approaches for the development of synthetic vaccines
- Miniaturized medical devices for cancer diagnosis, drug screening and delivery
- Inherent therapeutic properties of some nanomaterials (for example, gold nanoshells and nanorods, and iron oxide nanoparticles) upon stimulation

| Therapy modality | Generic name and/or proprietary name | Nanotechnology platform | Active pharmaceutical ingredients | Cancer type | Status | Refs |
|-------------------------------------|---|-------------------------|--|---|-------------------------------|---------|
| Chemotherapy: non-targeted delivery | Liposomal doxorubicin (Doxil) | Pegylated liposome | Doxorubicin | HIV-related Kaposi sarcoma, ovarian cancer, and multiple myeloma | Approved by FDA | 6 |
| | Liposomal daunorubicin (DaunoXome) | Liposome | Daunorubicin | HIV-related Kaposi sarcoma | Approved by FDA | 6 |
| | Liposomal vincristine (Marqibo) | Liposome | Vincristine sulfate | Acute lymphoblastic leukaemia | Approved by FDA | 6 |
| | Liposomal irinotecan (Onivyde or MM-398) | Pegylated liposome | Irinotecan | Post-gemcitabine metastatic pancreatic cancer | Approved by FDA | 230 |
| | Liposomal doxorubicin (Myocet) | Liposome | Doxorubicin | Metastatic breast cancer | Approved in Europe and Canada | 6 |
| | Mifamurtide (Mepact) | Liposome | Muramyl tripeptide phosphatidyl-ethanolamine | Nonmetastatic, resectable osteosarcoma | Approved in Europe | 6 |
| | Nab-paclitaxel (Abraxane) | Albumin NP | Paclitaxel | Breast, lung and pancreatic cancer | Approved by FDA | 6 |
| | SMANCS | Polymer conjugate | Neocarzinostatin | Liver and renal cancer | Approved in Japan | 6 |
| | Polymeric micelle paclitaxel (Genexol-PM) | Polymeric micelle | Paclitaxel | Breast cancer and NSCLC | Approved in Korea | 6 |
| | Liposomal cisplatin (Lipoplatin) | Pegylated liposome | Cisplatin | NSCLC | Phase III | 231 |
| | NK-105 | Polymeric micelle | Paclitaxel | Metastatic or recurrent breast cancer | Phase III | 232 |
| | Liposomal paclitaxel (EndoTAG-1) | Liposome | Paclitaxel | Pancreatic cancer, liver metastases and HER2-negative and triple-negative breast cancer | Phase II | 233–236 |
| | Nab-rapamycin (ABI-009) | Albumin NP | Rapamycin | Advanced malignant PEComa and advanced cancer with mTOR mutations | Phase II | 237,238 |

NSCLC, metastatic renal cell carcinoma and recurrent ovarian, tubal or peritoneal cancer

| | | | | | | |
|--|---|-----------------------------|-----------------------------------|--|--------------|---------|
| Chemotherapy: targeted delivery | MM-302 | HER2-targeting liposome | Doxorubicin | HER2-positive breast cancer | Phase II/III | 242 |
| | BIND-014 | PSMA-targeting polymeric NP | Docetaxel | NSCLC and mCRPC | Phase II | 243–245 |
| | MBP-426 | TfR-targeting liposome | Oxaliplatin | Gastric, oesophageal and gastro-oesophageal adenocarcinoma | Phase I/II | 246 |
| | Anti-EGFR immunoliposomes loaded with doxorubicin | EGFR-targeting liposome | Doxorubicin | Solid tumours | Phase I | 247 |
| Chemotherapy: stimuli-responsive delivery | ThermoDox | Liposome | Doxorubicin | Hepatocellular carcinoma | Phase III | 248 |
| Chemotherapy: combinatorial delivery | Liposomal cytarabine–daunorubicin (CPX-351 or Vyxeos) | Liposome | Cytarabine and daunorubicin (5:1) | High-risk acute myeloid leukaemia | Phase III | 249 |
| | CPX-1 | Liposome | Irinotecan and floxuridine (1:1) | Advanced colorectal cancer | Phase II | 250 |

| Therapy modality | Generic name and/or proprietary name | Nanotechnology platform | Active pharmaceutical ingredients | Cancer type | Status | Refs |
|----------------------|--------------------------------------|-----------------------------------|---|--|--------------------|---------|
| Hyperthermia | NanoTherm | Iron oxide NP | NA | Glioblastoma | Approved in Europe | 6 |
| | AuroLase | Silica core with a gold nanoshell | NA | Head and neck cancer, and primary and metastatic lung tumours | Pilot study | 251,252 |
| Radiotherapy | NBTXR3 | Hafnium oxide NP | NA | Adult soft tissue sarcoma | Phase II/III | 253 |
| Gene or RNAi therapy | SGT53 | TfR-targeting liposome | Plasmid encoding normal human wild-type p53 DNA | Recurrent glioblastoma and metastatic pancreatic cancer | Phase II | 254,255 |
| | PNT2258 | Liposome | DNA oligonucleotide against BCL-2 | Relapsed or refractory non-Hodgkin lymphoma and diffuse large B-cell lymphoma | Phase II | 256,257 |
| | SNS01-T | Polyethylenimine NP | siRNA against eIF5A and plasmid expressing eIF5A-K50R | Relapsed or refractory B cell malignancies | Phase I/II | 258 |
| | Atu027 | Liposome | siRNA against protein kinase N3 | Advanced or metastatic pancreatic cancer | Phase I/II | 259 |
| | TKM-080301 | Lipid NP | siRNA against PLK1 | Neuroendocrine tumours, adrenocortical carcinoma and advanced hepatocellular carcinoma | Phase I/II | 260,261 |
| | DCR-MYC | Lipid NP | Dicer-substrate siRNA against MYC | Hepatocellular carcinoma | Phase I/II | 262 |
| | MRX34 | Liposome | miR-34 mimic | Primary liver cancer, solid tumours and haematological malignancies | Phase I | 263 |
| | CALAA-01 | TfR-targeting polymeric NP | siRNA against ribonucleotide reductase M2 | Solid tumours | Phase I | 227 |
| | ALN-VSP02 | Lipid NP | siRNAs against KSP and VEGFA | Solid tumours | Phase I | 264,265 |
| | siRNA-EPHA2-DOPC | Liposome | siRNA against EPHA2 | Advanced cancers | Phase I | 266 |
| | pbi-shRNA STMN1 LP | Lipid NP | shRNA against stathmin 1 | Advanced and/or metastatic cancer | Phase I | 267 |

| | | | | | | |
|---------------|--------------|-------------------|--|--|------------|-----|
| Immunotherapy | Tecemotide | Liposome | MUC1 antigen | NSCLC | Phase III | 268 |
| | dHER2 + AS15 | Liposome | Recombinant HER2 (dHER2) antigen and AS15 adjuvant | Metastatic breast cancer | Phase I/II | 269 |
| | DPX-0907 | Liposome | Multi-tumour associated antigens | HLA-A2-positive advanced stage ovarian, breast and prostate cancer | Phase I | 270 |
| | Lipovaxin-MM | Liposome | Melanoma antigens | Malignant melanoma | Phase I | 271 |
| | JVRS-100 | Lipid NP | Plasmid DNA | Relapsed or refractory leukaemia | Phase I | 272 |
| | CYT-6091 | Colloidal gold NP | TNF | Advanced solid tumours | Phase I | 273 |

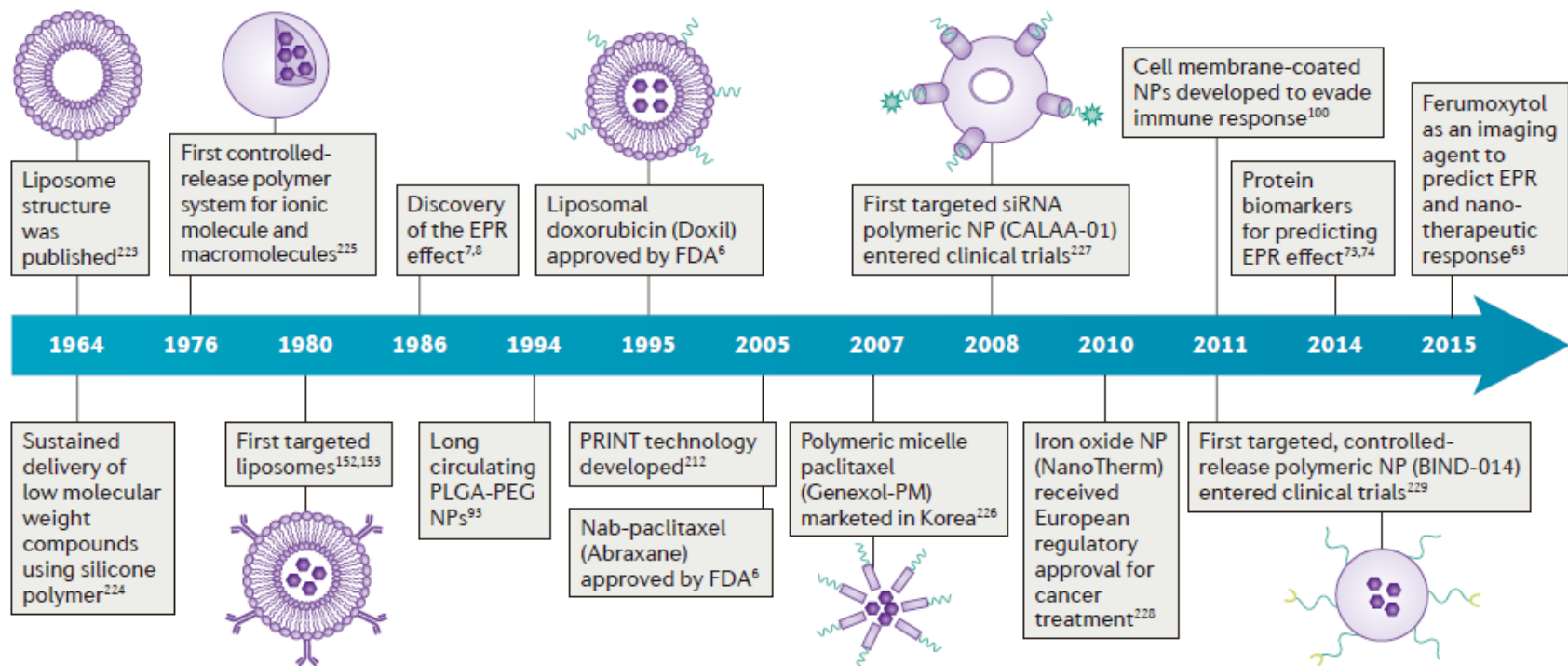
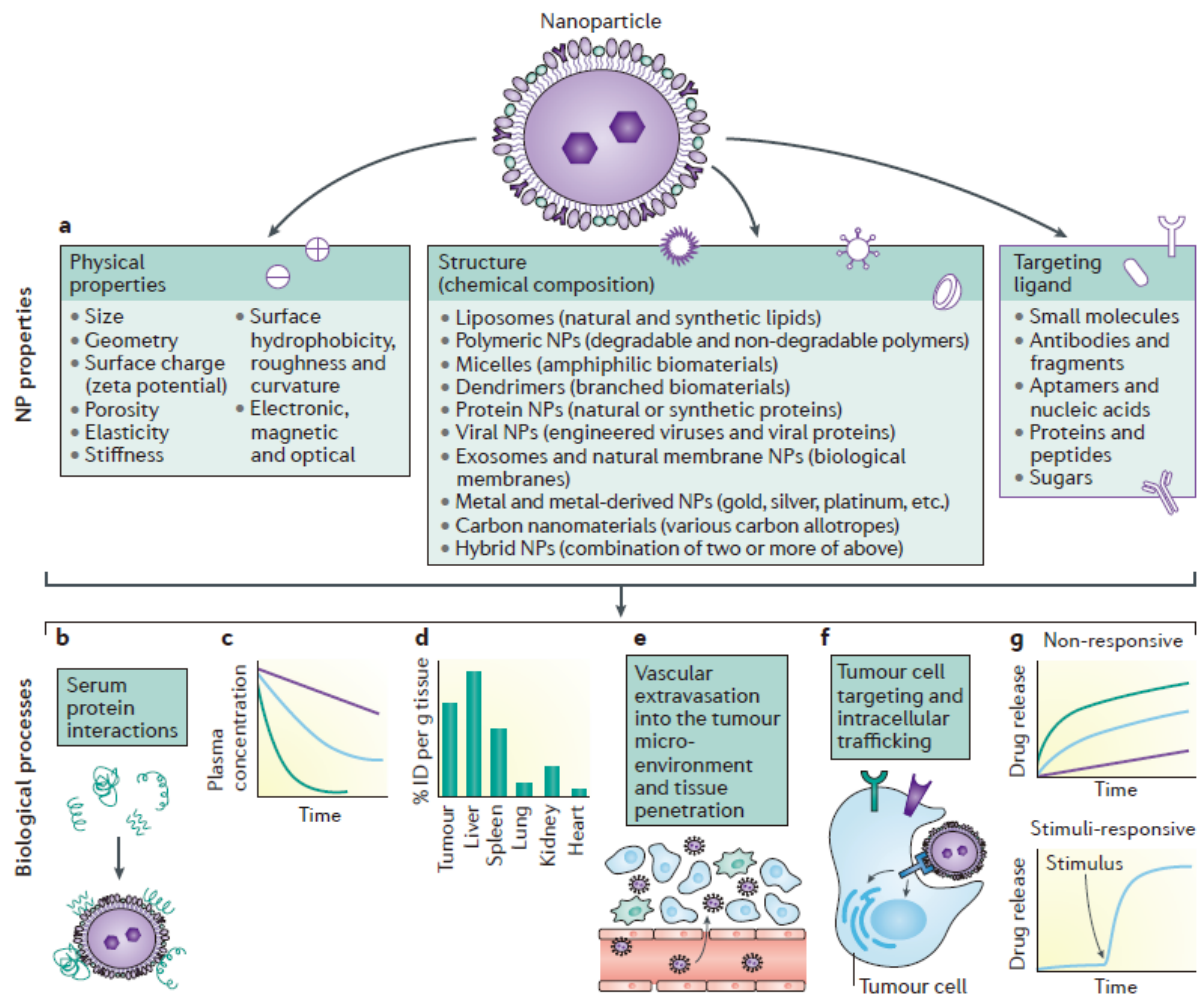


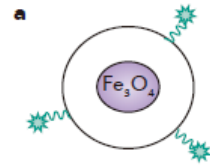
Figure 1 | **Historical timeline of major developments in the field of cancer nanomedicine.** EPR, enhanced permeability and retention; FDA, US Food and Drug Administration; nab, nanoparticle albumin-bound; NP, nanoparticle; PLGA-PEG, poly(D,L-lactic-co-glycolic acid)-b-poly(ethylene glycol); PRINT, particle replication in non-wetting template; siRNA, small interfering RNA.



Patients with heterogeneous tumour EPR effect



Potential EPR markers



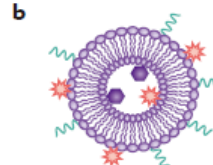
Companion imaging NPs

Pros

- No modification of therapeutic NPs
- Proof-of-concept available in animal models and in patients
- Non-invasive imaging

Cons

- Regulatory, marketing and use complexity



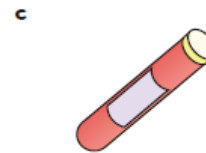
Theranostic NPs

Pros

- More precise tracking
- Proof-of-concept available in animal models and in patients
- Non-invasive imaging

Cons

- Complexity of chemistry and manufacturing



Serum or tissue biomarkers

Pros

- Detection using patient samples
- Proof-of-concept available in animal models

Cons

- Require serum sample or tumour biopsy
- Need more biological understanding



Patients with high EPR effect to receive nanotherapeutics



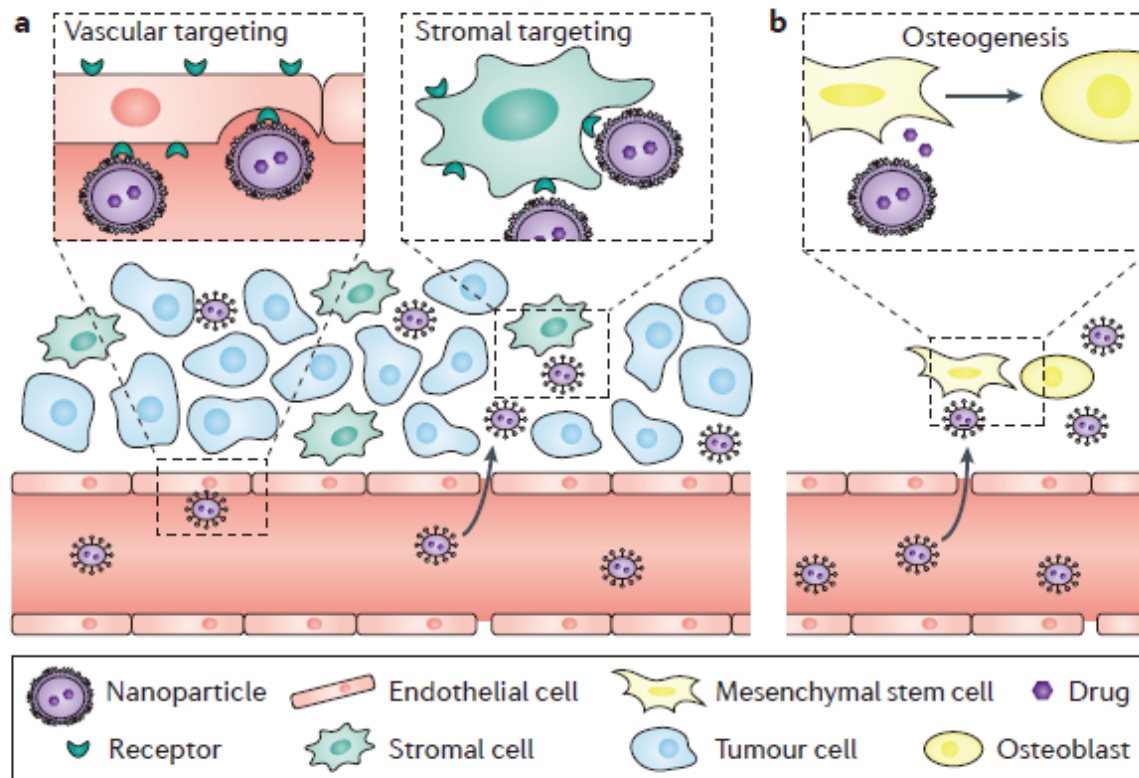
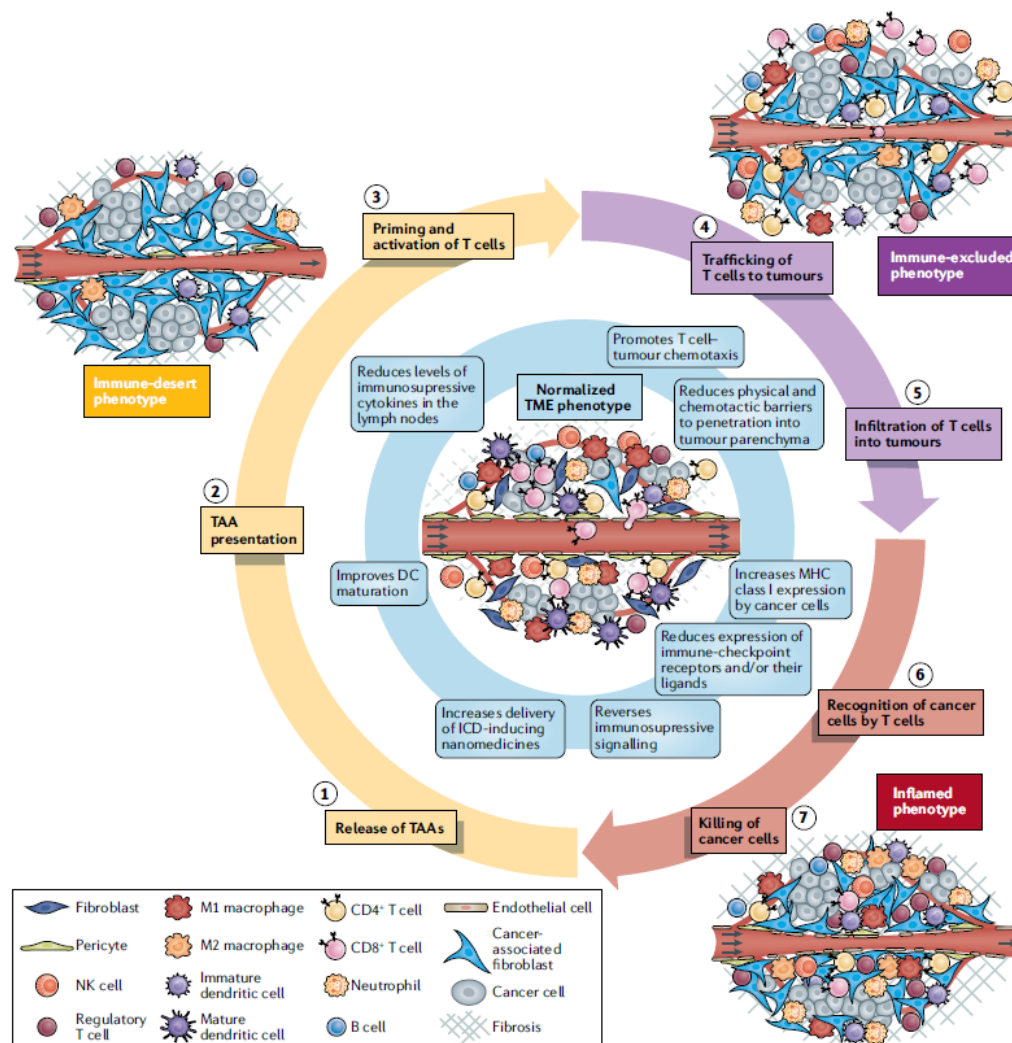
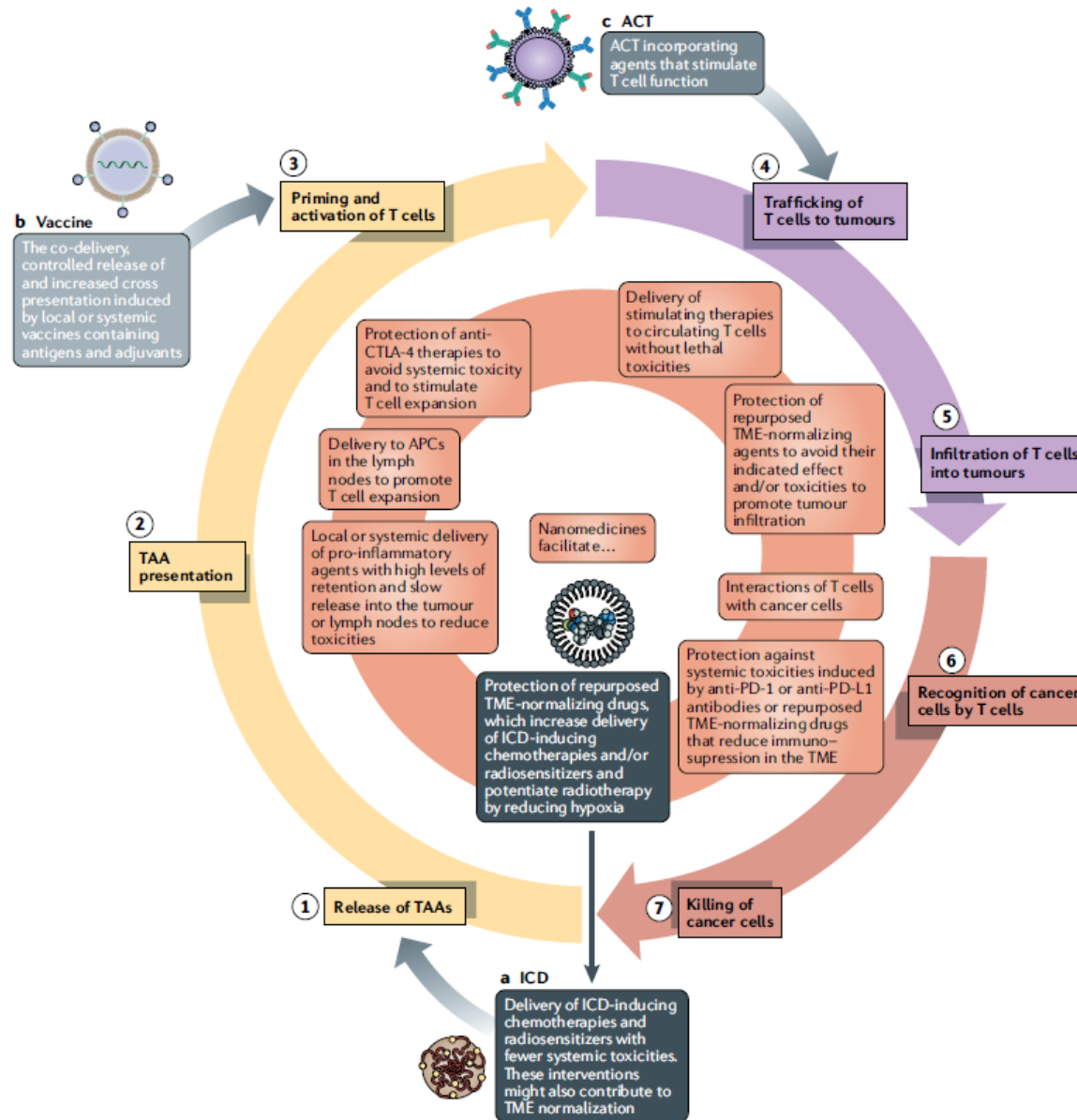


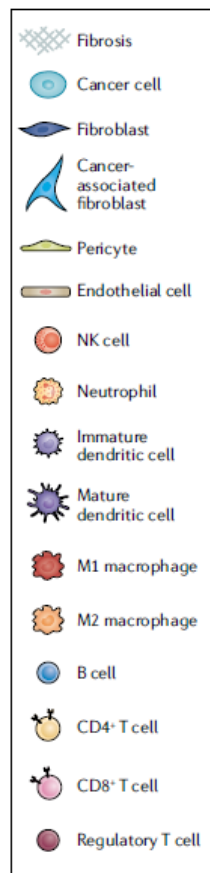
Figure 4 | Nanoparticle targeting of the tumour microenvironment and the premetastatic niche. Targeting of the tumour vasculature or stromal cells in the tumour microenvironment (part **a**) and the premetastatic microenvironments such as the bone marrow niche, where induction of the osteogenic differentiation of mesenchymal stem cells enhances bone strength and volume (part **b**). Cell-specific targeting can be achieved via the modification of nanoparticles (NPs) with ligands that bind to specific receptors (for example, $\alpha\beta_3$ integrin and mannose receptor) on the surface of tumour endothelial cells, stromal cells or other target cells. It should be noted that even without targeting ligands, NPs can be engineered for preferential cellular uptake. The payloads released from NPs localized in tumours or premetastatic tissues can also be nonspecifically taken up by these cells.

Improving cancer immunotherapy using nanomedicines: progress, opportunities and challenges

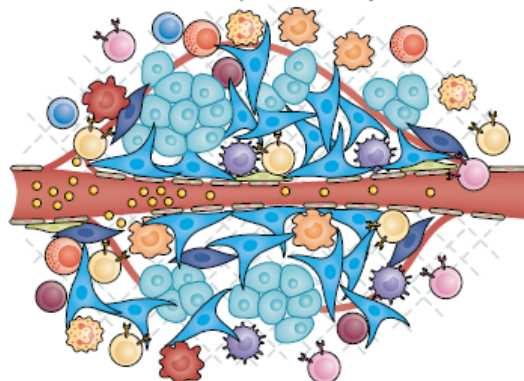
John D. Martin¹, Horacio Cabral, Triantafyllos Stylianopoulos¹ and Rakesh K. Jain¹





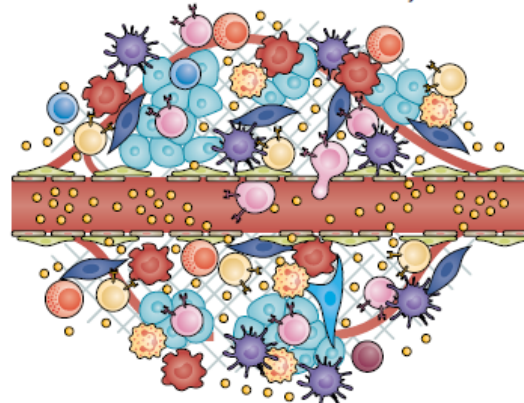


The TME compromises delivery



Targeted, functionalized and/or combination nanomedicines (such as those responding to pH, temperature, heat, or sound waves) to enhance intratumoural drug distribution are compromised by the TME

TME normalization increases delivery



TME normalization increases nanomedicine distribution

Targeted, functionalized and/or combination nanomedicines widely distribute throughout tumour lesion

Vaccine or ACT

TME normalization increases immune cell distribution

Enhancing cancer immunotherapy with nanomedicine

Darrell J. Irvine^{1,2,3,4,5*} and Eric L. Dane¹

NATURE REVIEWS | IMMUNOLOGY

VOLUME 20 | MAY 2020 | 321

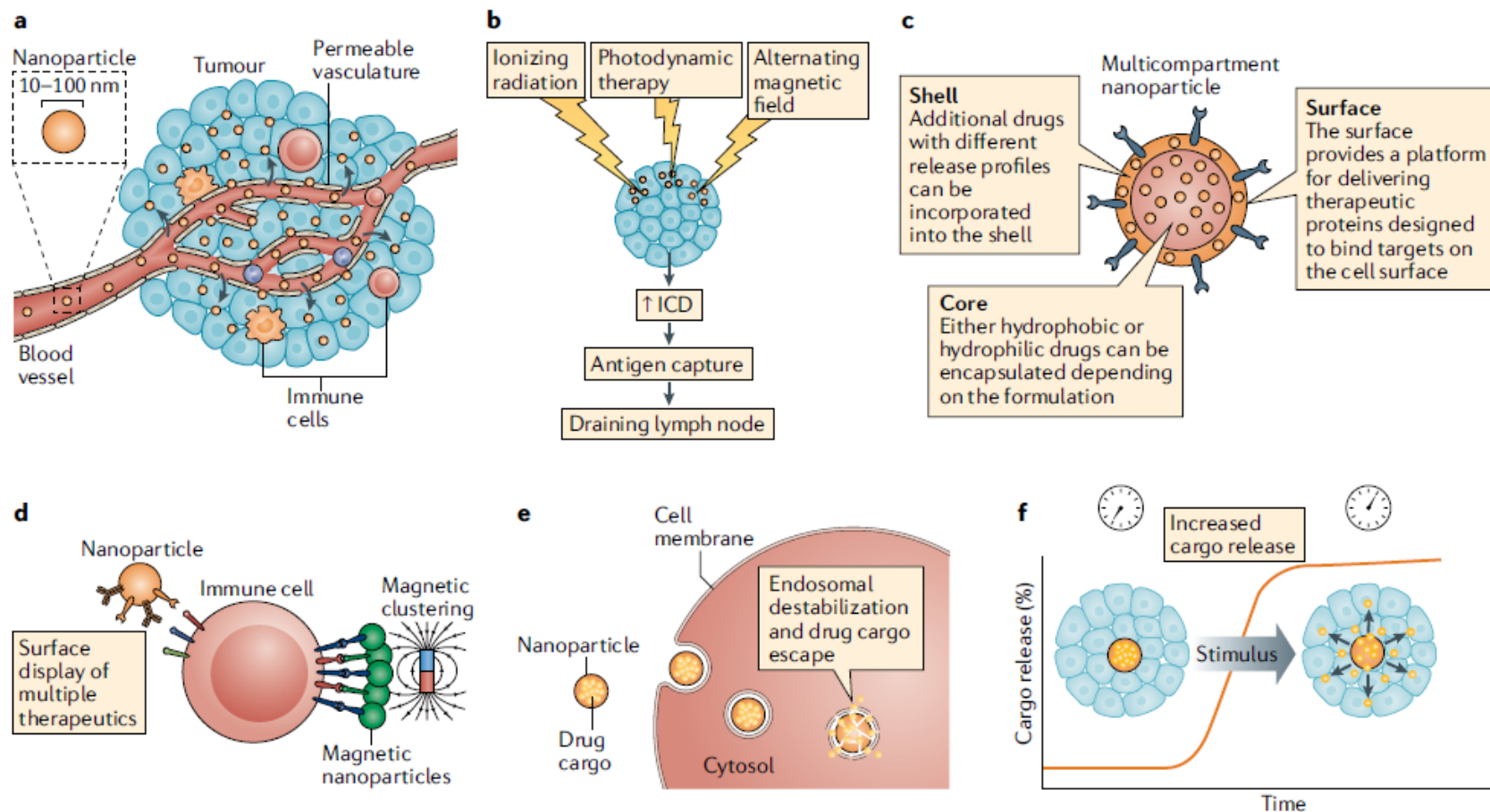


Table 1 | Clinical translation of cancer immunotherapy nanomedicines

| Developer | Concept | Indications | Clinical stage | ClinicalTrials.gov identifiers | Refs |
|---|---|--|-----------------------------|---|-------------|
| NanoBiotix | Metal nanoparticle radioenhancers in combination with checkpoint blockade | Various solid tumours | Phase I–III | NCT03589339 | 25–27 |
| Oslo University Hospital/Bristol-Myers Squibb | Pegylated liposomal doxorubicin in combination with checkpoint blockade | Metastatic breast cancer | Phase IIb | NCT03409198 | 16 |
| Nektar Therapeutics | Reversibly pegylated IL-2 in combination with checkpoint blockade | Various solid tumours | Phase I, phase II | NCT02983045, NCT03138889, NCT03282344, NCT03635983, NCT03785925, NCT03729245, NCT03435640 | 81–83 |
| Exicure | Intratumoural administration of TLR9 agonist-functionalized nanoparticles in combination with checkpoint blockade | Various solid tumours | Phase Ib/II | NCT03684785 | 48,50 |
| Torque Therapeutics | Nanoparticle-functionalized antigen-primed T cell therapy | Various solid tumours and lymphomas | Phase I | NCT03815682 | 113,115,120 |
| Rimo Therapeutics | Metal–organic framework nanoparticles as radioenhancers combined with IDO inhibitors and/or checkpoint blockade | Various solid tumours | Phase I | NCT03444714 | 29 |
| Coordination Pharma | Nanoscale coordination polymer-based particles | Various solid tumours | Phase I | NCT03781362, NCT03953742 | 35–37 |
| Moderna Therapeutics | Lipid nanoparticle-delivered mRNA encoding OX40L, IL-23 and IL-36γ with or without checkpoint blockade | Relapsed or refractory solid tumour malignancies or lymphoma | Phase I | NCT03739931 | 53 |
| Moderna Therapeutics | Lipid nanoparticle-delivered mRNA encoding OX40L | Relapsed or refractory solid tumour malignancies or lymphoma | Phase I | NCT03323398 | 53 |
| OncoNano | STING-activating polymer micelles | TBD | Phase I projected 2020–2021 | NA | 40,142 |
| Tidal Therapeutics | Nanoparticles for gene transfer to macrophages and lymphocytes | TBD | Phase I projected 2020–2021 | NA | 127,128 |

IDO, indoleamine 2,3-dioxygenase; NA, not applicable; STING, stimulator of interferon genes; TBD, to be determined; TLR9, Toll-like receptor 9.

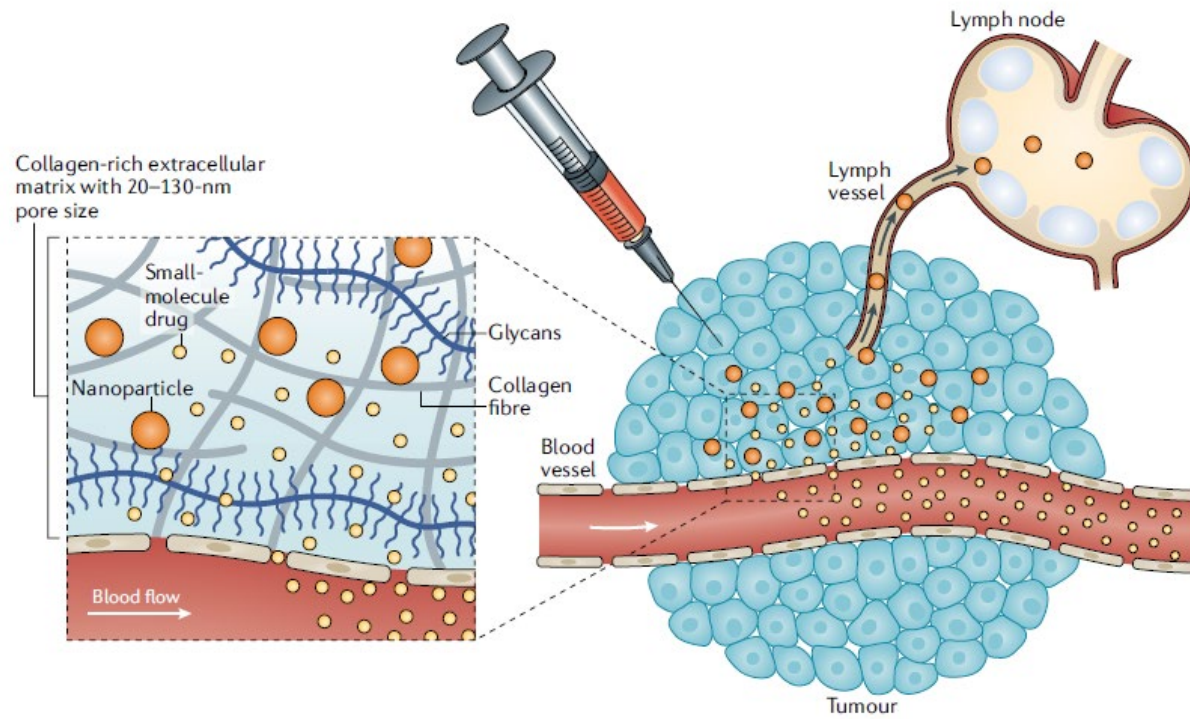
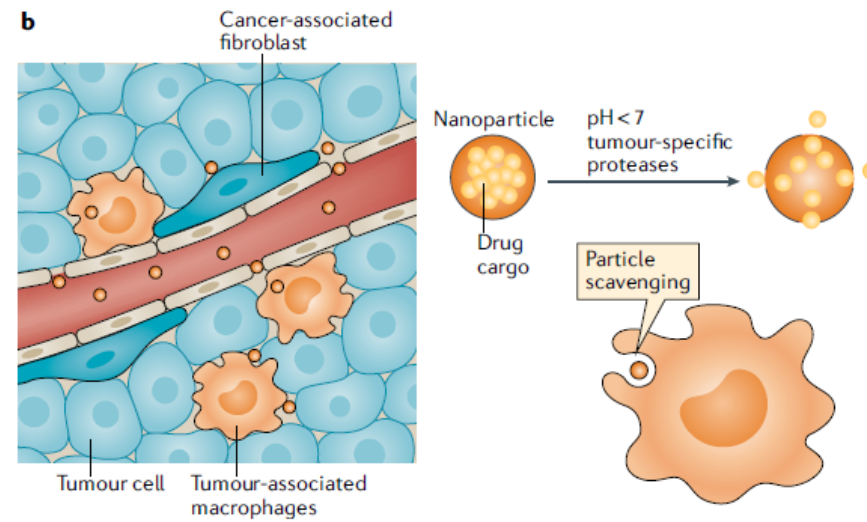
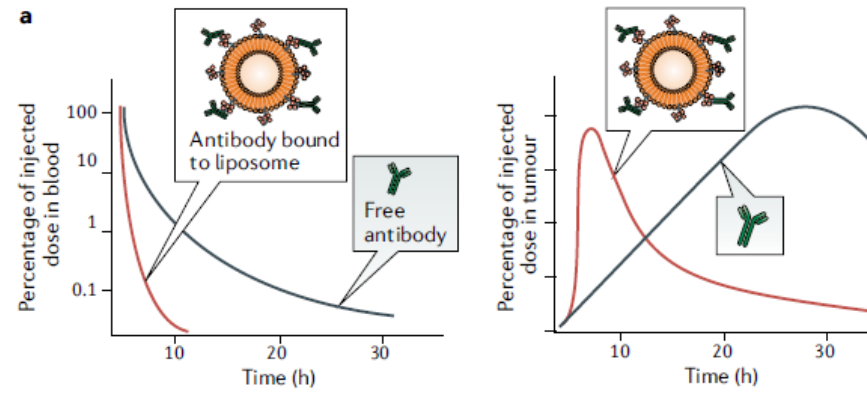
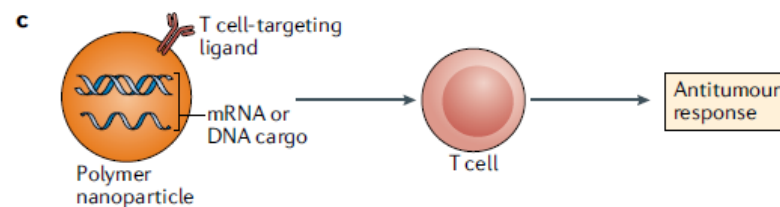
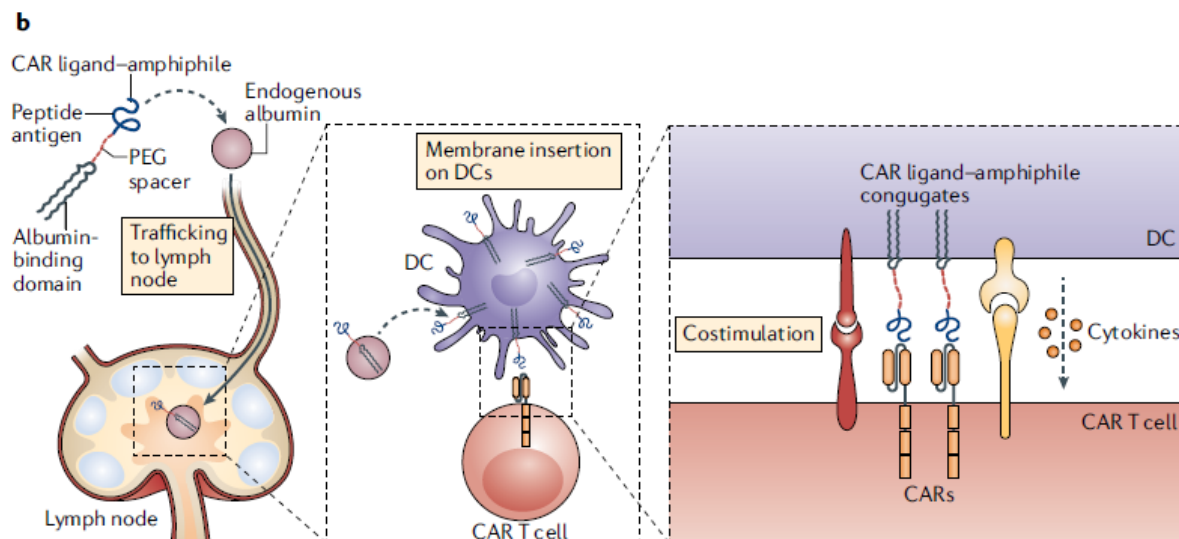
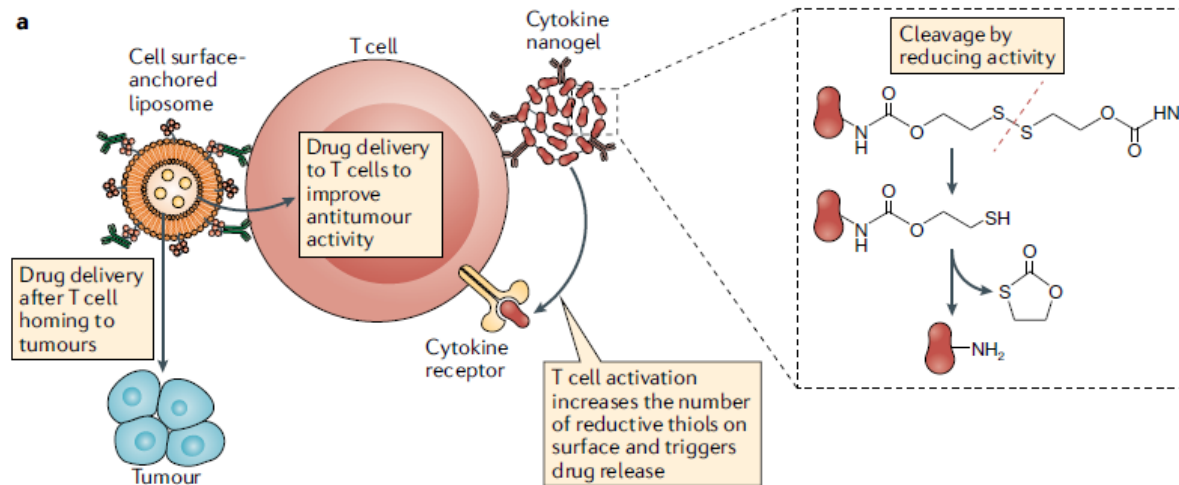


Fig. 6.18 Drug delivery to a tumor via the lymphatic system. The drug is injected into the tumor via a syringe. The drug is then transported through the lymphatic system to the lymph node. The drug is then released from the lymph node into the tumor.





Regulating trained immunity with nanomedicine

NATURE REVIEWS | MATERIALS

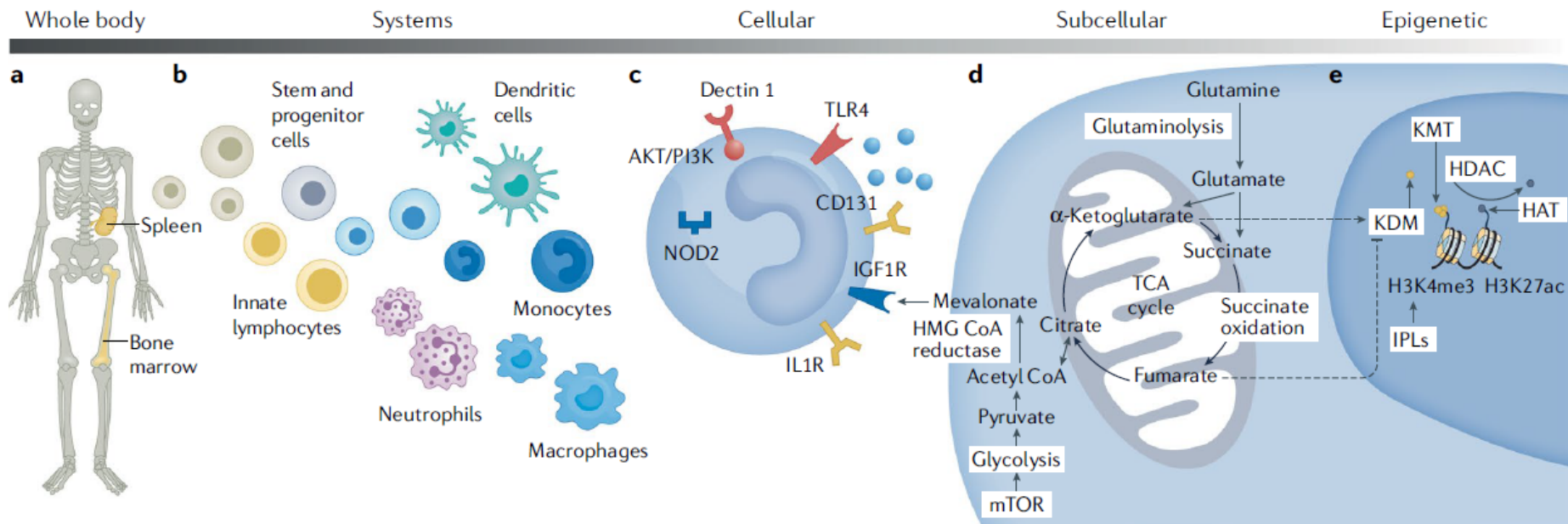
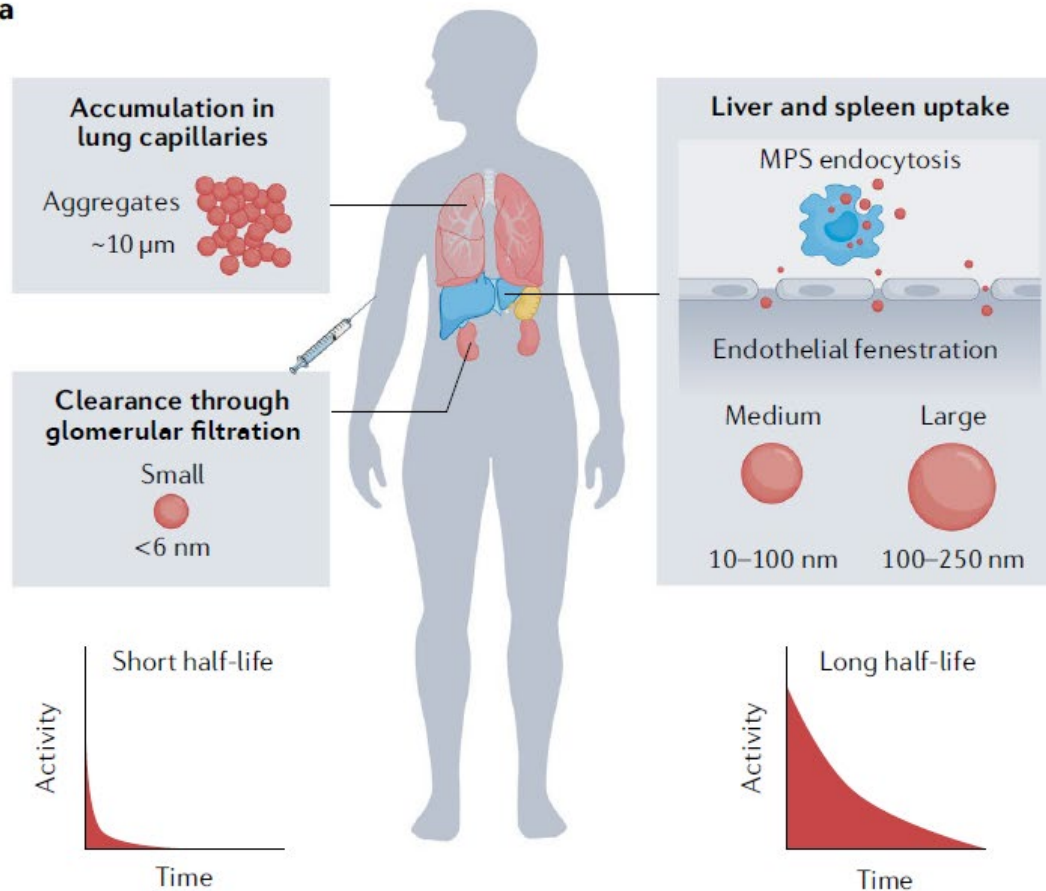
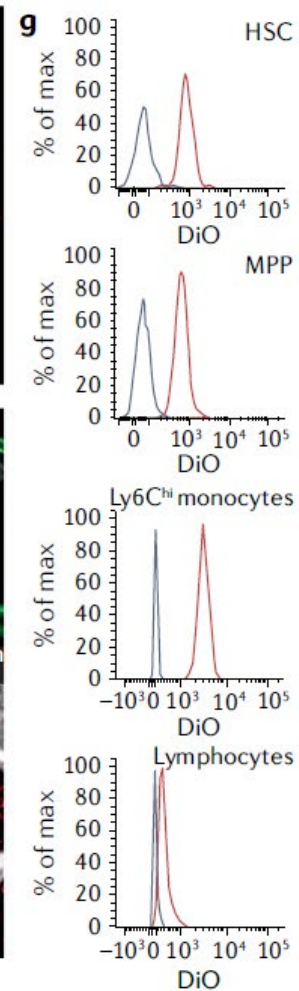
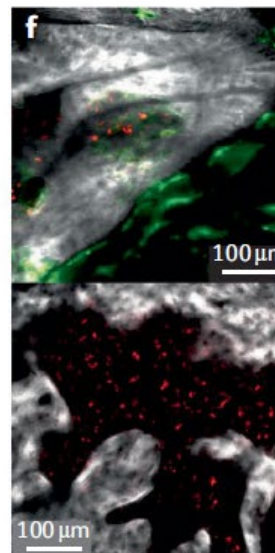
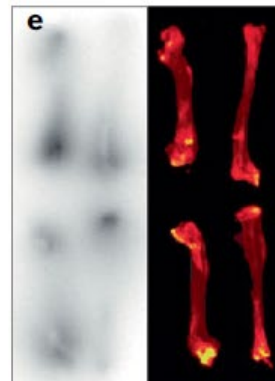
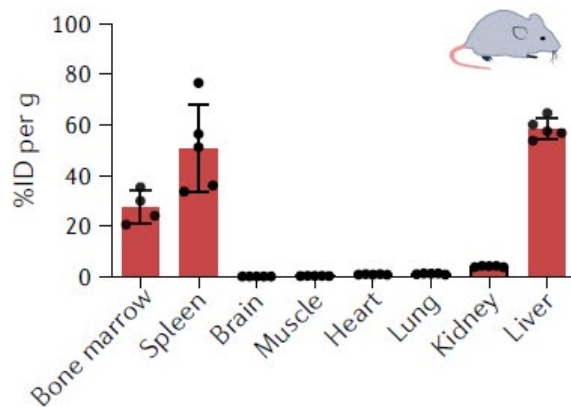
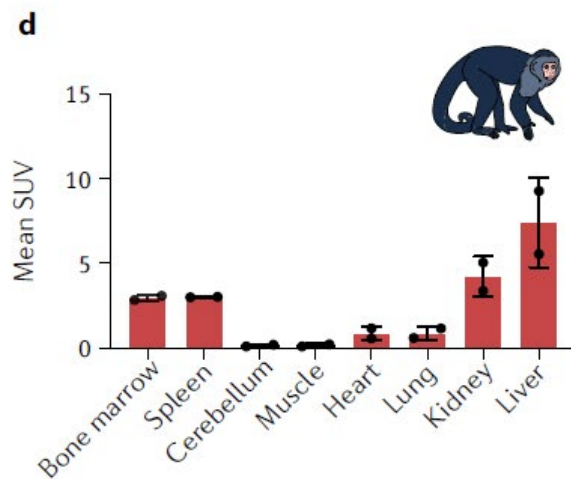
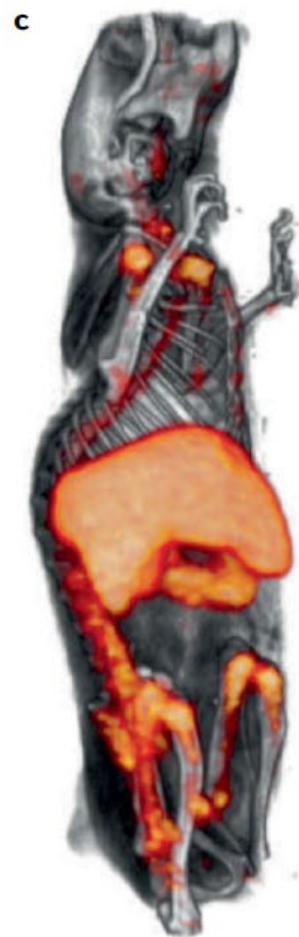
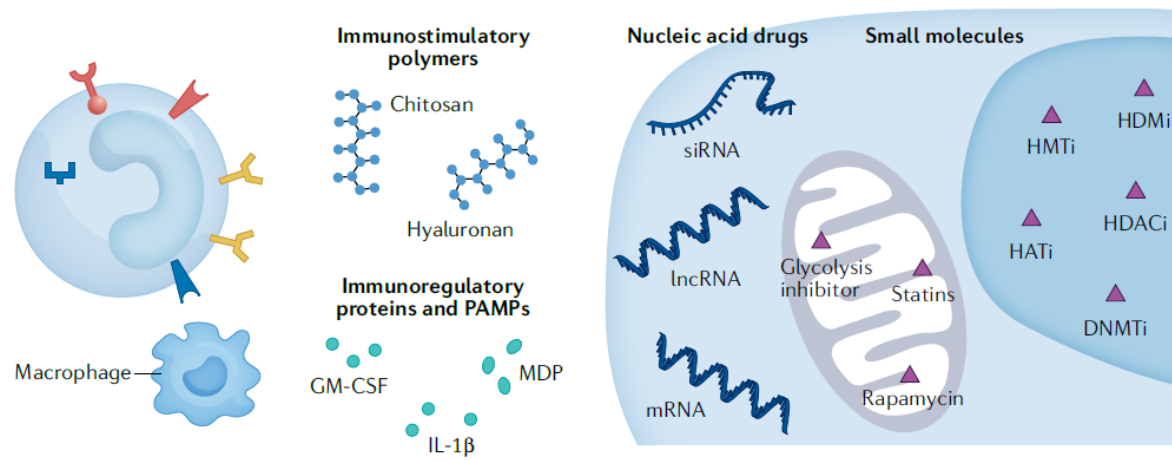
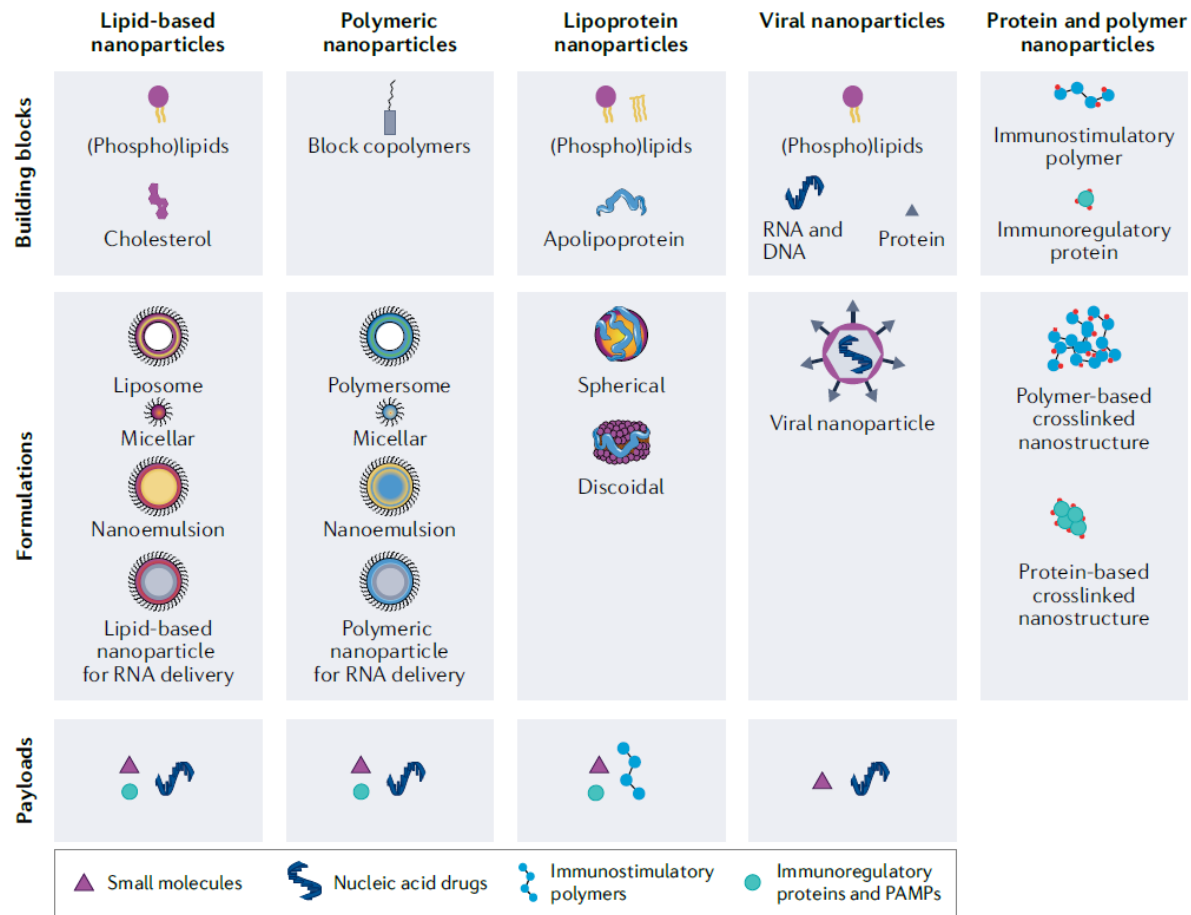


Fig. 1 | Trained immunity targeting levels. **a** | The spleen and bone marrow are important target organs, because they produce and contain large numbers of innate immune cells. **b** | Mature innate immune cells (innate lymphocytes, dendritic cells, monocytes, neutrophils and macrophages) and haematopoietic stem and progenitor cells can be targeted to prevent or enhance trained immunity. **c** | Pattern recognition receptors play an important part in trained immunity. Examples include dectin 1, Toll-like receptor 4 (TLR4) and nucleotide-binding oligomerization domain-containing protein 2 (NOD2). These receptors recognize pathogen-associated molecular patterns (PAMPs) and damage-associated molecular patterns (DAMPs). CD131 is the common β -subunit of granulocyte-macrophage colony-stimulating factor (GM-CSF) and interleukin-3 (IL-3) receptors. The IL-1 receptor (IL-1R)

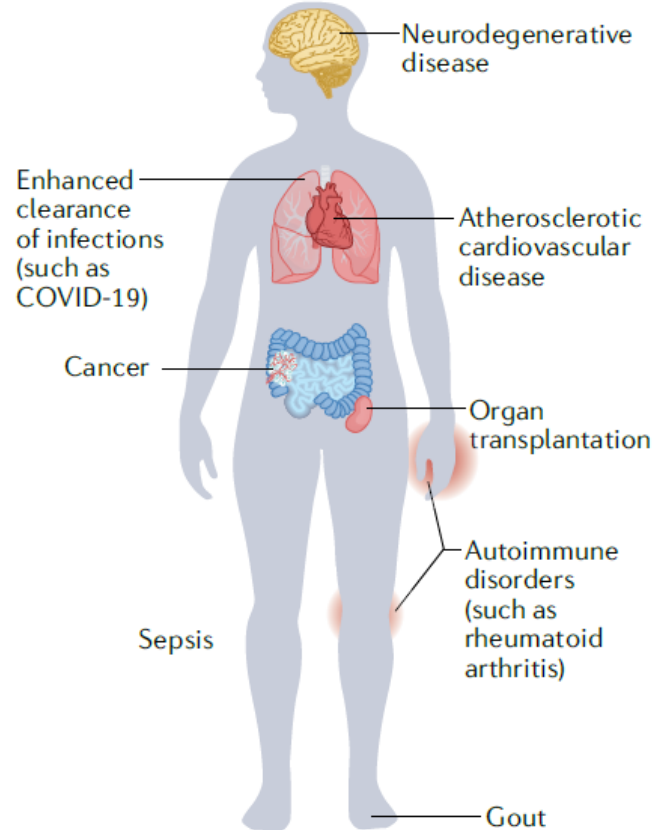
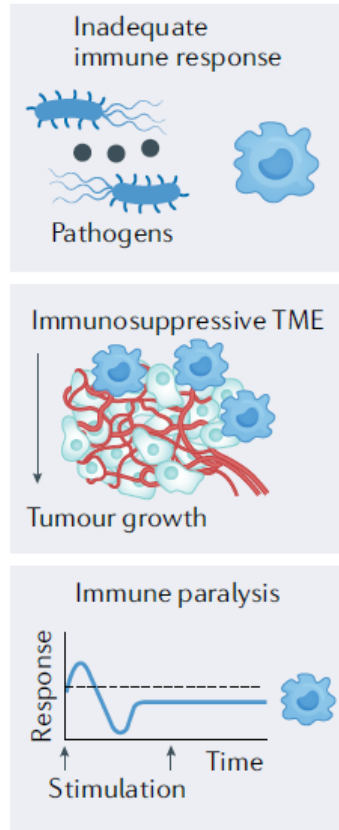
binds to IL-1 β . Insulin-like growth factor 1 receptor (IGF1R) recognizes extracellular mevalonate. **d** | Intracellular metabolic pathways that can be targeted include glycolysis⁴ (through interference with glycolytic enzymes or indirect through mechanistic target of rapamycin (mTOR) inhibition), cholesterol metabolism⁵⁴ (by targeting HMG CoA reductase), glutaminolysis⁶⁰ (through glutaminase inhibitors) and the tricarboxylic acid cycle (TCA) cycle (for example, by restricting succinate oxidation). **e** | H3K4me3 and H3K27ac are hallmark epigenetic signatures of trained immunity, which can be modified by targeting lysine demethylase (KDM), lysine methyltransferase (KMT), histone deacetylase (HDAC) and histone acetyltransferase (HAT) activity. Immune gene-priming long non-coding RNAs (IPLs) facilitate trimethylation of cytokine promoters⁶⁶. PI3K, phosphatidylinositol 3-kinase.

a**b**





Promotion of trained immunity



Inhibition of trained immunity

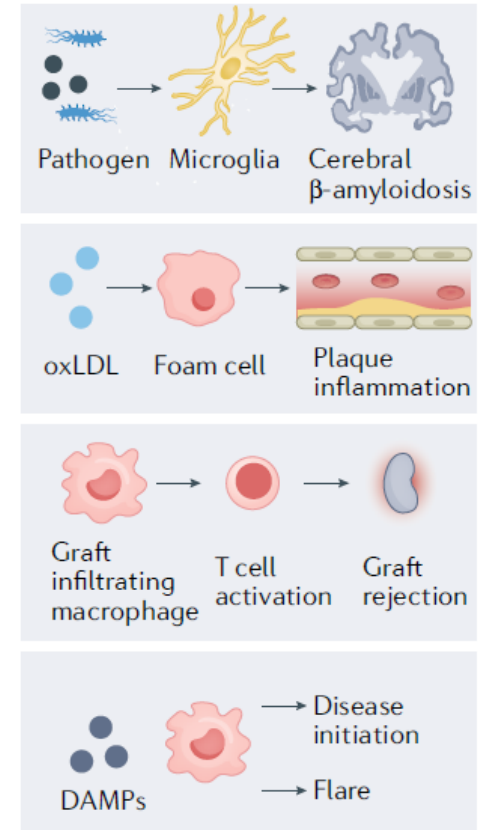
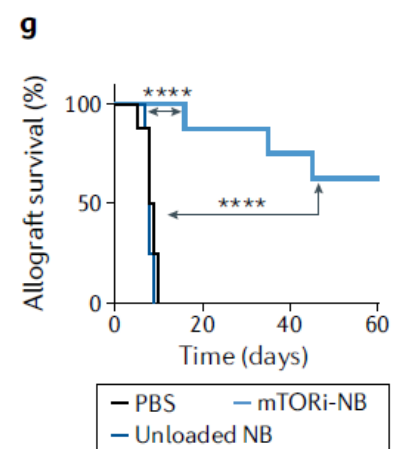
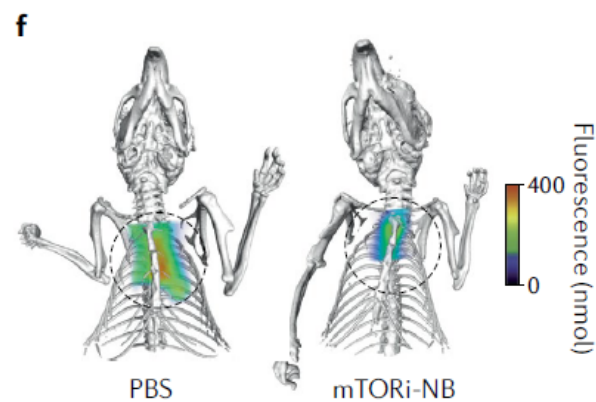
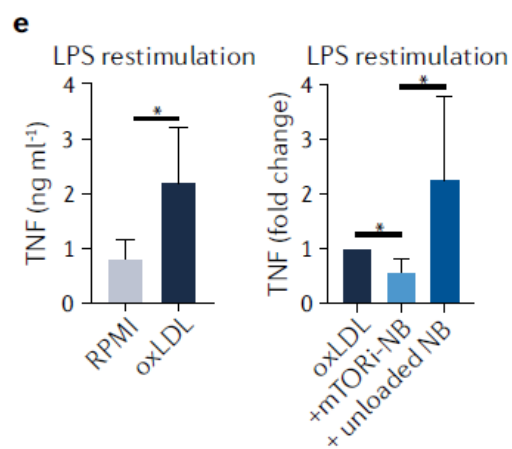
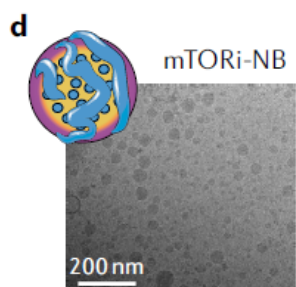
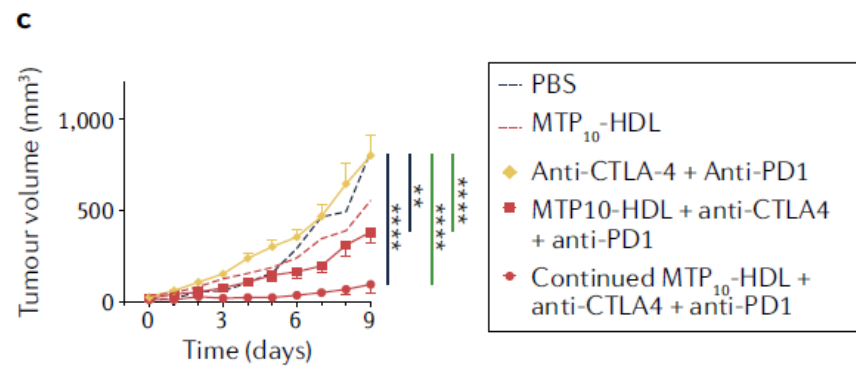
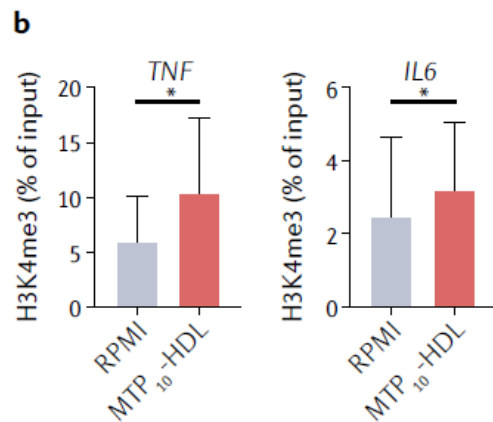
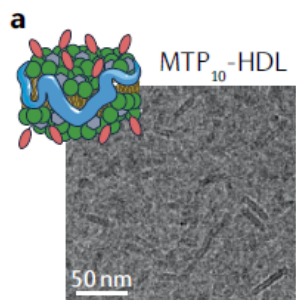
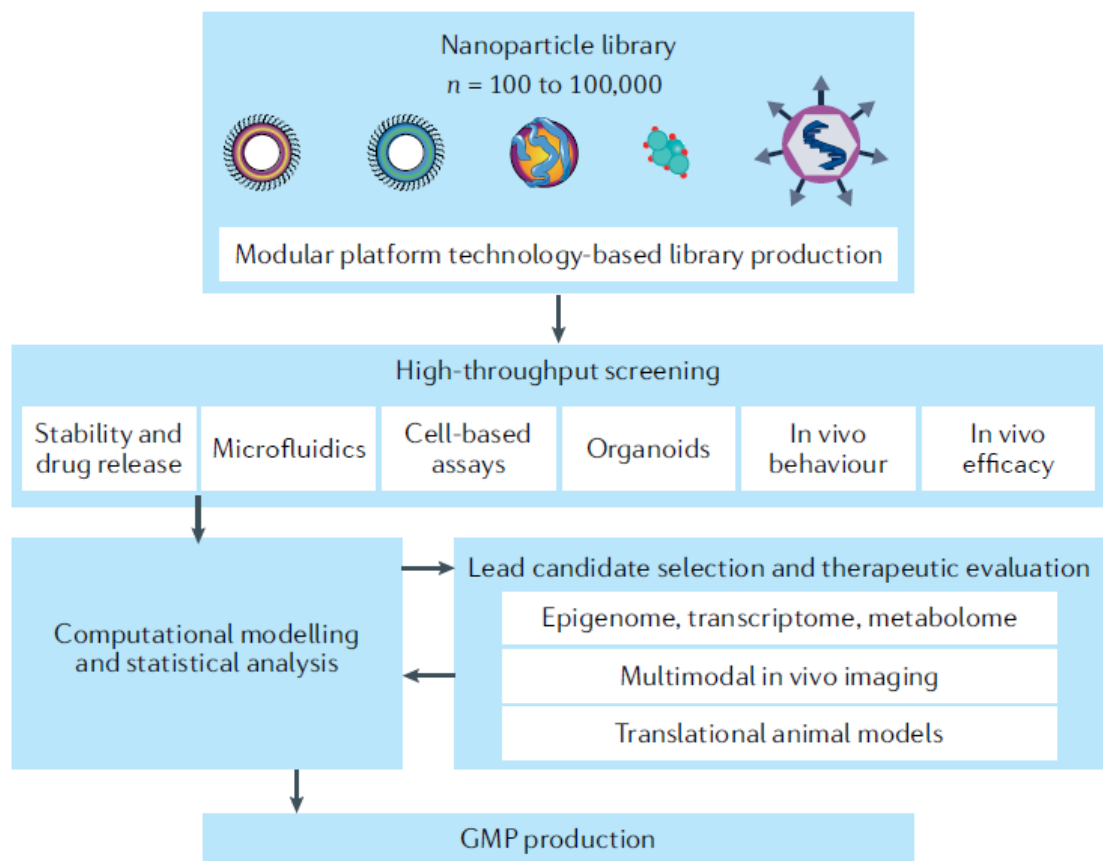


Fig. 4 | Trained-immunity-regulating nanotherapies in clinical scenarios. Trained immunity can be induced to combat cancer and increase resistance to infection, for example, against COVID-19, or trained immunity can be inhibited in conditions characterized by an exacerbated immune response. DAMP, damage-associated molecular pattern; oxLDL, oxidized low-density lipoprotein; TME, tumour microenvironment.





Nanomaterials for T-cell cancer immunotherapy

NATURE NANOTECHNOLOGY | VOL 16 | JANUARY 2021 | 25–36 | 5

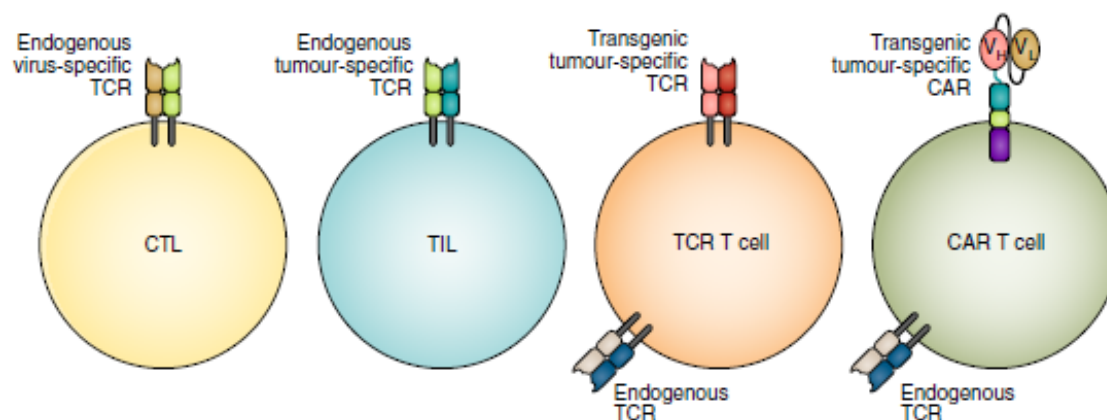


Fig. 1 | Classes of T cells deployed in ACT. Adoptive T-cell therapy makes use of either naturally occurring or redirected T cells. The naturally occurring T cells include CTLs against viral antigens for virus-induced cancers, or TILs for solid tumours. The redirected T cells are generated by the addition of a gene encoding a tumour-antigen-specific TCR or CAR. The antigen specificity of TILs is often not characterized but, where delineated, typically consists of a mix of populations targeting tumour-associated antigens, which are upregulated self-antigens found at lower levels in healthy tissues, cancer germline antigens, which are normally only expressed in the gonads or during foetal development, and neoepitopes, which are cancer-specific mutations. While TIL therapy can achieve excellent clinical responses, the TILs must be isolated from surgically resected tumour biopsies, which is not feasible in many indications. When bulk T cells from the peripheral blood or cord blood, or derived from induced pluripotent stem cells are redirected by addition of a transgenic receptor, the endogenous TCR may be deleted using gene editing tools if doing so enhances the activity of the T-cell product or improves the safety profile. Therapeutic T cells encoding both a tumour-antigen-specific TCR and a CAR have been reported. V_H , variable domain of heavy chain; V_L , variable domain of light chain.

| Table 1 Characteristics of the T cells used for ACT | | | | |
|---|---|--|--|---|
| | CTL | TIL | TCR-T | CAR T |
| Source | Isolated from healthy donors sharing relevant MHC alleles. | Isolated from patient's own tumour. | Manufactured from autologous or allogeneic peripheral blood T cells, cord blood T cells or iPSC-derived T cells. | |
| Specificity | EBV, CMV or HPV antigens. | Mixed population with various specificities. | Single tumour antigen. | Single or multiple tumour antigens depending on design. |
| Target type | TCR binds peptide from target antigen presented in complex with self MHC molecule. | | | CAR binds antigen directly. |
| Target location | Antigen can be expressed in any subcellular location since the antigen presentation pathway will result in surface-expressed peptide-MHC complexes. | | | Cell surface or secreted targets only. |
| Pros | Safety | Safety, efficacy | Evidence for activity in solid cancers. | HLA independence |
| Cons | Virus-driven tumours only. | Difficult to manufacture. Not feasible for many tumours. | Few patients express both antigen and correct HLA allele. | Few responses in solid cancers thus far. |
| EBV, Epstein-Barr virus; CMV, cytomegalovirus; HPV, human papillomavirus; HLA, human leukocyte antigen. | | | | |

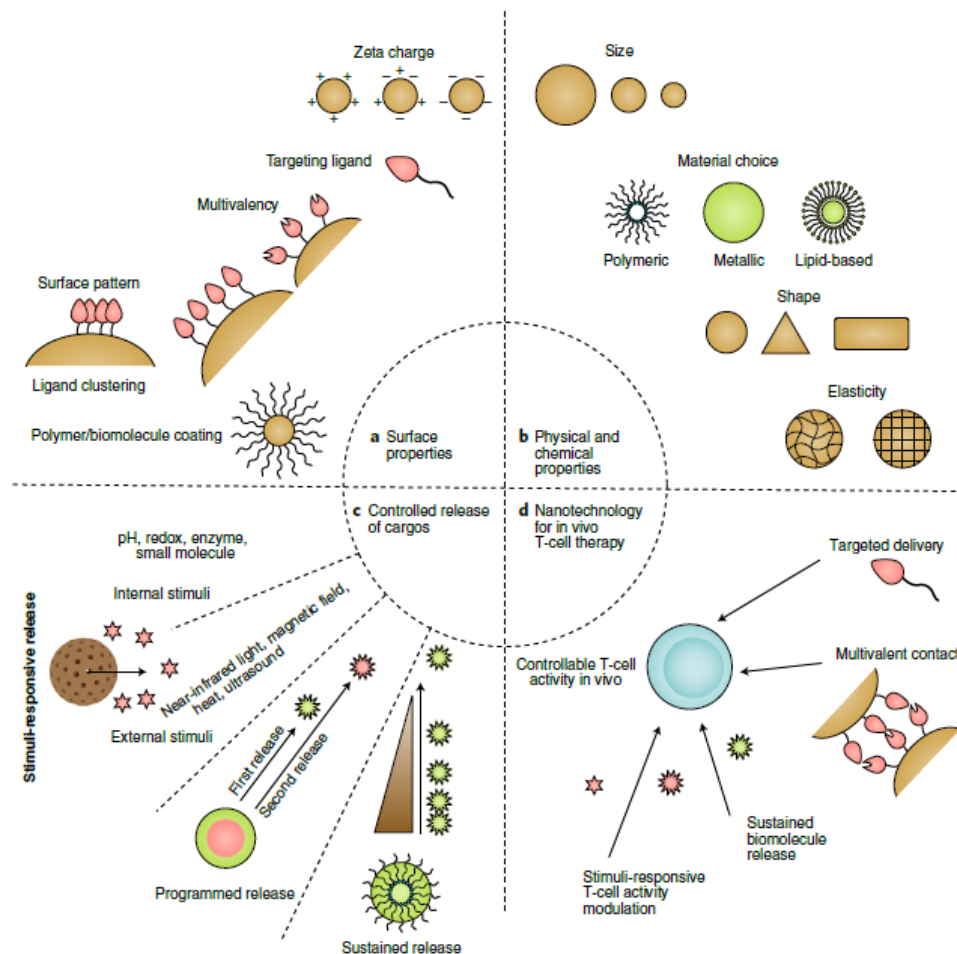


Fig. 2 | The current nanomaterial toolbox can be applied to in vivo T-cell therapies. a-c, Current strategies for expanding the functionalities of nanotechnologies include surface characteristics (a), physicochemical properties (b) and encapsulation and release features (c) of nanomaterials. **d,** Nanomaterials with optimized features could greatly benefit future T-cell cancer immunotherapies in vivo.

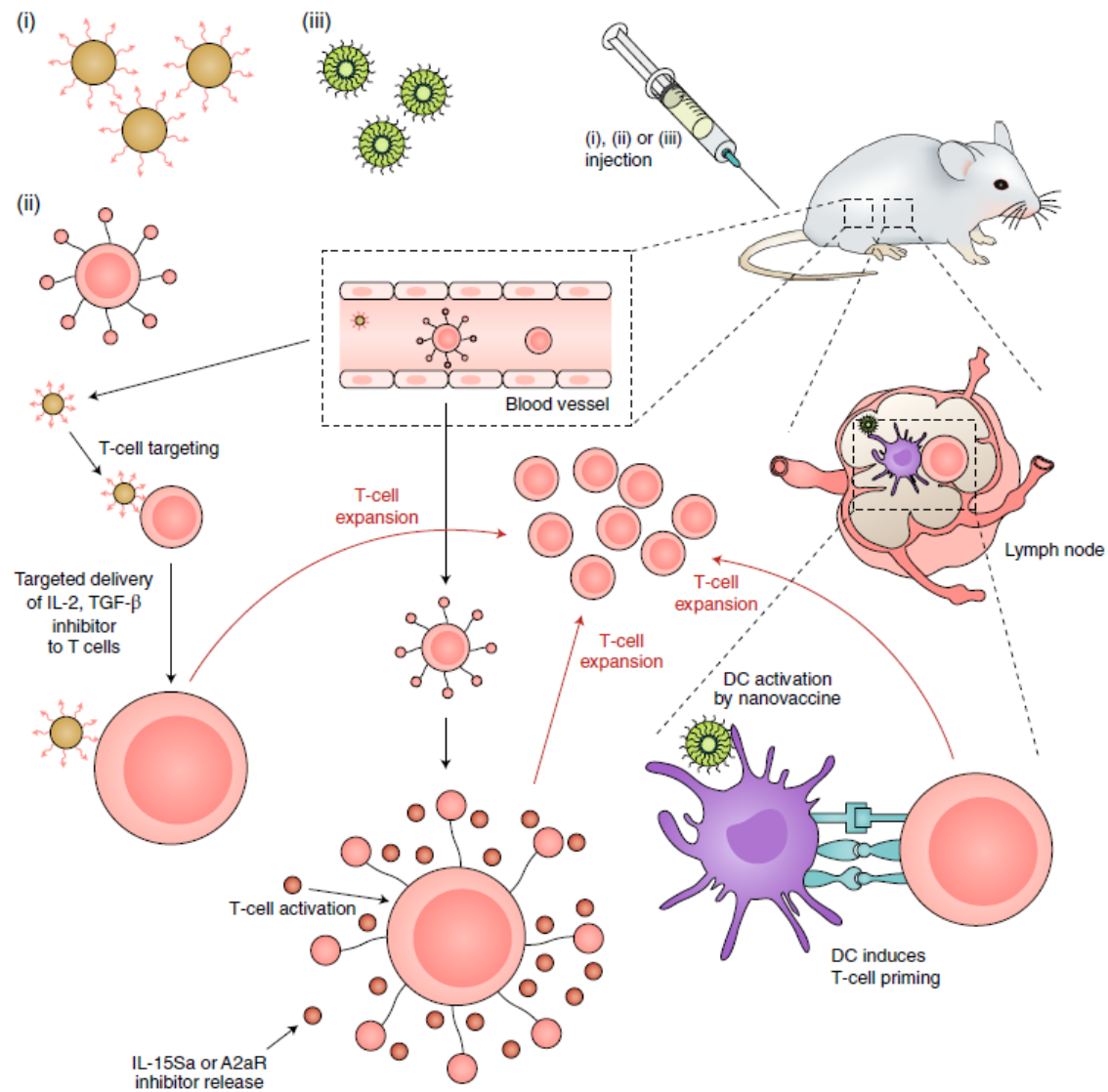


Fig. 3 | Nanomaterials for in vivo T-cell expansion. Nanomaterials can be designed for targeted delivery to T cells and induce T-cell activation and expansion in vivo (i). Backpacking nanoparticles are attached to the T-cell surface and release their cargo of stimulatory cues in response to environmental or applied stimuli, leading to precise control over the expansion of T cells in vivo (ii). Vaccine nanoparticles that target antigen-presenting cells, such as DCs, can activate these cells and induce T-cell expansion in vivo (iii).

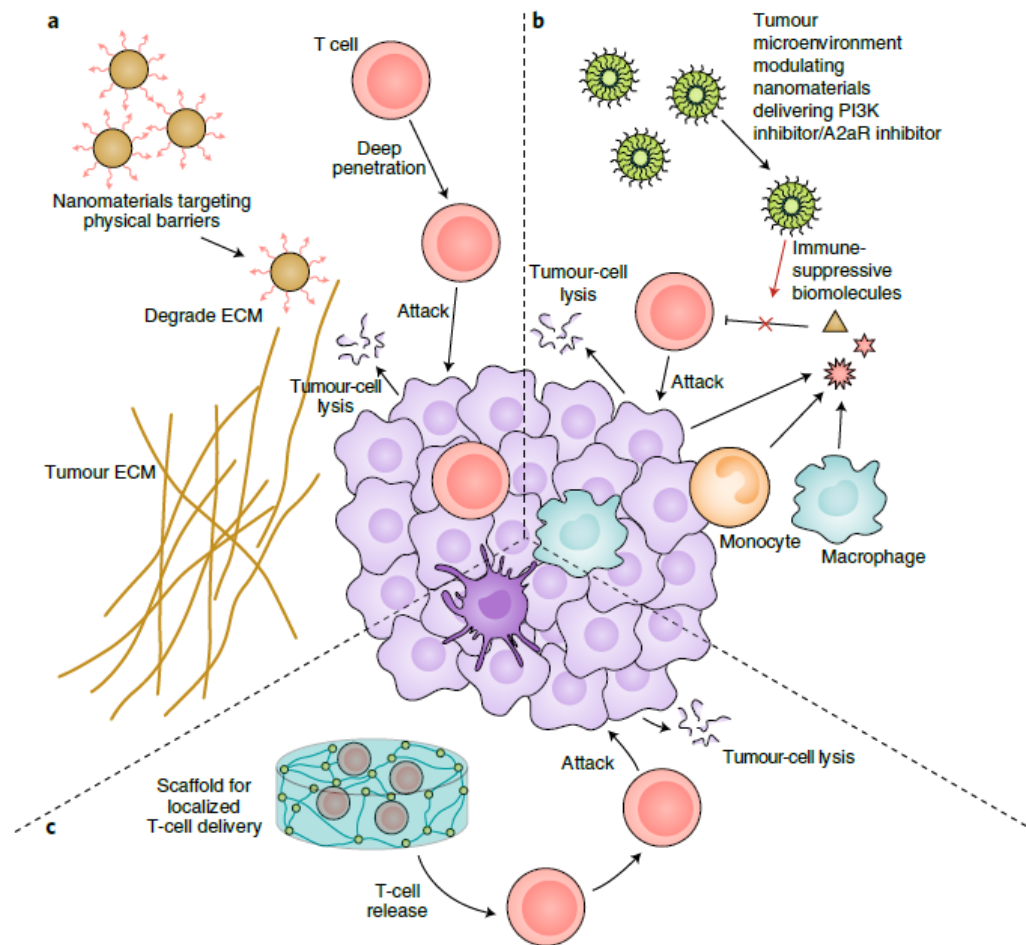


Fig. 4 | Nanomaterials overcome physical barriers and immune-suppressive environments for T-cell therapy. **a**, Nanomaterials can be designed to target the ECM and degrade the physical barriers inhibiting T-cell penetration and tumour cell targeting. **b**, Nanomaterials targeting the tumour microenvironment can deliver stimulatory cues to the tumour tissue and reverse the suppressive tumour microenvironment (immunological barrier), thus activating T-cell activity. **c**, Nanomaterials can locally deliver T cells directly to the tumour tissue with sustained release, which enhances tumour cell killing.

Table 2 | Preclinical and clinical studies of nanomaterials-based T-cell cancer immunotherapies

| Nanomaterials | Cargo molecules | Model/indication | Stage | |
|--|---|---|-------------------------------------|-----------------------------|
| Nanomaterials for T-cell expansion in vivo | T-cell-targeted delivery | | | |
| | Poly(beta-amino ester)-based nanomaterial | Plasmids encoding a 194-1BBz CAR and a piggyBac transposase | TBD | Phase 1 projected 2020–2021 |
| | Liposome | IL-2-Fc fusion protein | Mouse melanoma | Preclinical |
| | Liposome | TGF-β inhibitor (SB525334) | Mouse melanoma | Preclinical |
| | PLGA-PEG nanomaterial | TGF-β receptor inhibitor (SD-208) | Mouse colon cancer | Preclinical |
| | T-cell (Treg)-targeted hybrid nanomaterial | STAT3/STAT5 pathway inhibitor (imatinib) | Mouse melanoma | Preclinical |
| | Iron nanomaterial | Anti-CD137 and anti-PD-L1 | Mouse melanoma | Preclinical |
| | Liposome-coated polymeric gel | Mouse IL-2 and a TGF-β inhibitor (SB505124) | Mouse melanoma | Preclinical |
| | Backpacking nanomaterials | | | |
| | IL-15 superagonist complex nanogel | IL-15 superagonist complex | Various solid tumours and lymphomas | Phase 1 |
| | Multilamellar liposomal vesicles | A2a adenosine receptor inhibitor (SCH-58261) | Mouse model of human ovarian cancer | Preclinical |
| | Nanomaterials-based vaccines | | | |
| | Amphiphile ligands (EGFRvIII peptide-conjugated DSPE-PEG) | NA | Mouse glioma expressing EGFRvIII+ | Preclinical |
| | Lipid nanomaterial | mRNA encoding the tight junction protein claudin 6 (CLDN6) | Mouse melanoma expressing CLDN6 | Preclinical |

| | | junction protein claudin 6 (CLDN6) | expressing CLDN6 | | |
|--|--|--|--|-------------|-----|
| Nanomaterials overcome physical barriers and hostile tumour microenvironments | Nanomaterials that target physical barriers | | | | |
| | PLGA nanomaterial | Photothermal agent indocyanine green | Mouse melanoma | Preclinical | 104 |
| | Calcium phosphate nanomaterials with lipid bilayer coating | An antifibrotic compound α -mangostin and a plasmid encoding the stimulatory cytokine LIGHT | Mouse pancreatic cancer | Preclinical | 59 |
| | Nanomaterials that reverse the immune-suppressive environment | | | | |
| | Lipid nanomaterial | A PI3K inhibitor (PI-3065) and a T-cell stimulator (7DW8-5) | Mouse breast cancer | Preclinical | 61 |
| | Multilamellar liposomal vesicles | A2a adenosine receptor inhibitor (SCH-58261) | Mouse model of human ovarian cancer | Preclinical | 93 |
| | Nanomaterials for local T-cell delivery | | | | |
| | Macroporous alginate scaffolds | IL-15 superagonists, antibodies for CD3, CD28 and CD137 | Mouse breast cancer, mouse ovarian cancer | Preclinical | 60 |
| Nanomaterials as NBiTEs | Nickel-titanium alloys | Antibodies for CD3, CD28, CD137 | Mouse model of human pancreatic cancer expressing receptor tyrosine kinase-like orphan receptor (ROR1) | Preclinical | 111 |
| | Liposome | Human epidermal growth factor receptor 2 (HER2) and CD20 antibodies | Mouse breast cancer | Preclinical | 131 |
| | Polystyrene nanomaterial | Antibodies for HER2 and calreticulin protein | Mouse breast cancer | Preclinical | 132 |
| | Exosome | Exosome expressing antibodies for CD3 and epidermal growth factor receptor (EGFR) | Mouse breast cancer | Preclinical | 58 |
| TBD, to be determined; NA, not applicable; LIGHT, tumour necrosis factor superfamily 14. | | | | | |

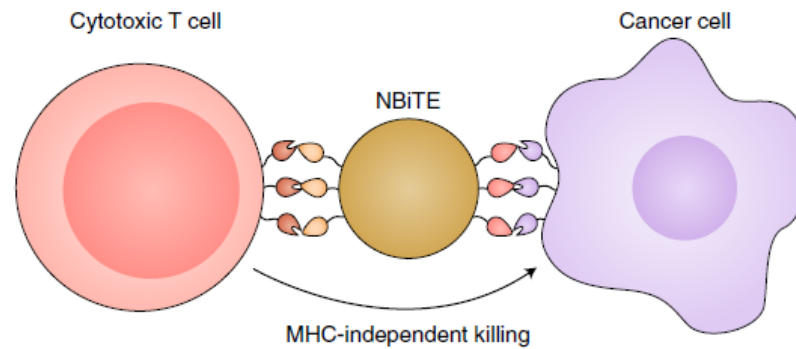
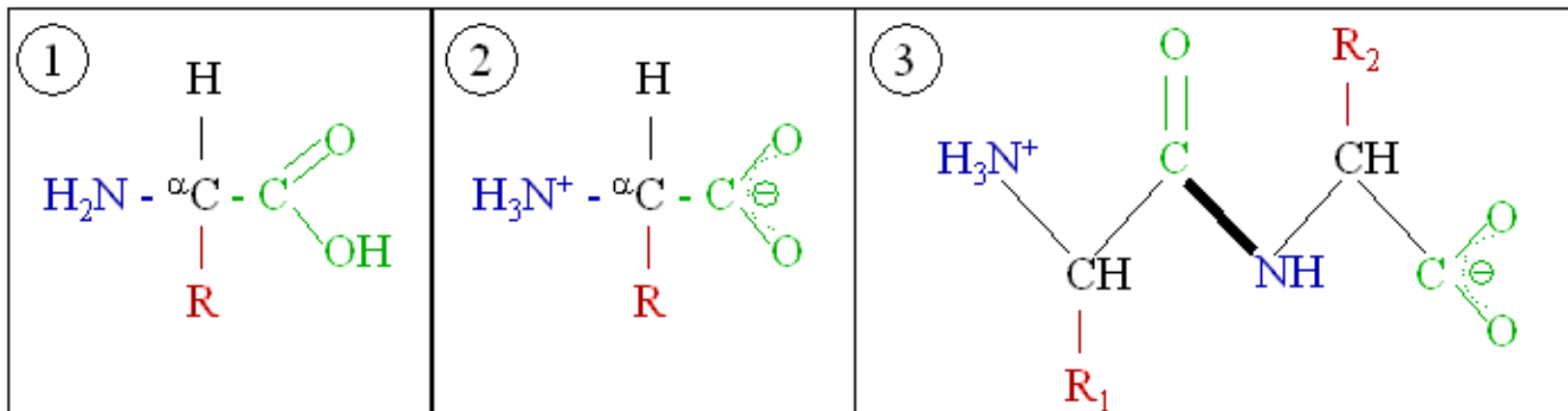
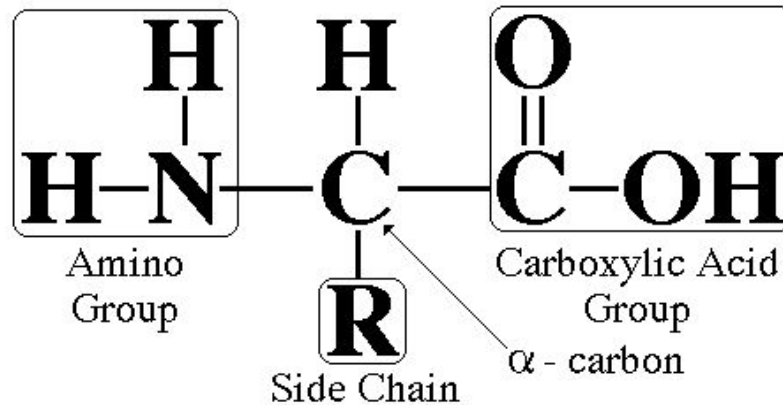


Fig. 5 | NBIETs for cancer immunotherapy. A typical NBIET is developed by adding two scFvs on the nanoparticle surface, with one scFv targeting a T-cell-specific antigen while the other targets a tumour-specific antigen. The multivalent contact at the nanomaterial/cell interfaces makes NBIETs bridge T cells and tumour cells more effectively than traditional BiETs and induces potent tumour cell killing.

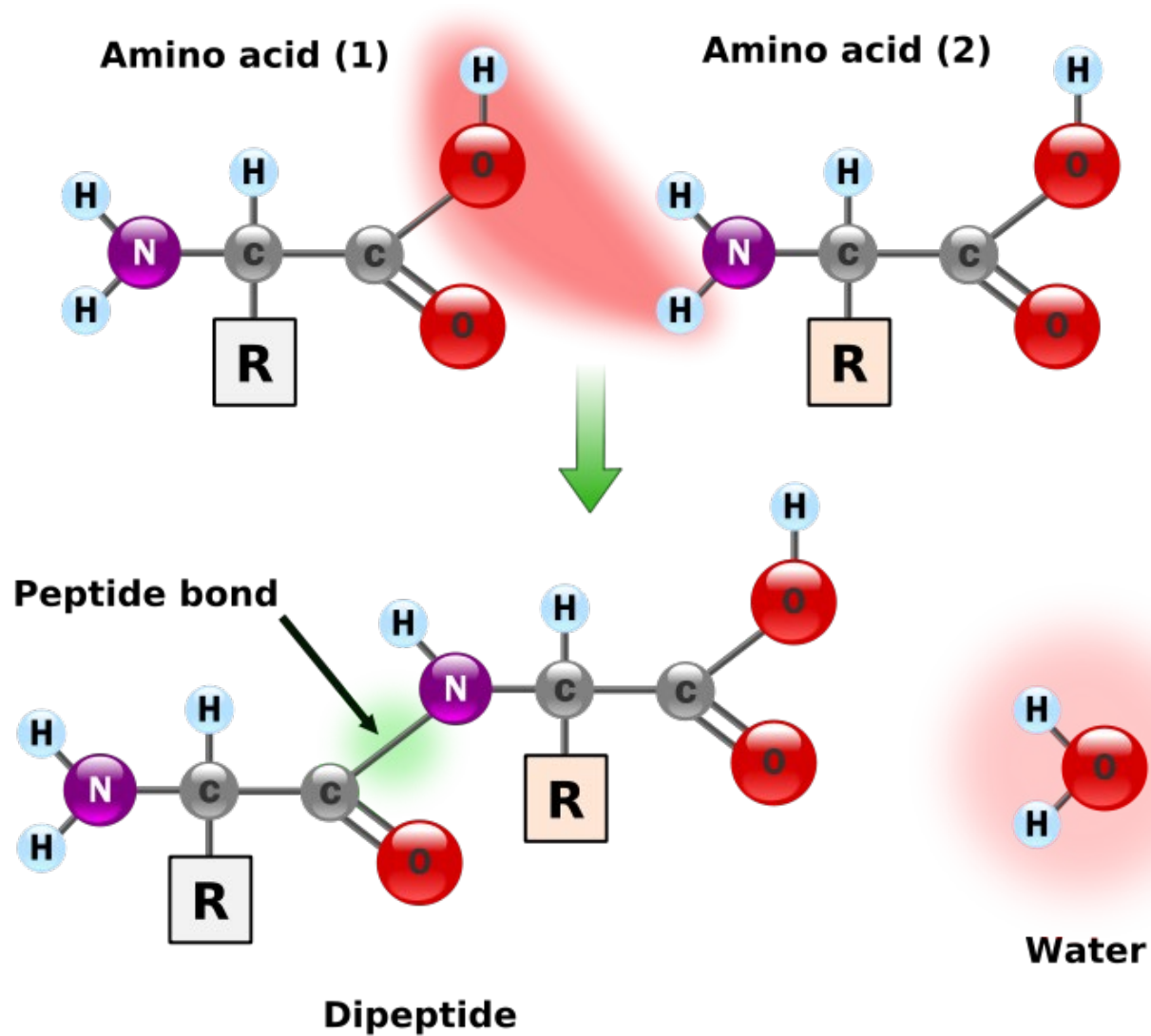
Review

Amino Acid

Amino Acid Structure



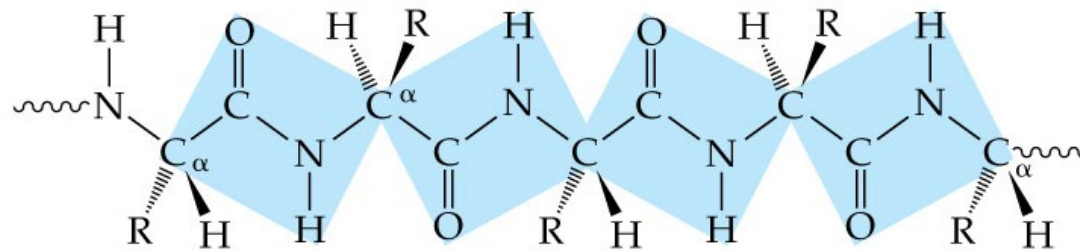
Peptide bond



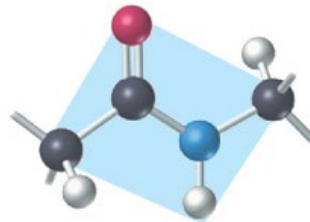
Primary Protein Structure

- Primary structure of a proteins is the sequence of amino acids connected by **peptide bonds**. Along the backbone of the proteins is a chain of alternating peptide bonds and α -carbons and the amino acid side chains are connected to these

Planar units along a protein chain



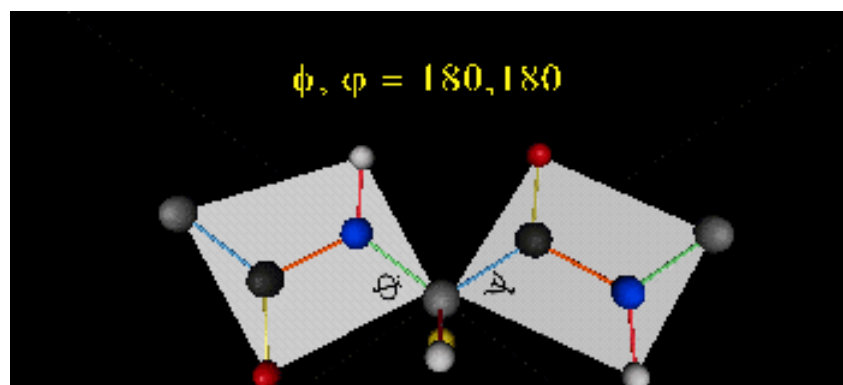
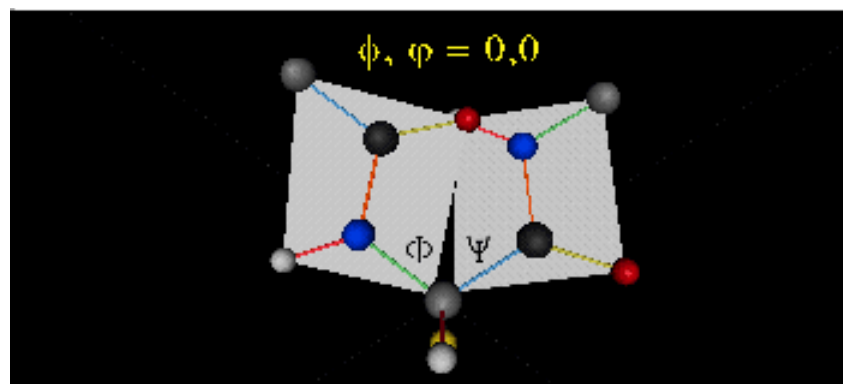
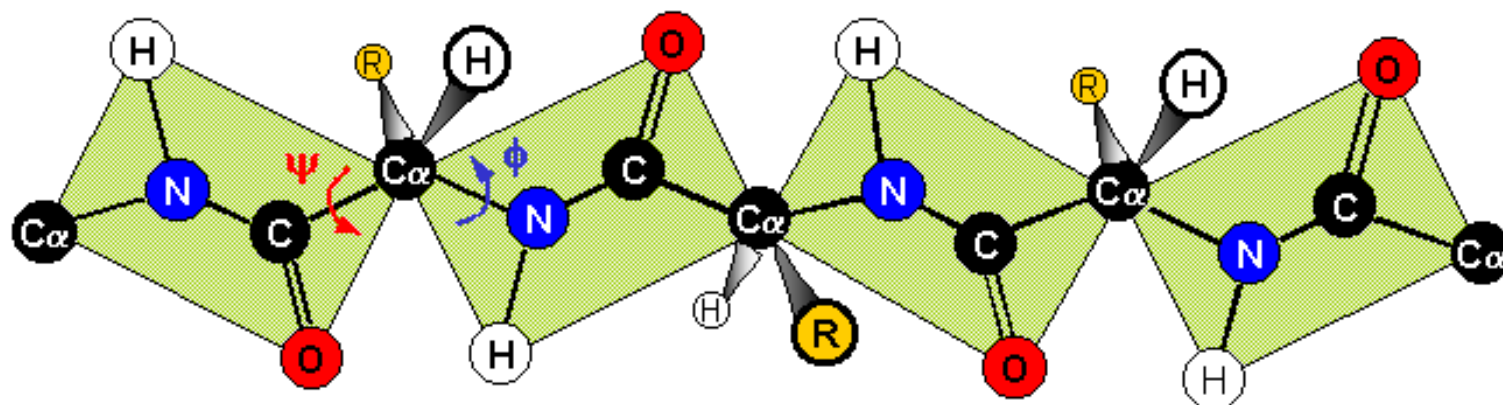
One planar unit



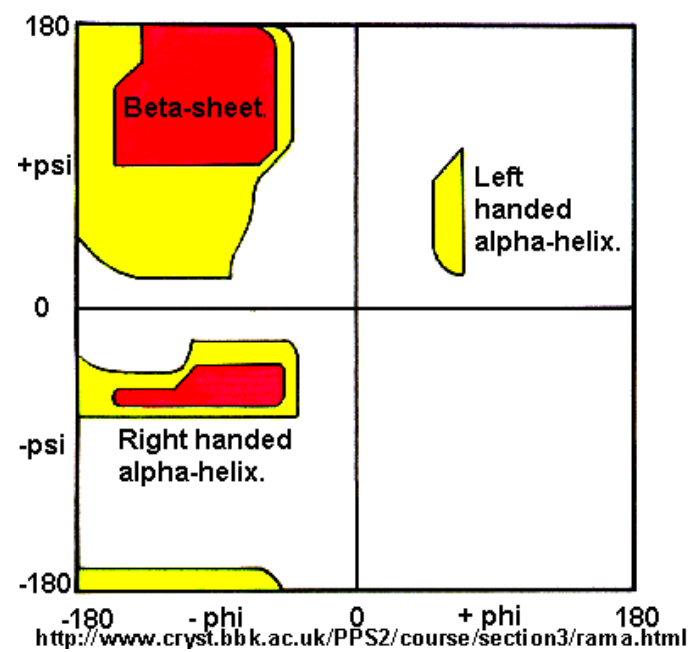
Secondary Protein Structure

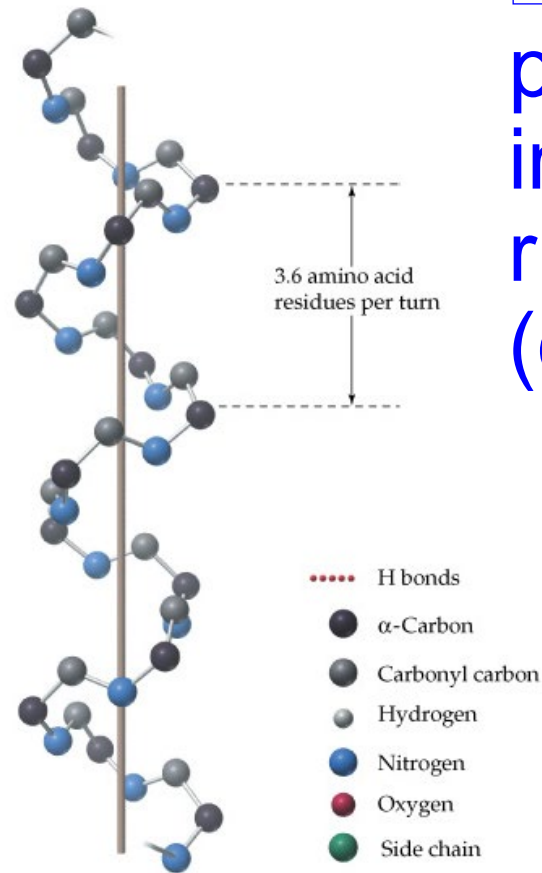
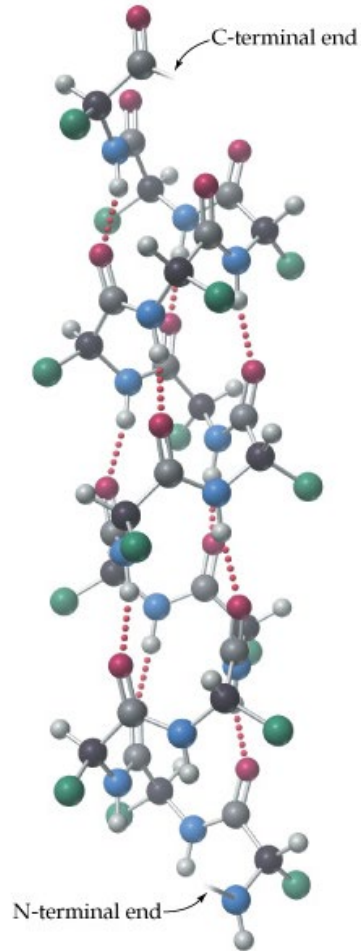
- Secondary structure of a protein is the arrangement of polypeptide backbone of the protein in space. The secondary structure includes two kinds of repeating pattern known as the *α -helix and β -sheet*.
- Hydrogen bonding between backbone atoms are responsible for both of these secondary structures.

FULLY EXTENDED POLYPEPTIDE CHAIN



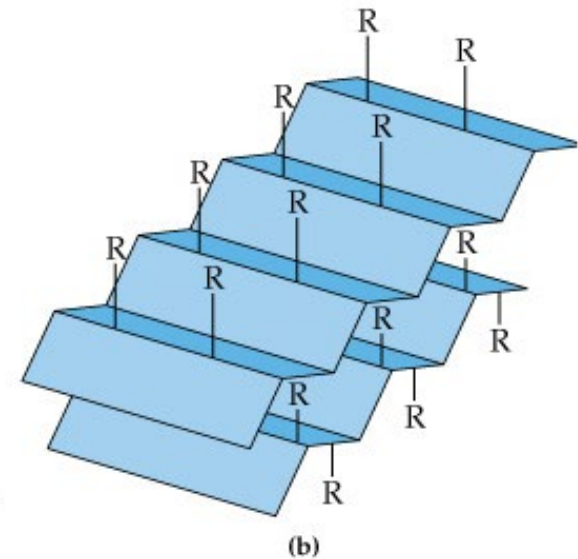
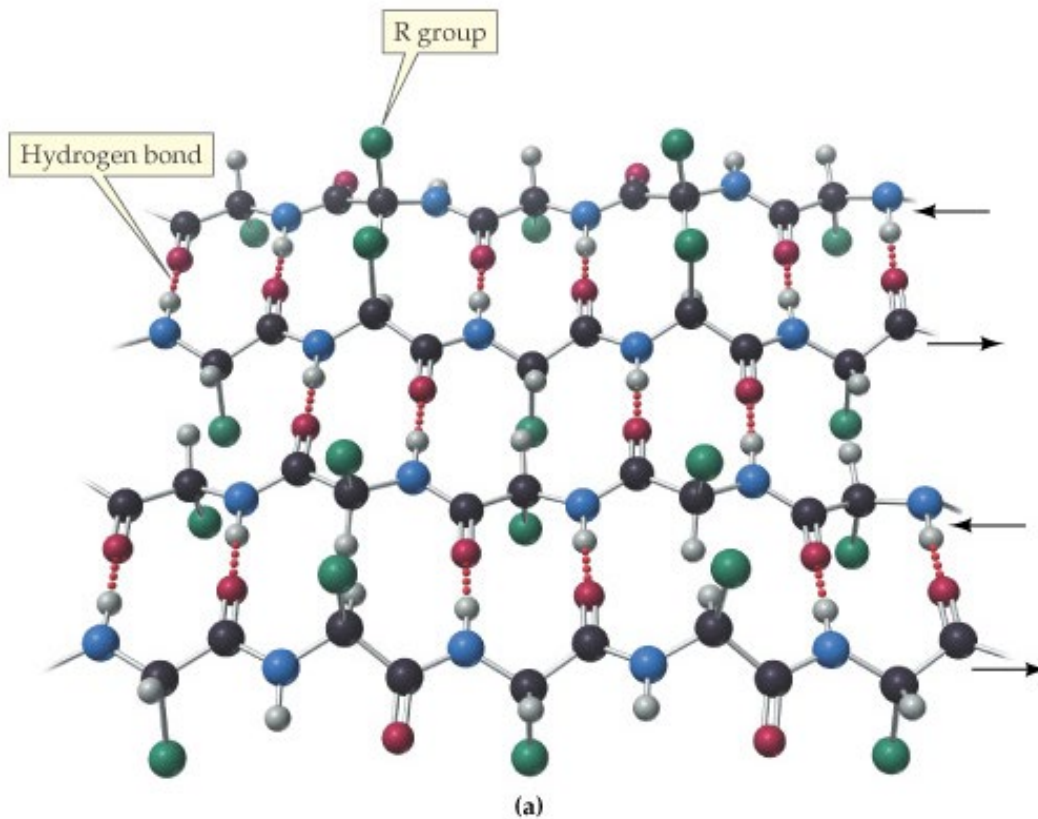
The Ramachandran Plot.





□ ***α -Helix:*** A single protein chain coiled in a spiral with a right-handed (clockwise) twist.

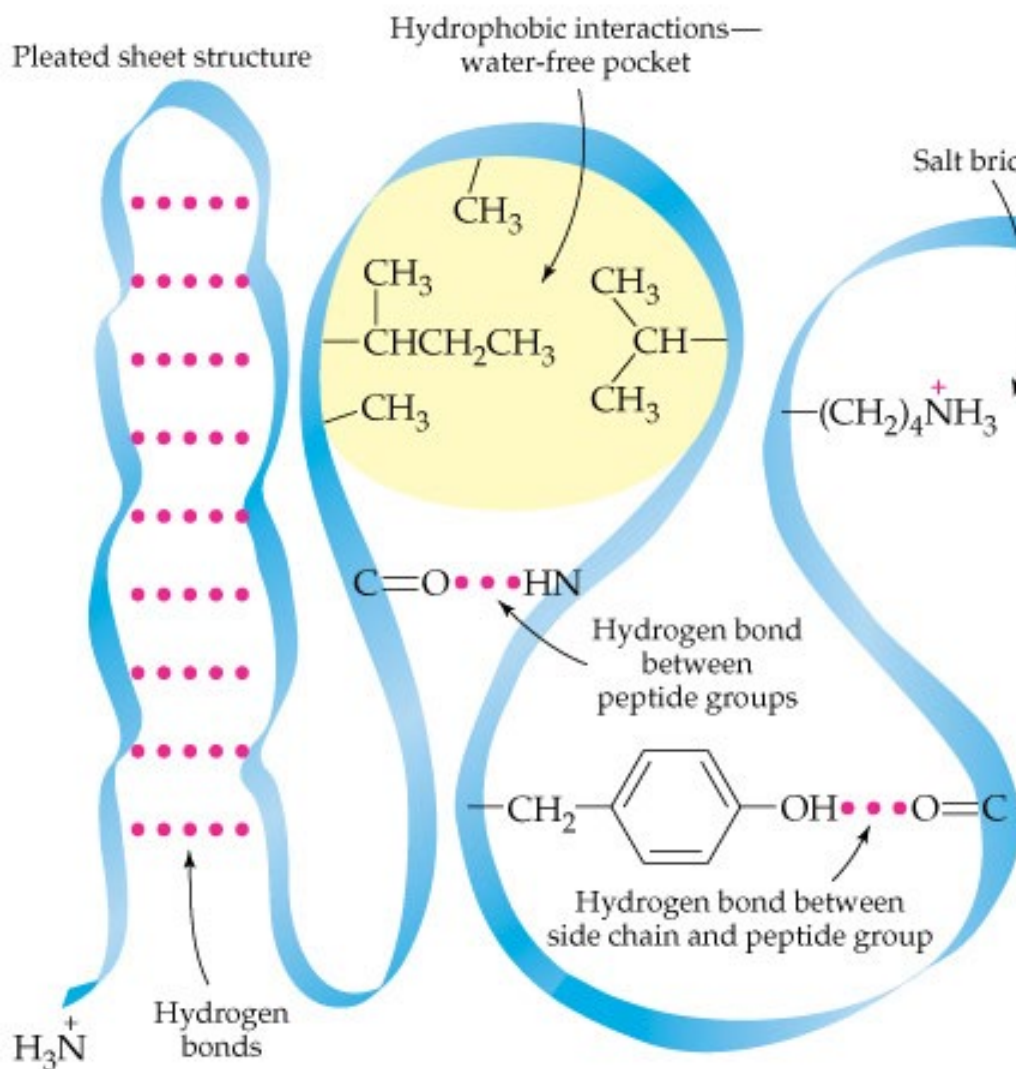
□ ***β-Sheet***: The polypeptide chain is held in place by hydrogen bonds between pairs of peptide units along neighboring backbone segments.



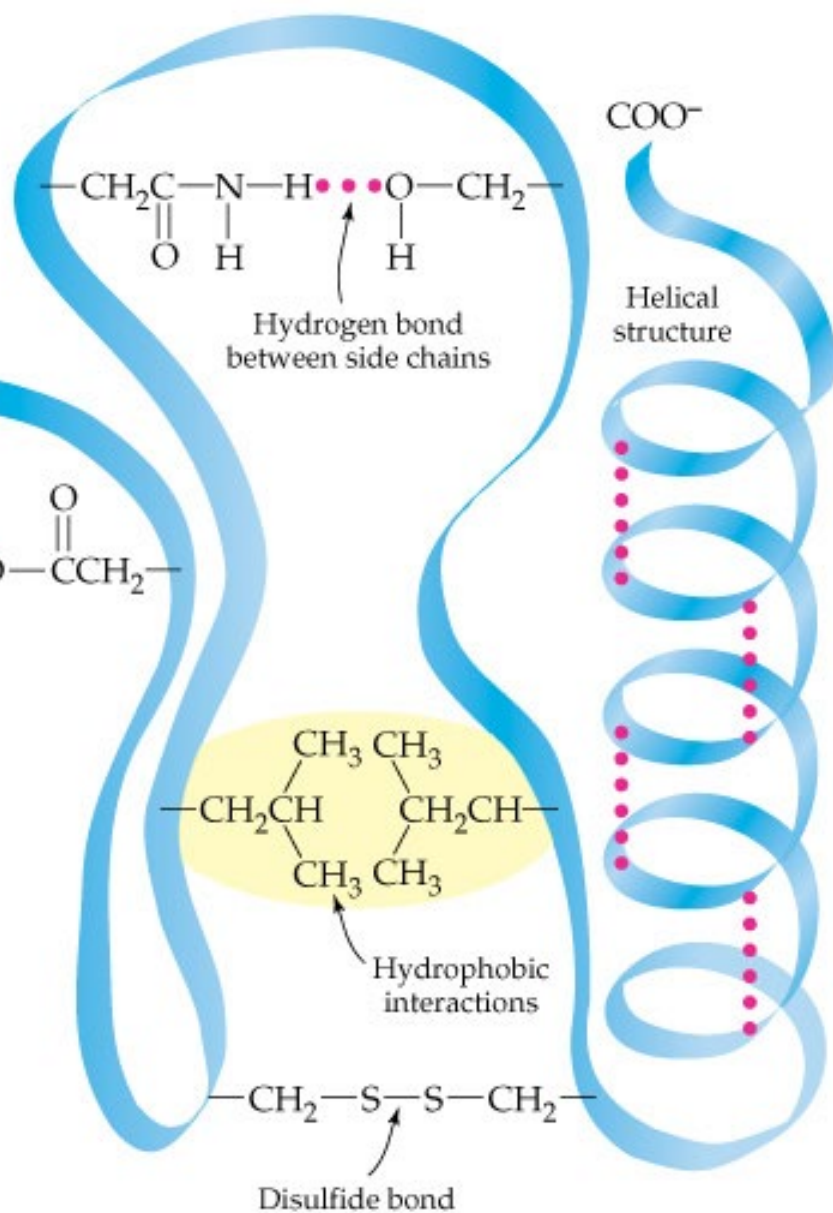
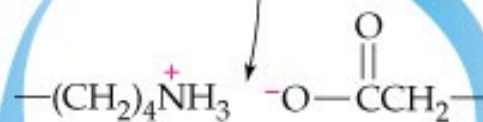
Tertiary Protein Structure

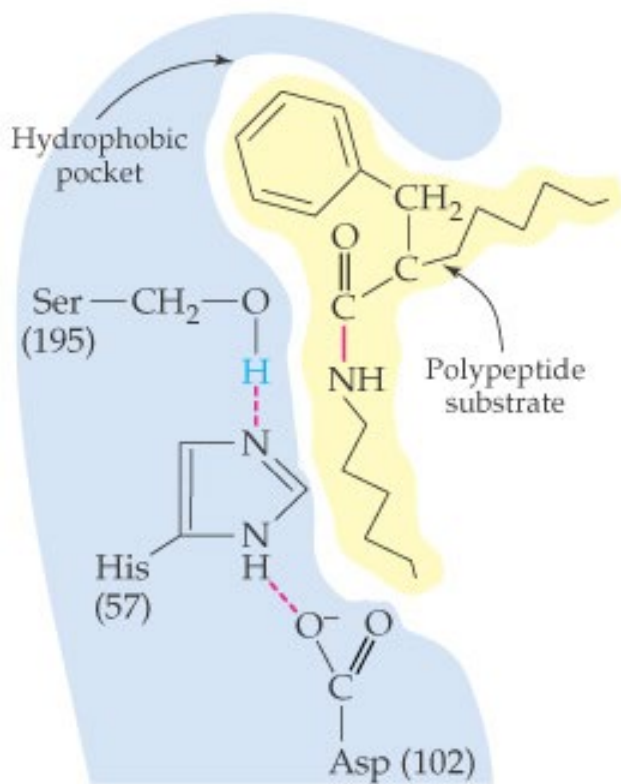
- ***Tertiary Structure of a proteins*** The overall three dimensional shape that results from the folding of a protein chain. Tertiary structure depends mainly on attractions of amino acid side chains that are far apart along the same backbone. **Non-covalent interactions and disulfide covalent bonds** govern tertiary structure.
- A protein with the shape in which it exist naturally in living organisms is known as a ***native protein***.

Pleated sheet structure

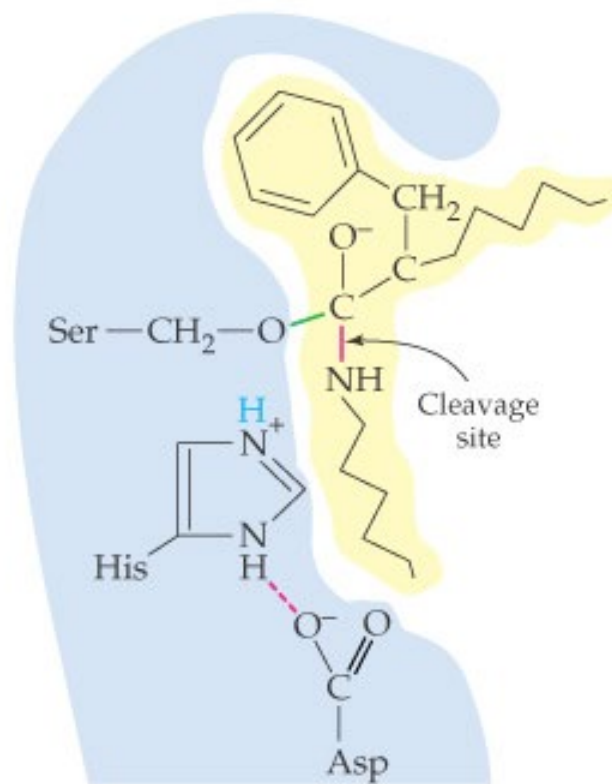


Salt bridge

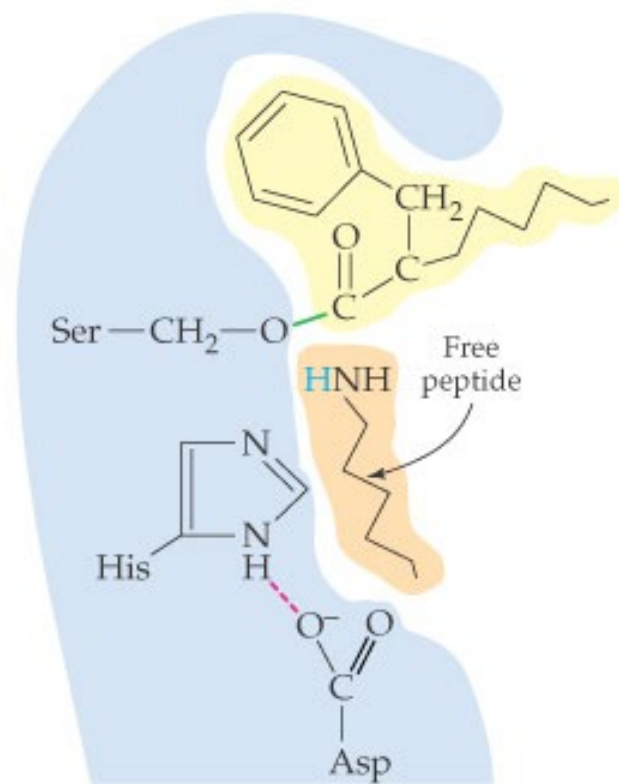




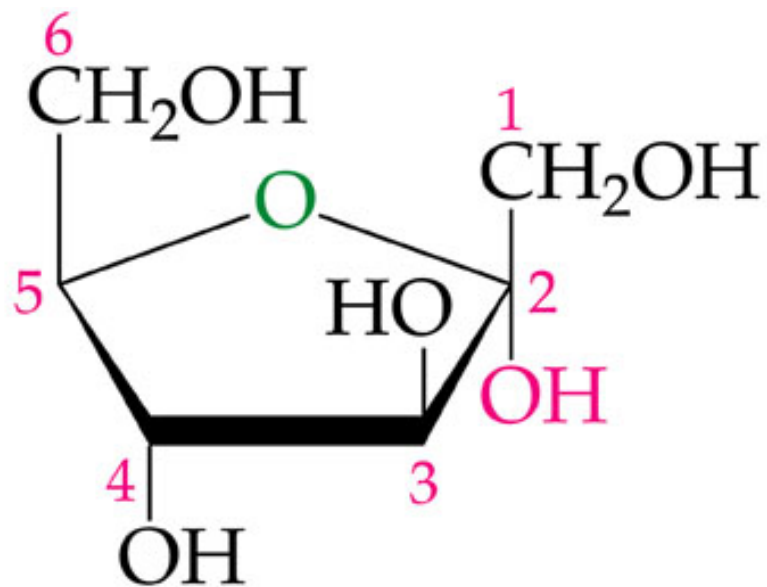
(a)



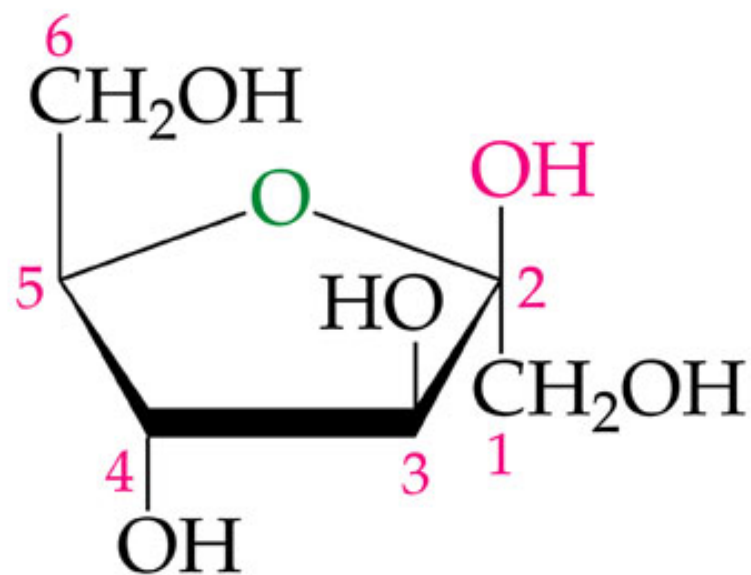
(b)



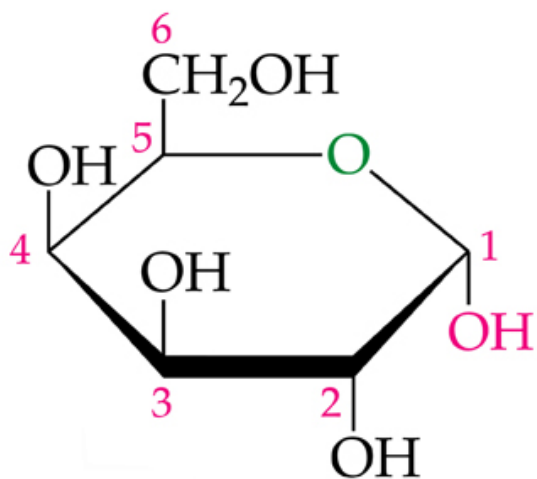
(c)



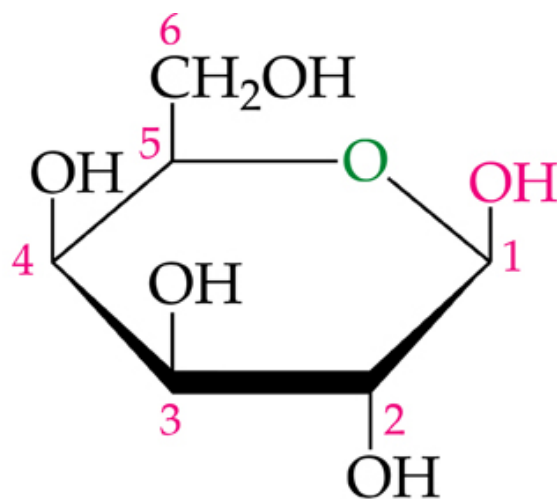
α -D-Fructose



β -D-Fructose

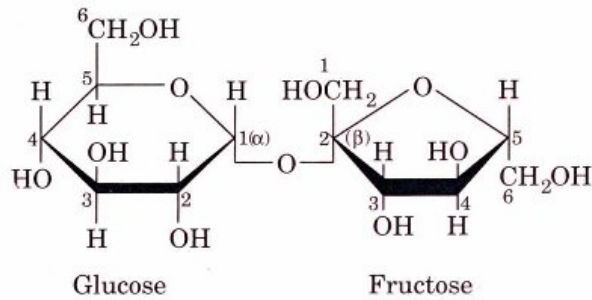


α -D-Galactose

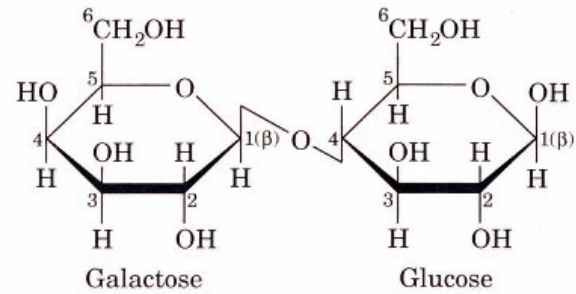


β -D-Galactose

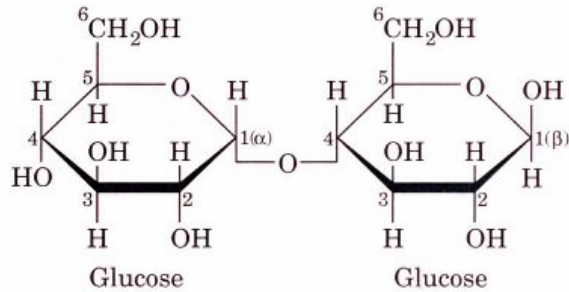
Some Common Disaccharides



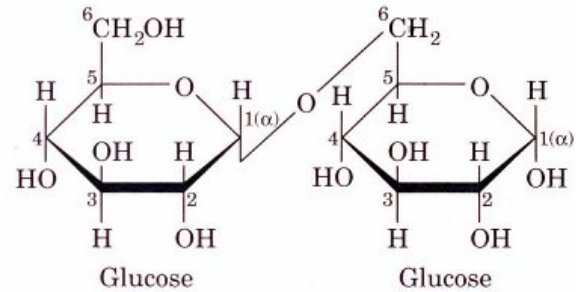
Sucrose



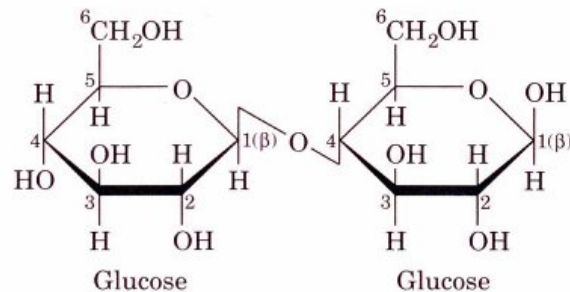
Lactose



Maltose

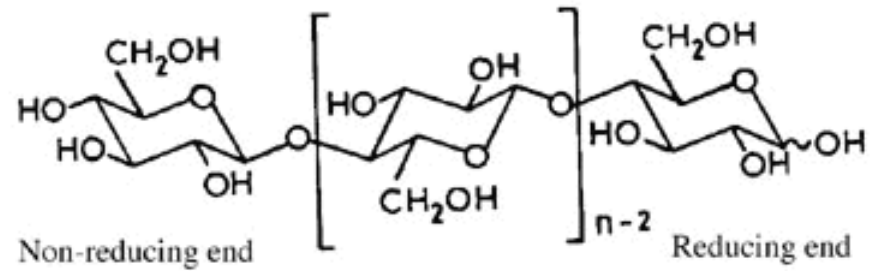
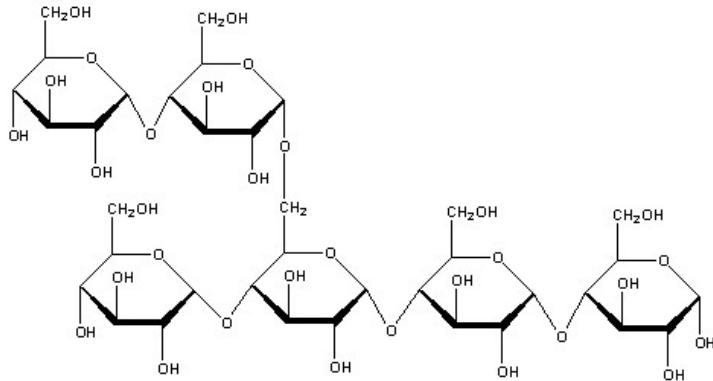


Isomaltose

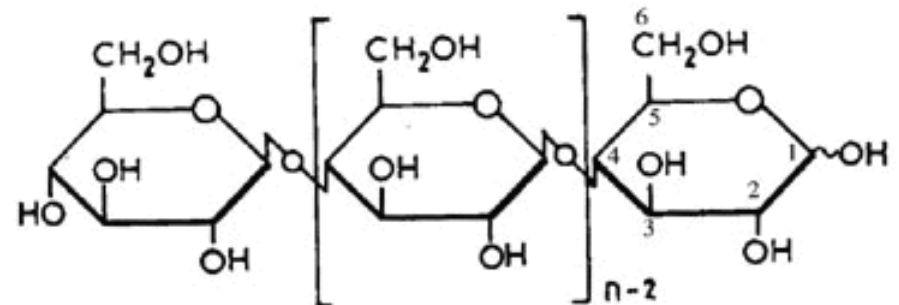
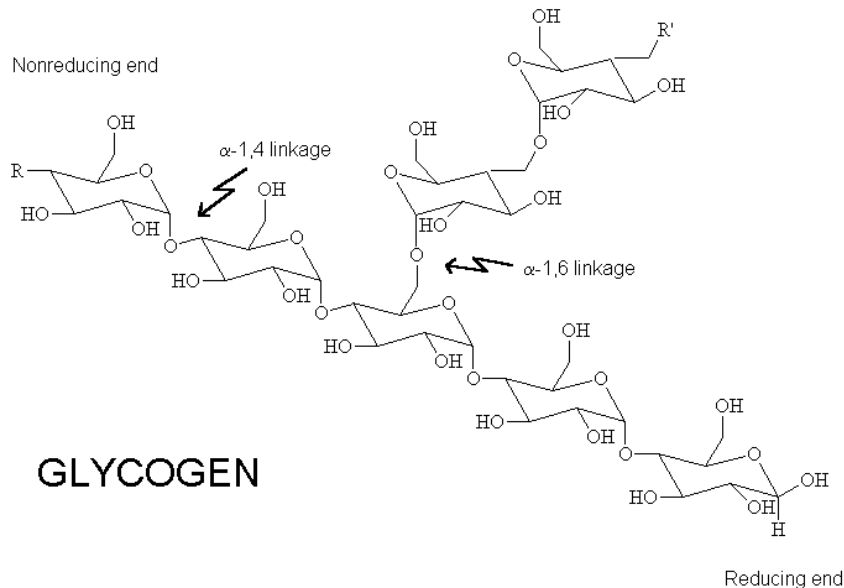


Cellobiose

Polysaccharides

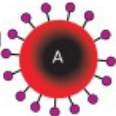
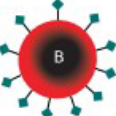
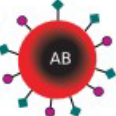










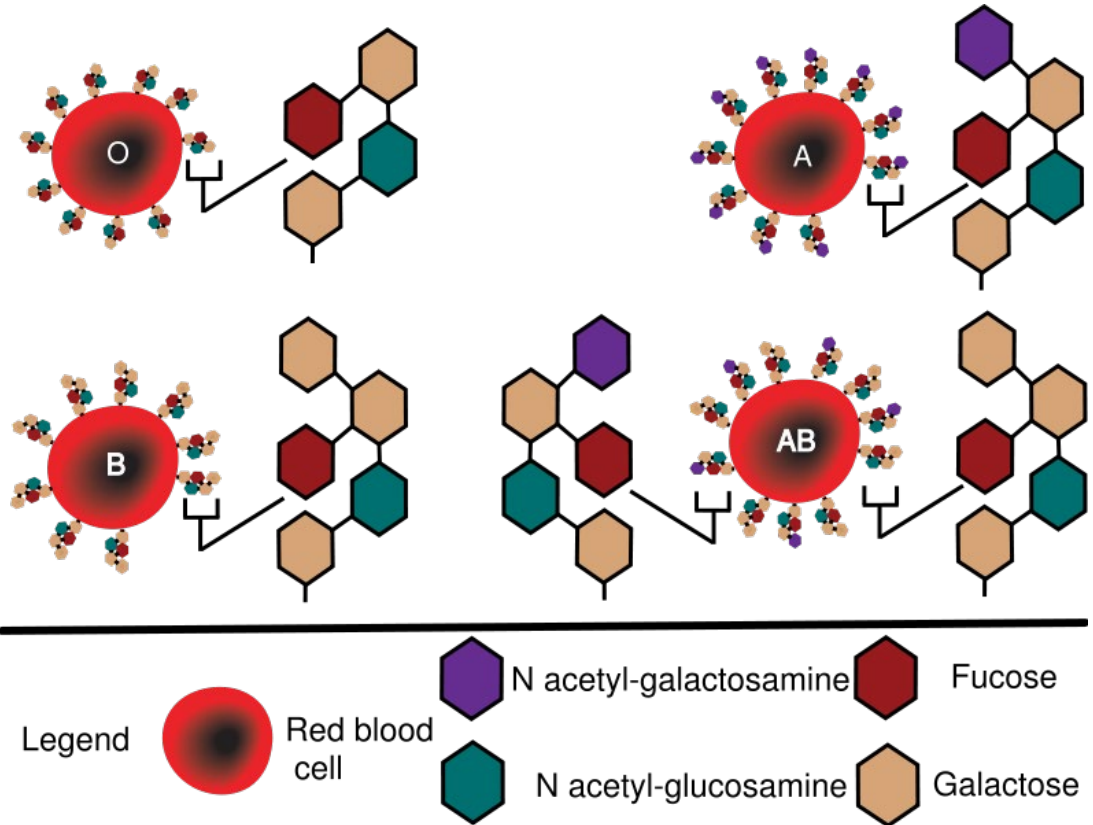
Sometimes shown as



Cellulose

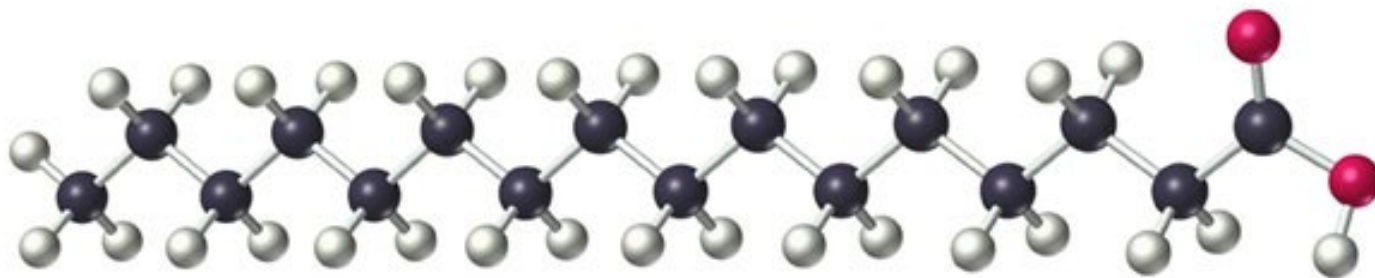
Blood Type

| | Group A | Group B | Group AB | Group O |
|---------------------|--|--|---|--|
| Red blood cell type |  |  |  |  |
| Antibodies present |  Anti-B |  Anti-A | None |  Anti-A and Anti-B |
| Antigens present | A antigen  | B antigen  | A and B antigens   | No antigens |

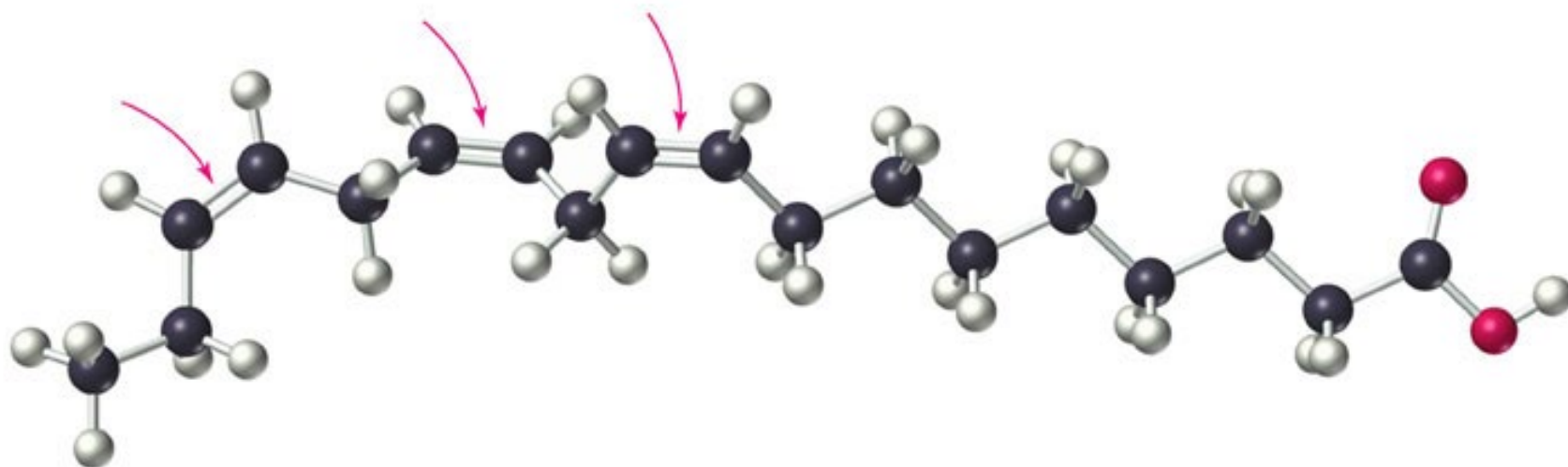
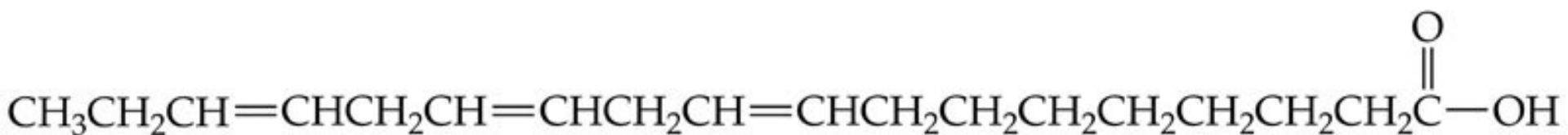


Lipid

- ***Lipids*** are naturally occurring molecules from plants or animals that are soluble in nonpolar organic solvents.
- Lipid molecules contain large hydrocarbon portion and not many polar functional group, which accounts for their solubility behavior.



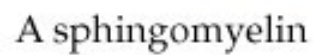
A saturated fatty acid
(palmitic acid)

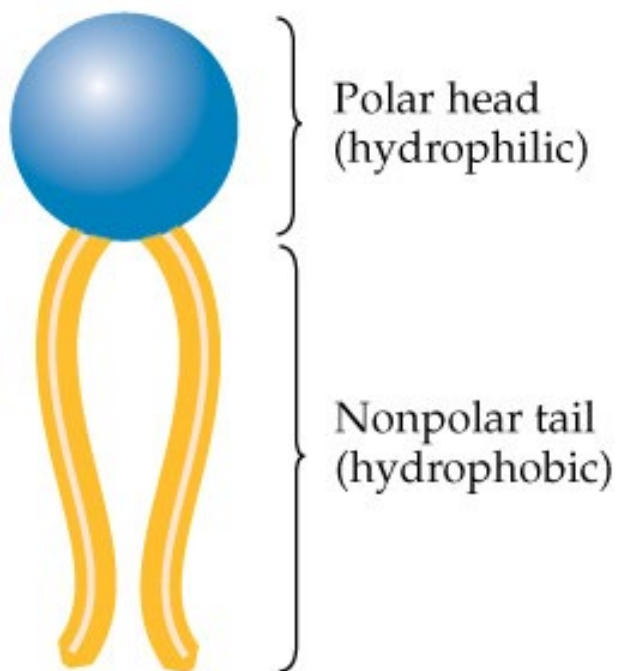


A *cis* unsaturated fatty acid
(linolenic acid)

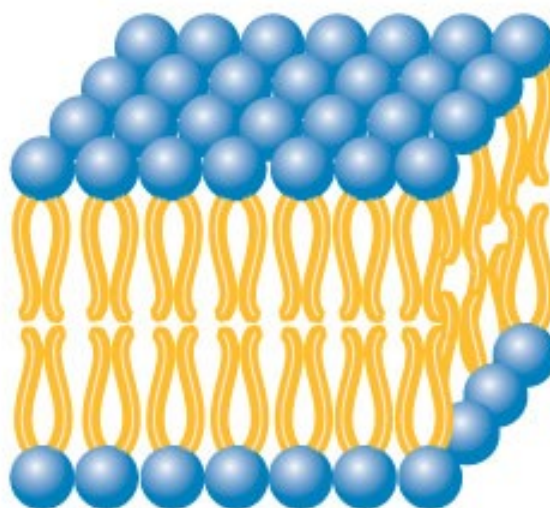


Stearic acid, an 18-carbon saturated fatty acid

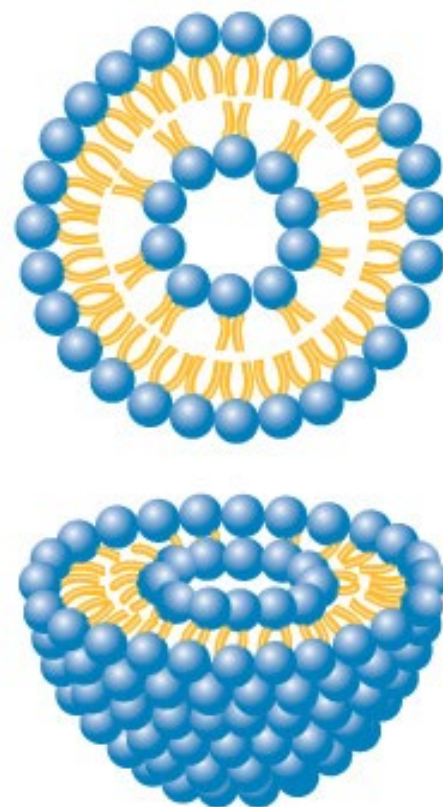




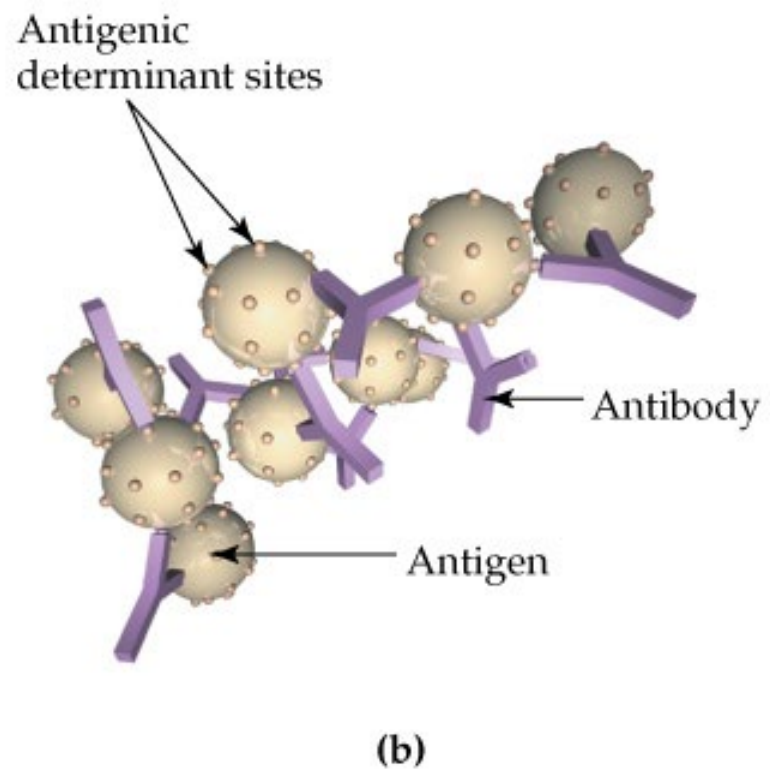
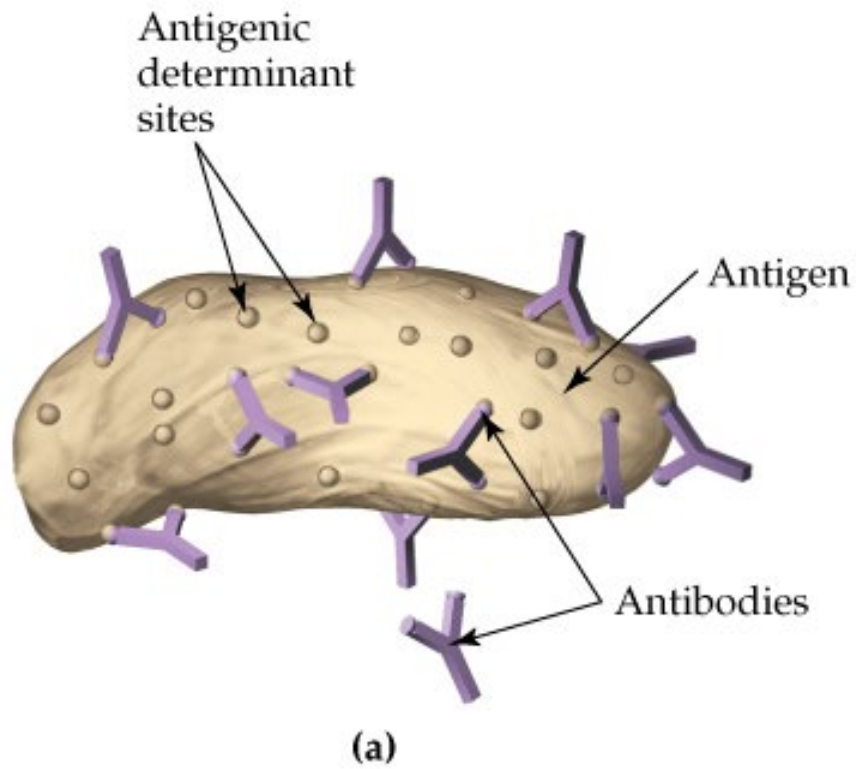
Membrane lipid



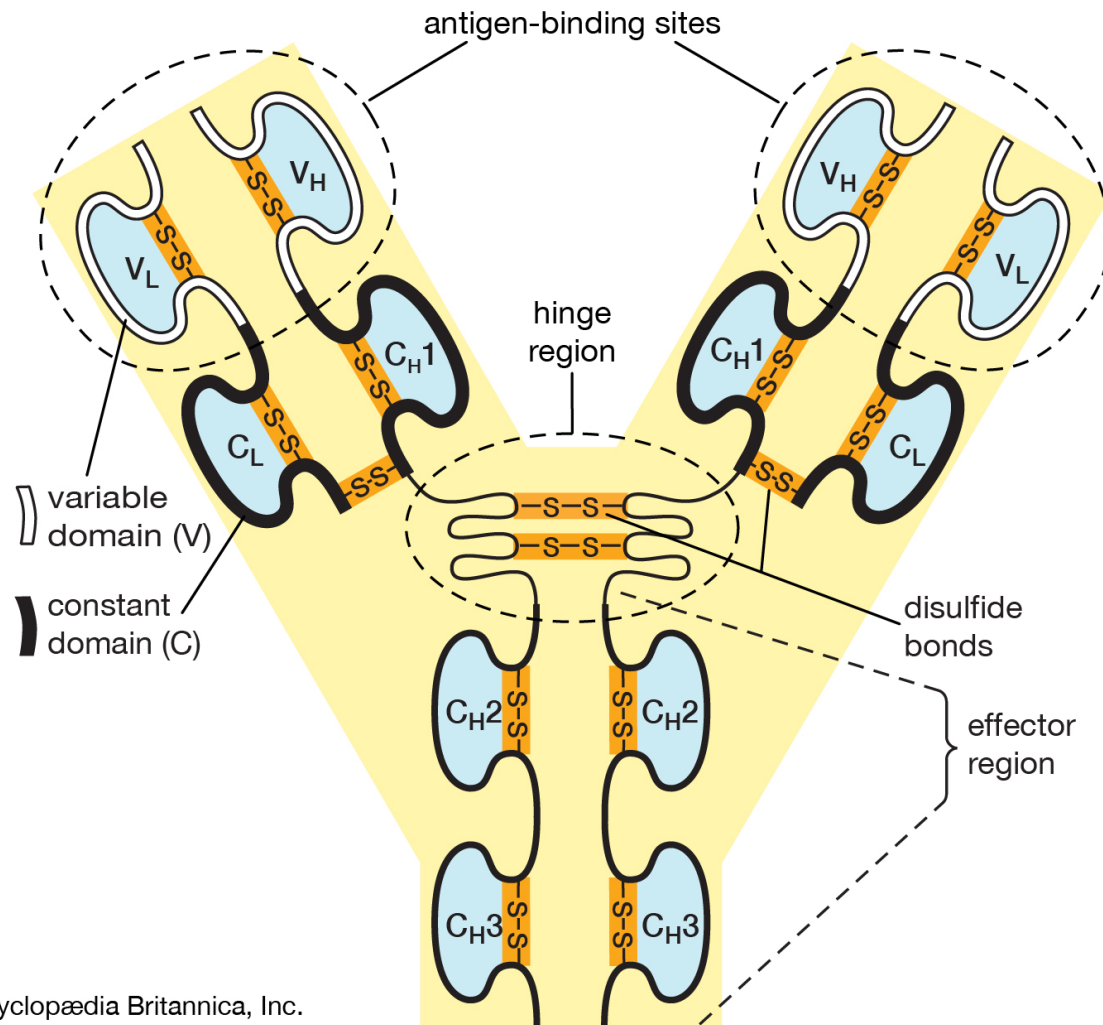
Lipid bilayer



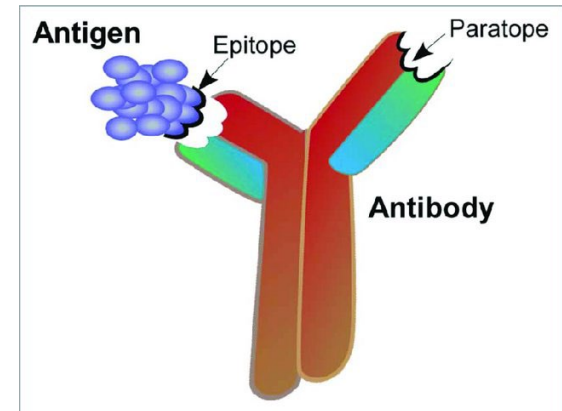
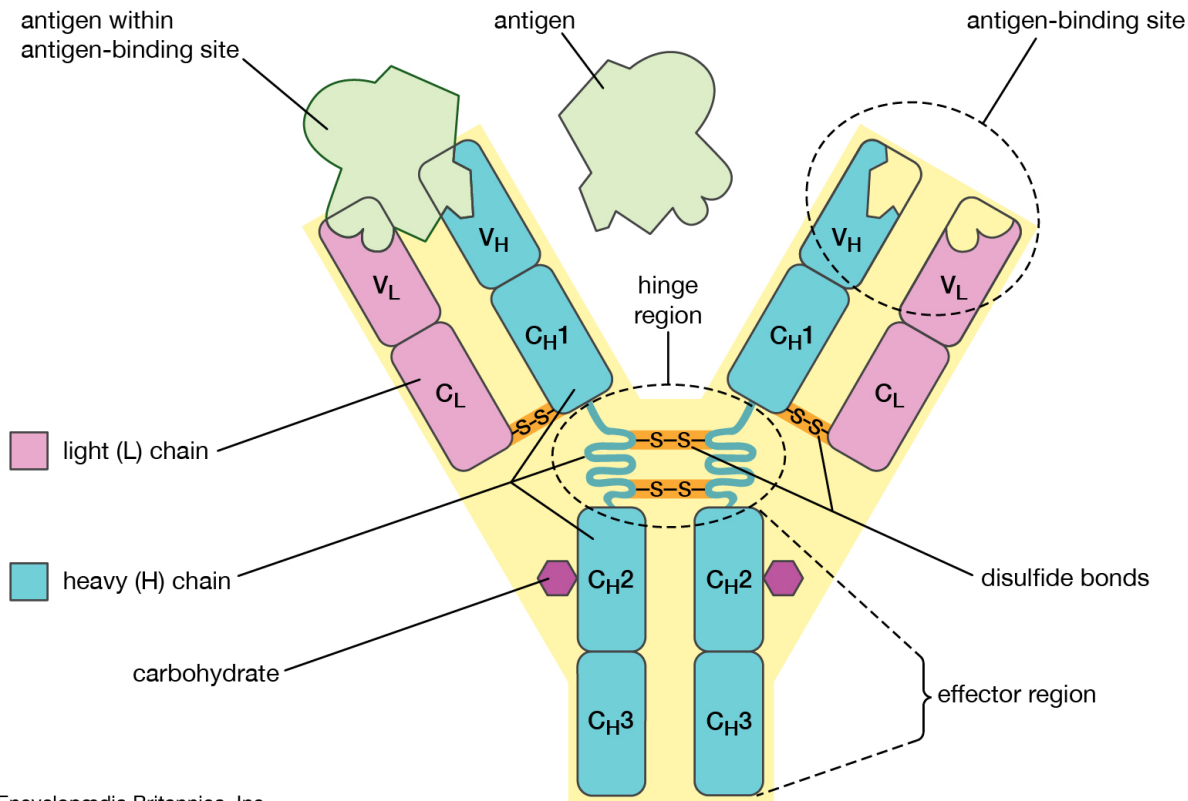
Liposome



Antibody

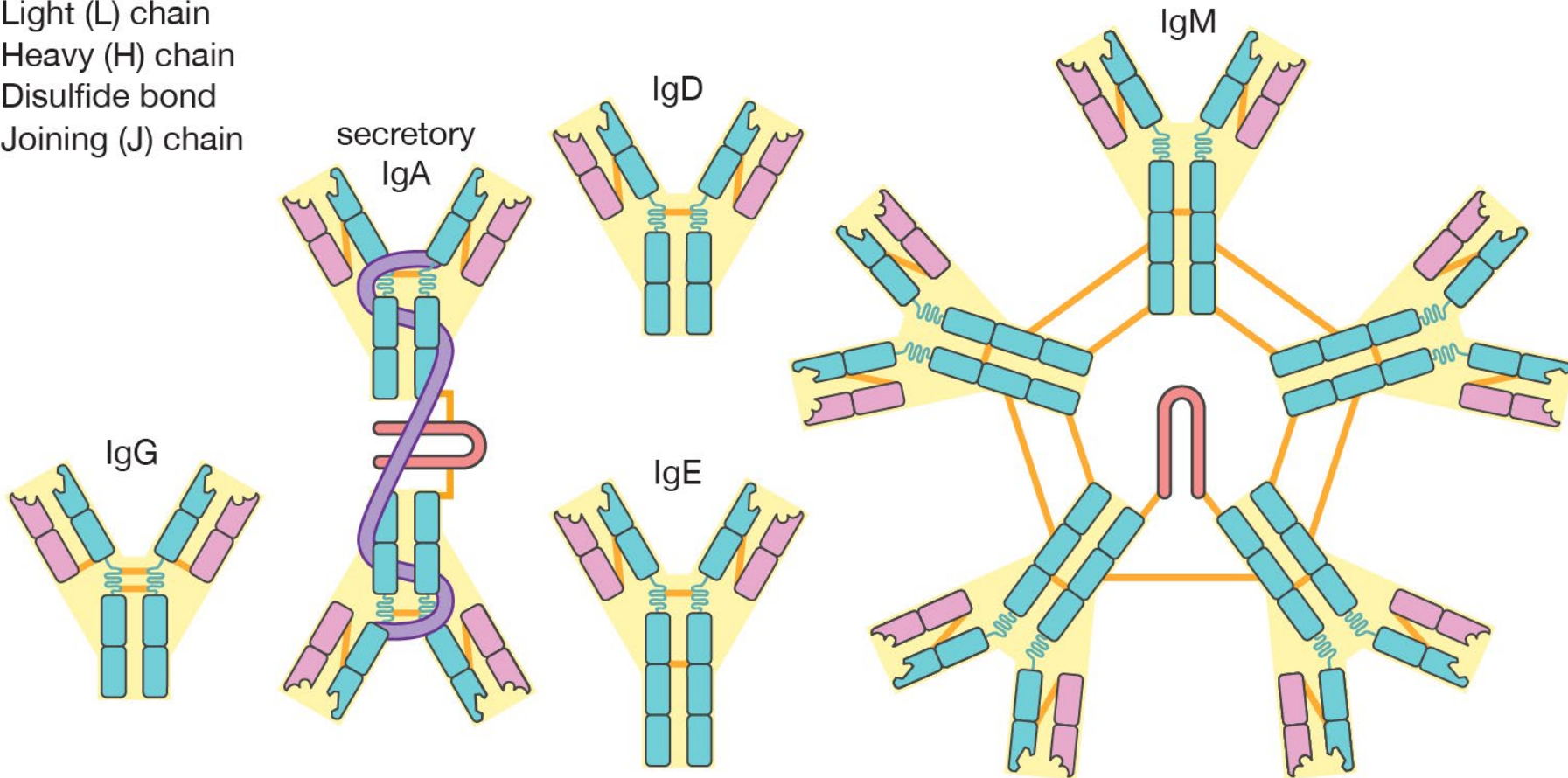


Antibody Binding Sites

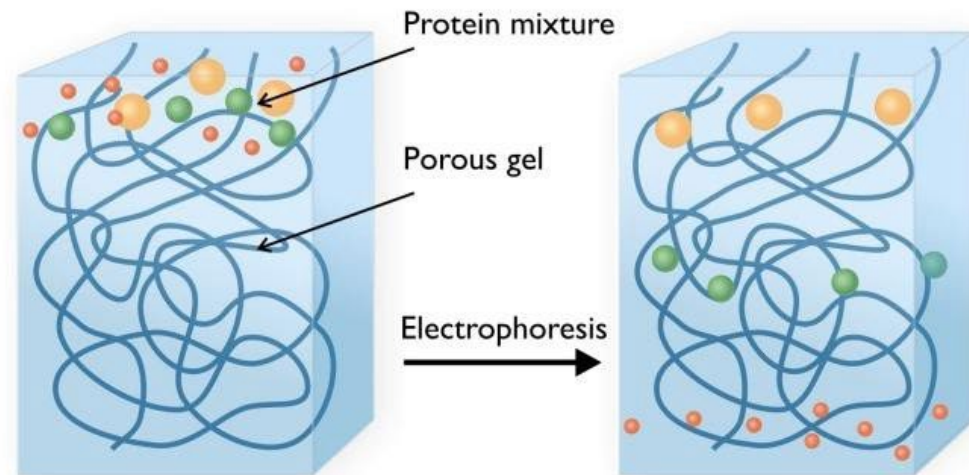
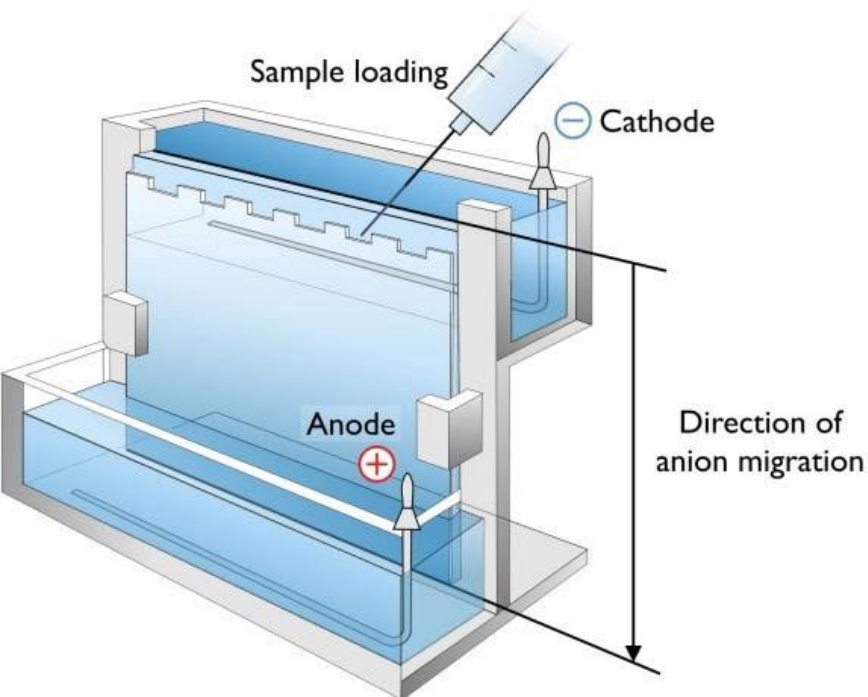


Different Types of Antibodies

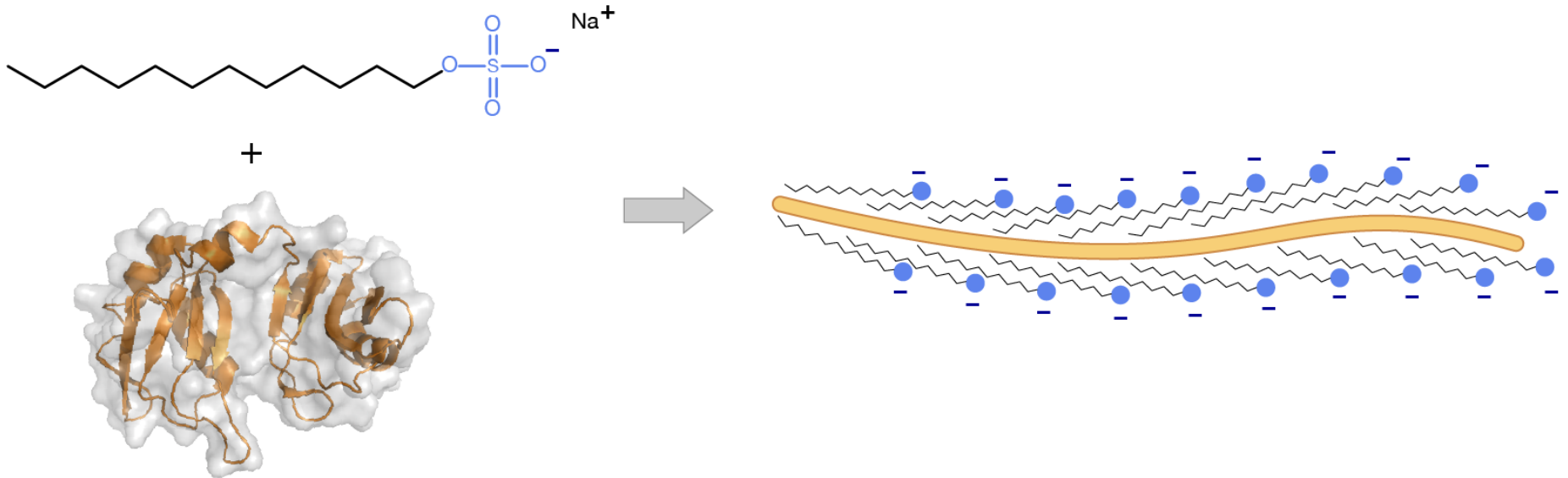
- Light (L) chain
- Heavy (H) chain
- Disulfide bond
- Joining (J) chain



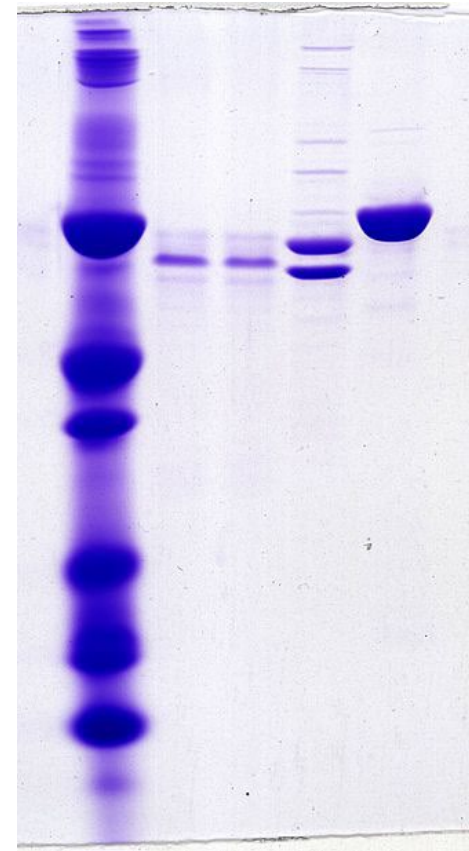
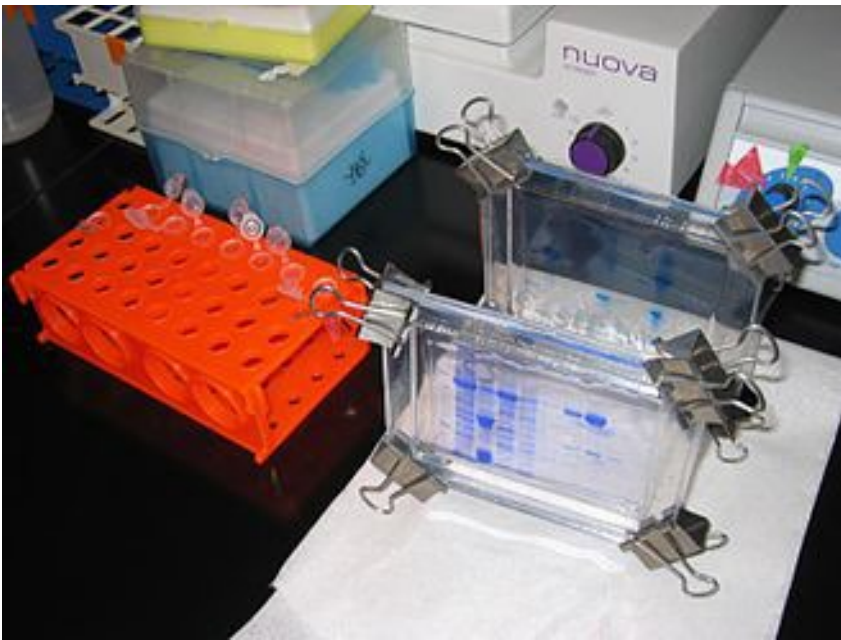
Sodium dodecyl sulfate polyacrylamide gel electrophoresis (SDS-PAGE)



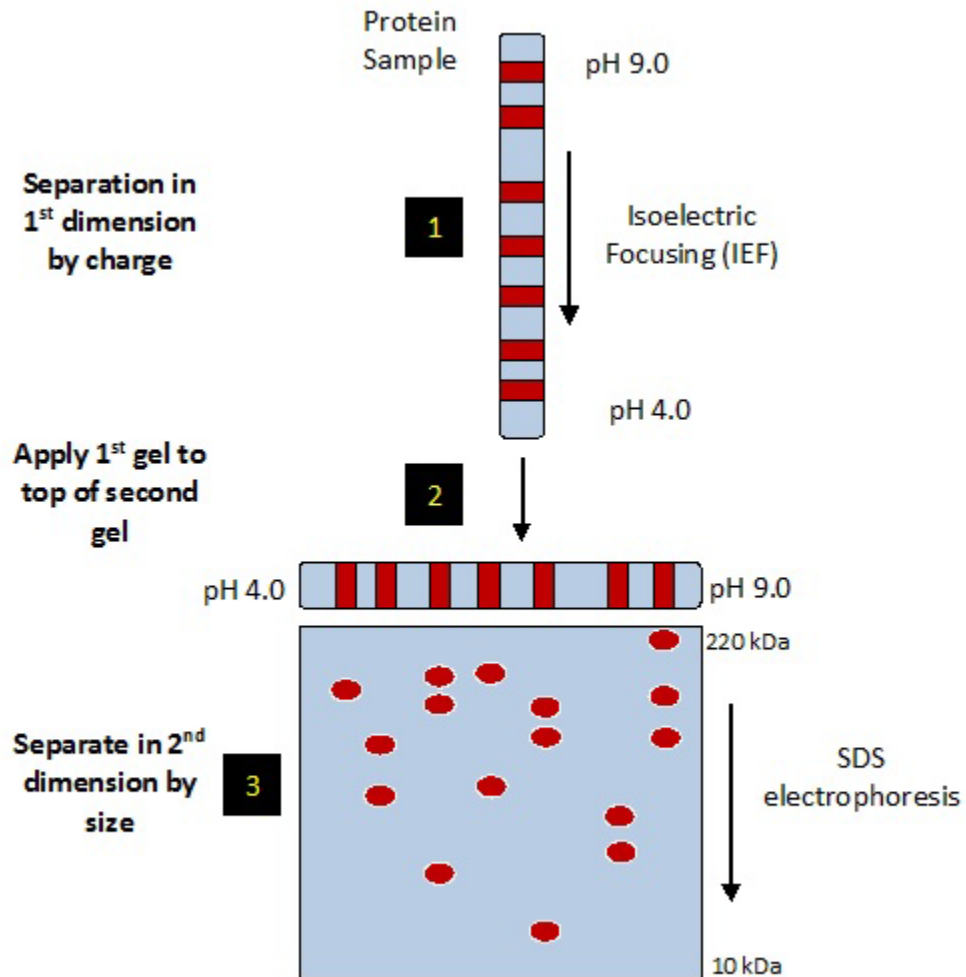
Protein Denature



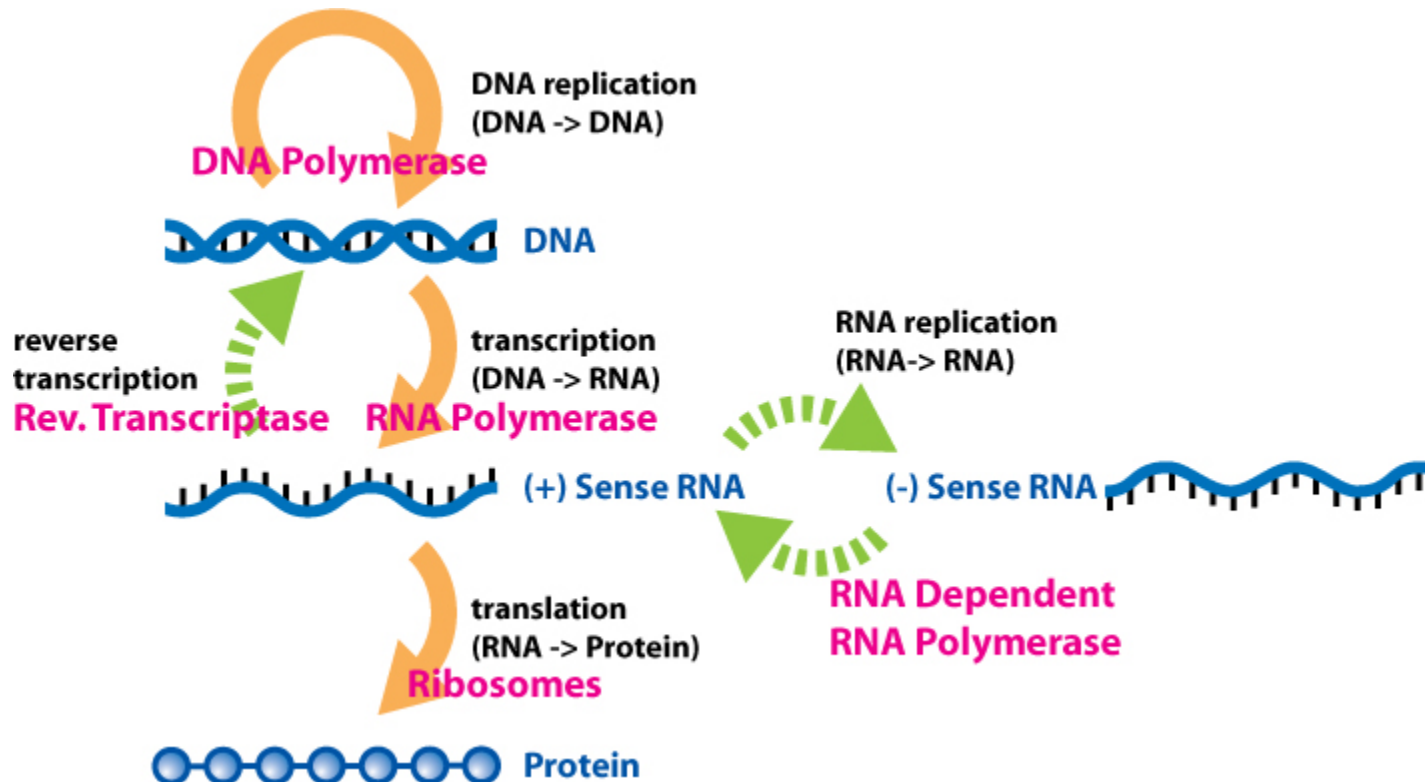
SDS-PAGE



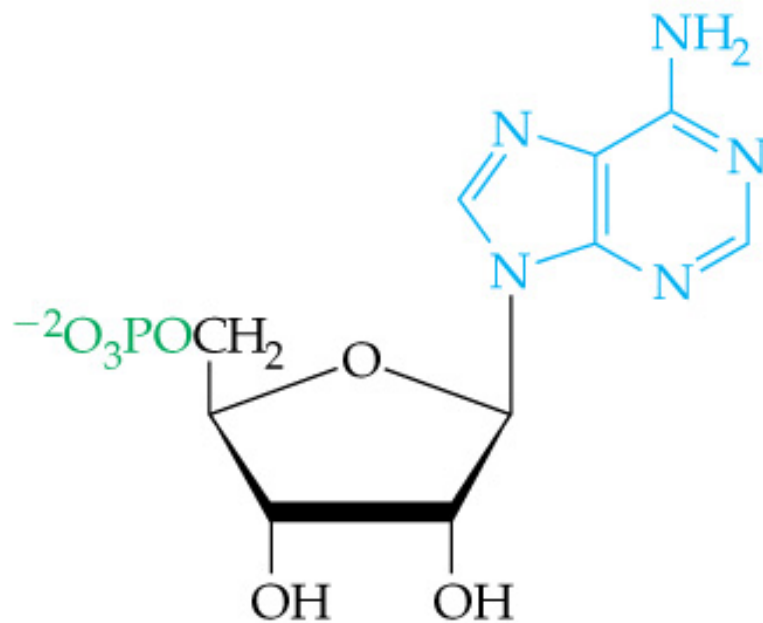
2D PAGE



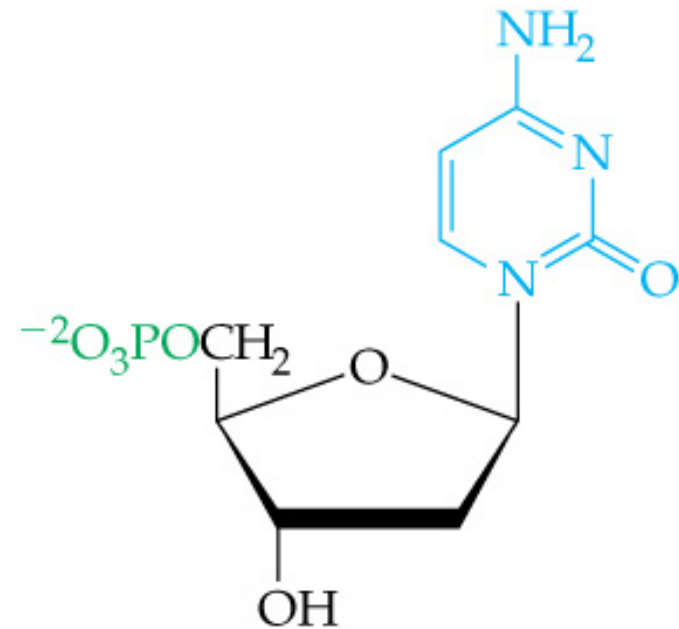
Central Dogma



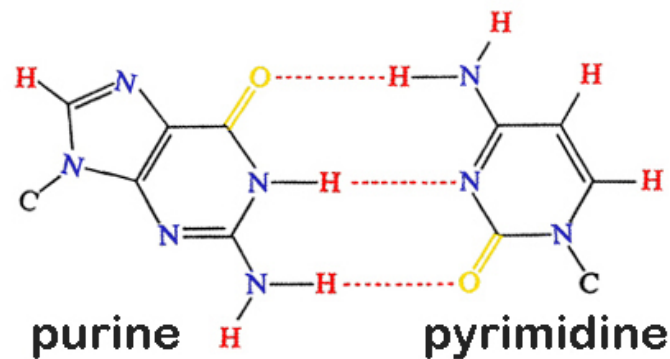
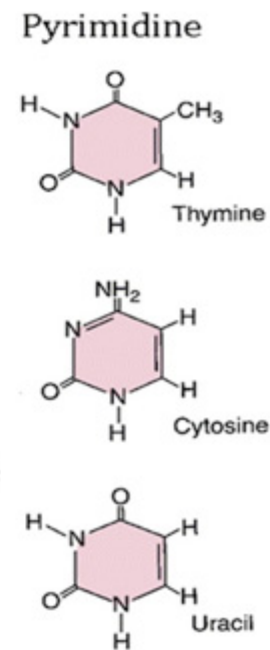
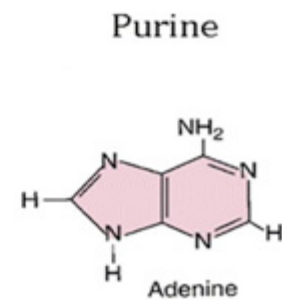
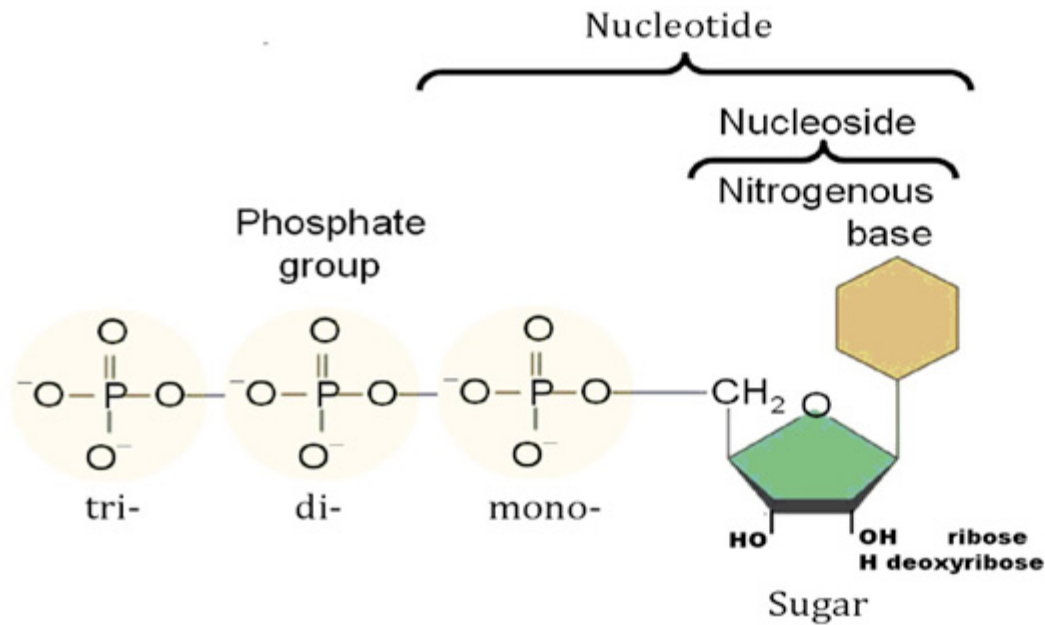
- In RNA, the sugar is ribose.
- In DNA, the sugar is deoxyribose.



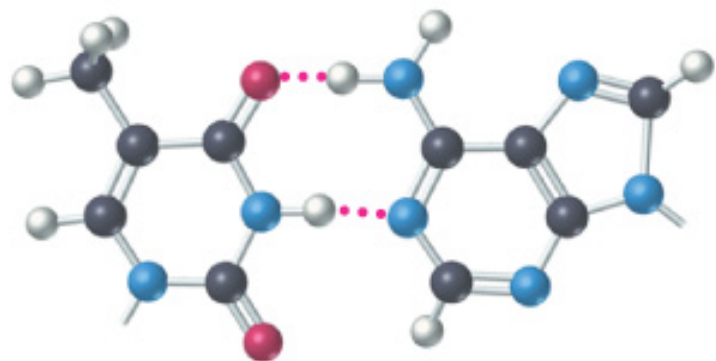
Adenosine 5'-monophosphate (AMP)
(a ribonucleotide)



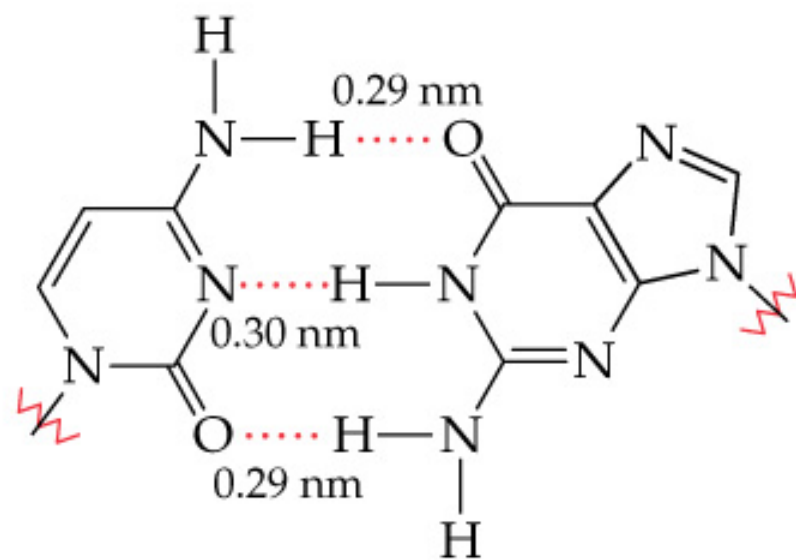
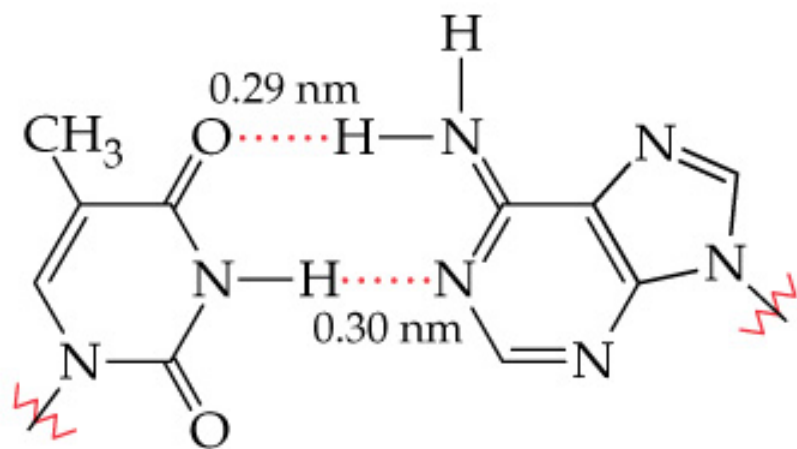
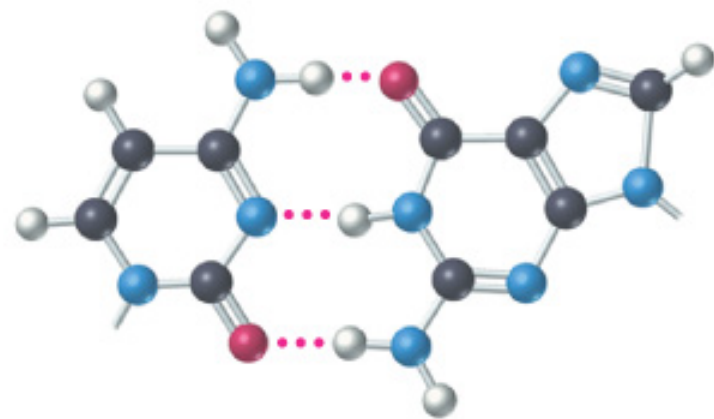
Deoxycytidine 5'-monophosphate (dCMP)
(a deoxyribonucleotide)

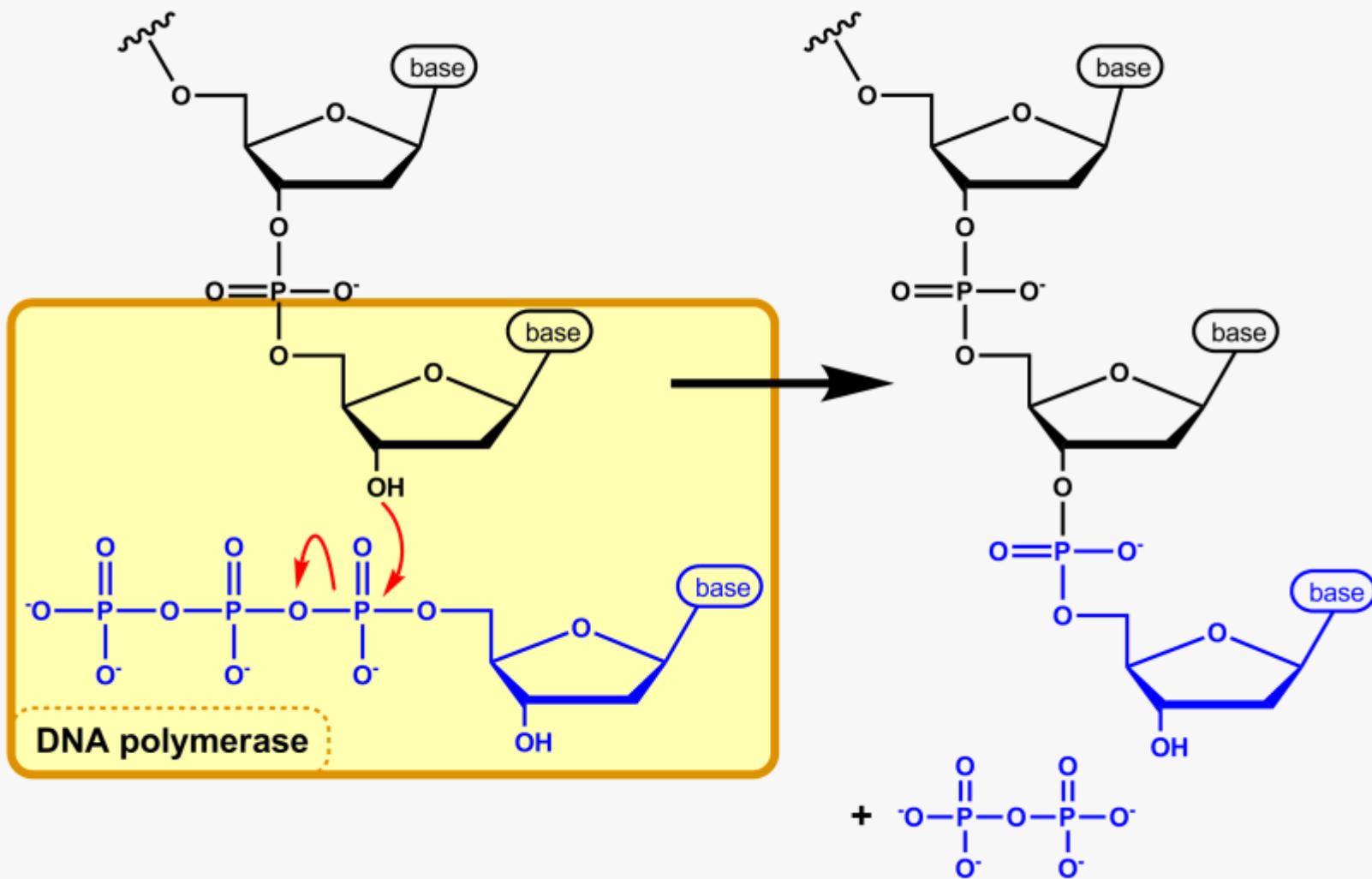


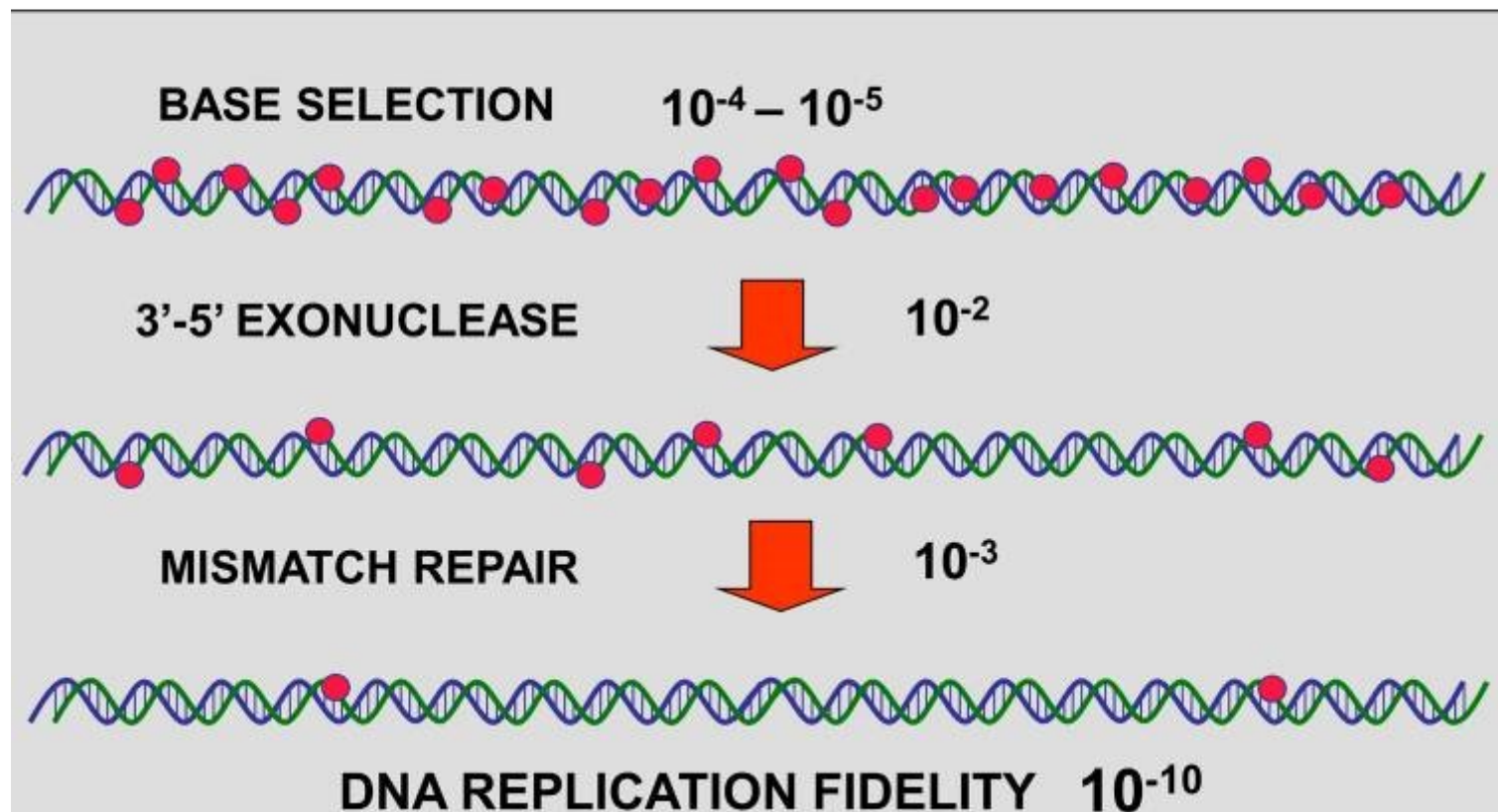
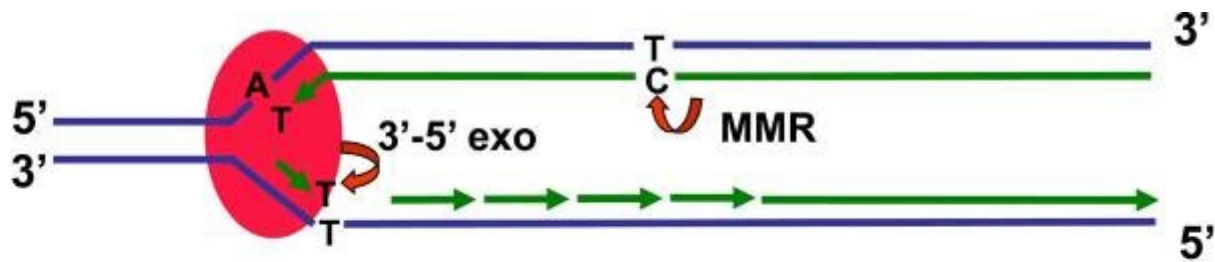
Thymine-Adenine

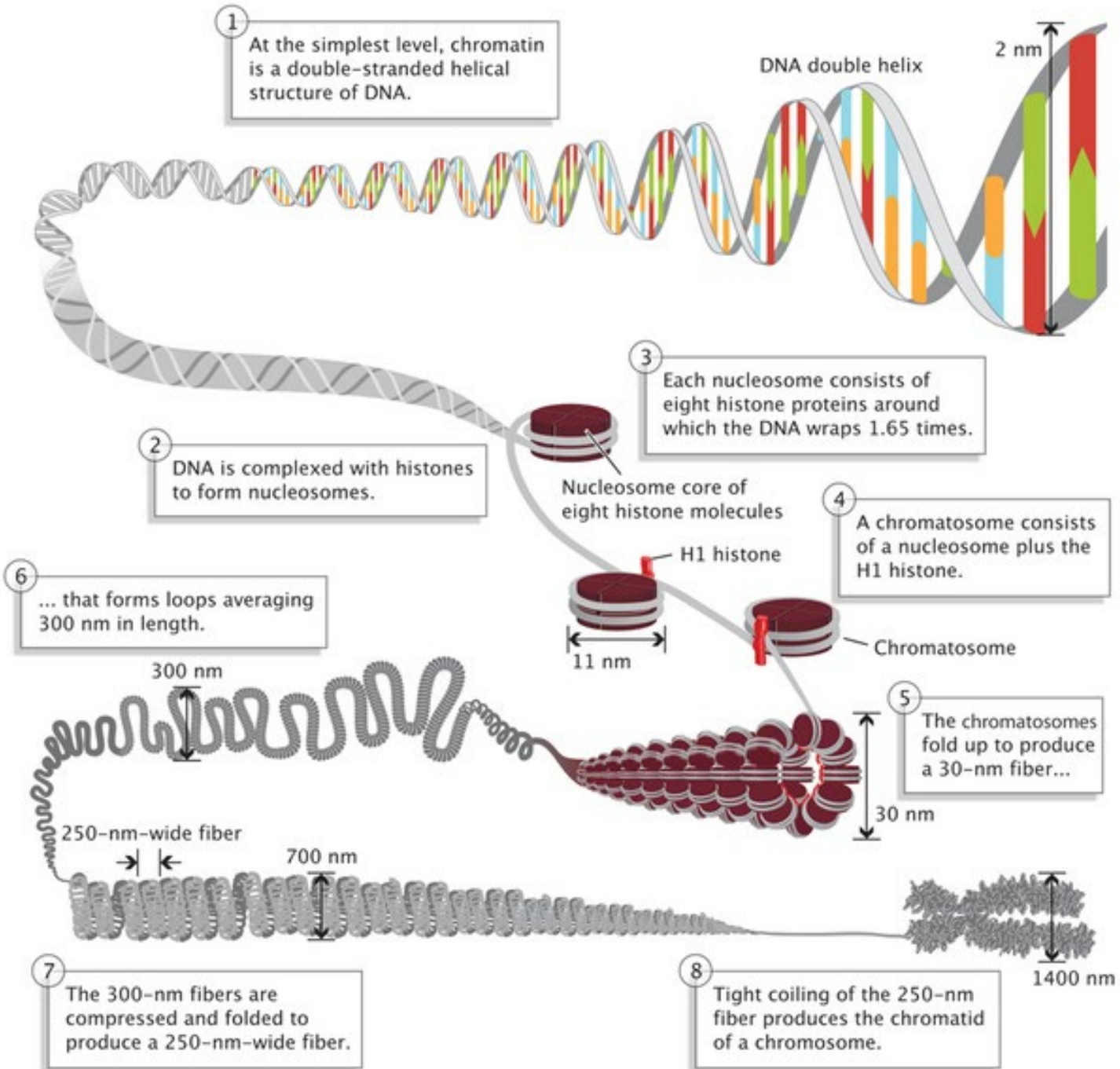


Cytosine-Guanine



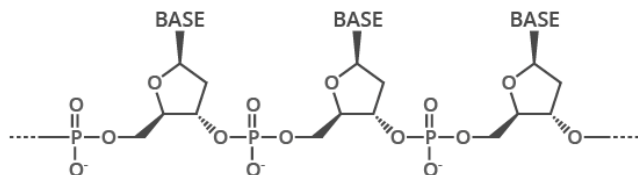






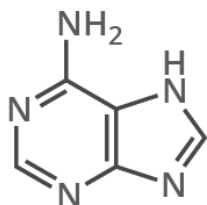
THE CHEMICAL STRUCTURE OF DNA

THE SUGAR PHOSPHATE 'BACKBONE'

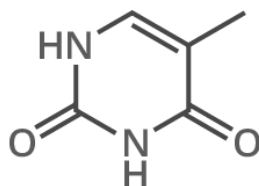


DNA is a polymer made up of units called nucleotides. The nucleotides are made of three different components: a sugar group, a phosphate group, and a base. There are four different bases: adenine, thymine, guanine and cytosine.

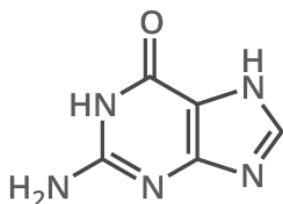
A ADENINE



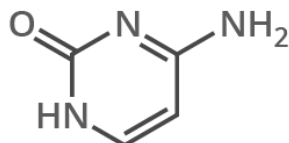
T THYMINE



G GUANINE

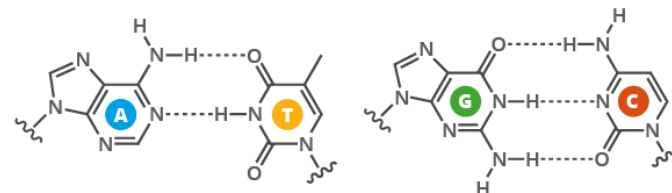


C CYTOSINE



WHAT HOLDS DNA STRANDS TOGETHER?

DNA strands are held together by hydrogen bonds between bases on adjacent strands. Adenine (A) always pairs with thymine (T), while guanine (G) always pairs with cytosine (C). Adenine pairs with uracil (U) in RNA.



FROM DNA TO PROTEINS

The bases on a single strand of DNA act as a code. The letters form three letter codons, which code for amino acids - the building blocks of proteins.

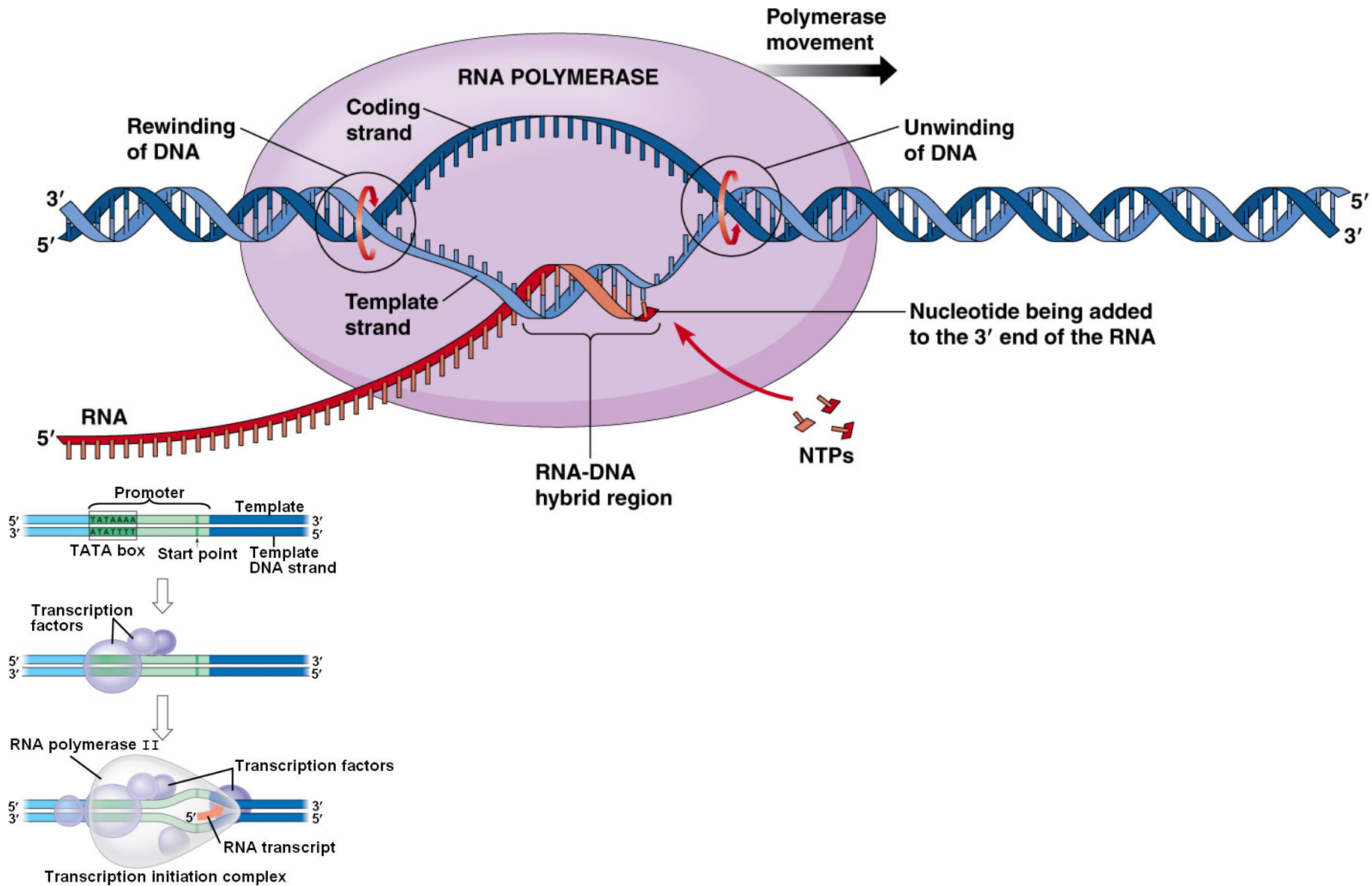


An enzyme, RNA polymerase, transcribes DNA into mRNA (messenger ribonucleic acid). It splits apart the two strands that form the double helix, then reads a strand and copies the sequence of nucleotides. The only difference between the RNA and the original DNA is that in the place of thymine (T), another base with a similar structure is used: uracil (U).

| | | | | | | | | | | | | | | | |
|---------------|---------------|---|---------|---|------------|---|---------|---|---------|---|---|---|---|---|---|
| DNA SEQUENCE | T | T | C | C | T | G | A | A | C | C | C | G | T | T | A |
| mRNA SEQUENCE | U | U | C | C | U | G | A | A | C | C | C | G | U | U | A |
| AMINO ACID | Phenylalanine | | Leucine | | Asparagine | | Proline | | Leucine | | | | | | |

In multicellular organisms, the mRNA carries genetic code out of the cell nucleus, to the cytoplasm. Here, protein synthesis takes place. 'Translation' is the process of turning the mRNA's 'code' into proteins. Molecules called ribosomes carry out this process, building up proteins from the amino acids coded for.





RNA

Base

G C U A C G G A G C U U C G G A G C U A G

Codon

Codon 1 Codon 2 Codon 3 Codon 4 Codon 5 Codon 6 Codon 7

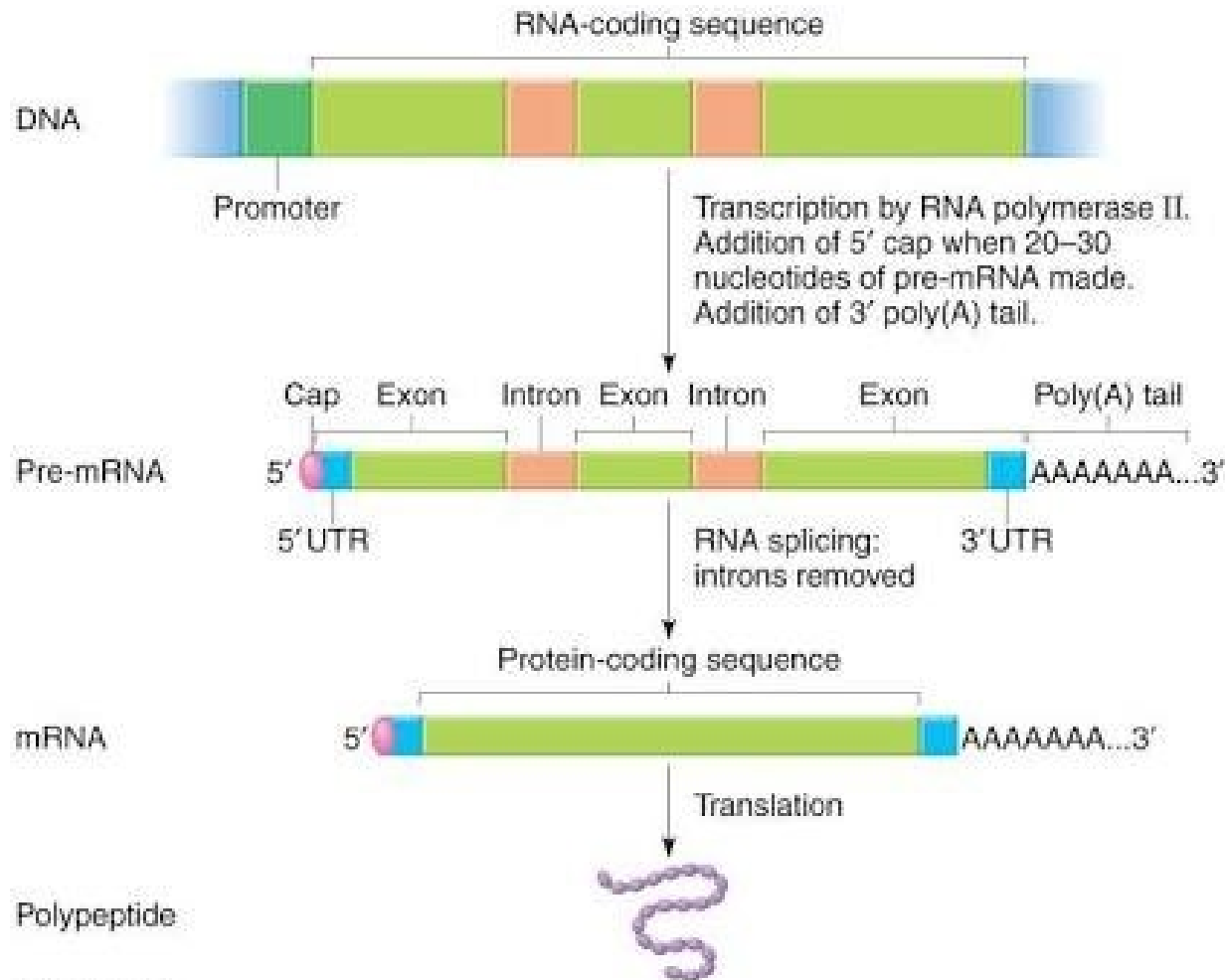
Aminoacid

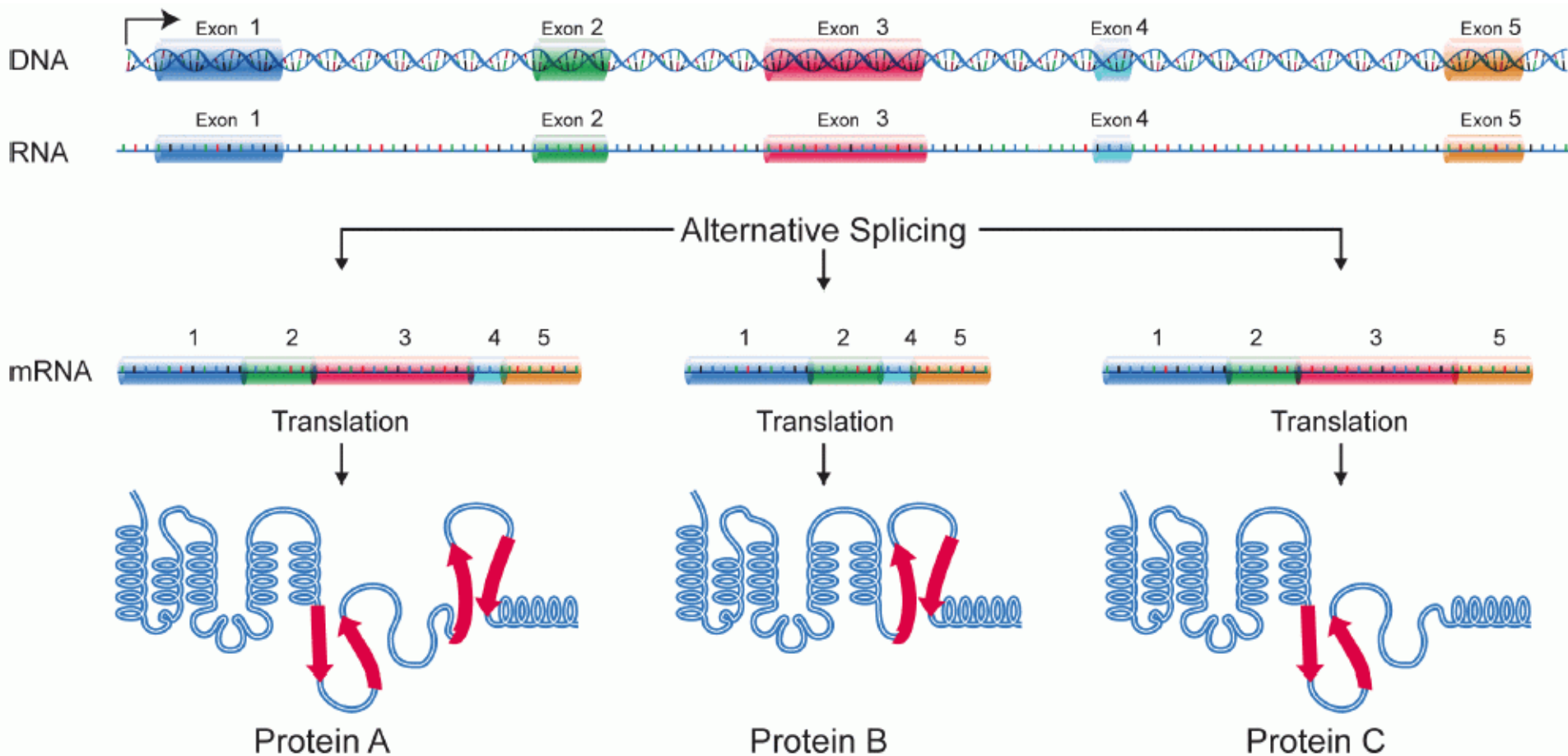
Alanine Threonine Glutamate Leucine Arginine Serine Stop

| | | Second letter | | | | |
|--------------|---|---|--------------------------------------|--|--|------------------|
| | | U | C | A | G | |
| First letter | U | UUU } Phe UUC } UUA } Leu UUG } | UCU } UCC } Ser UCA } UCG } | UAU } Tyr UAC } UAA Stop UAG Stop | UGU } Cys UGC } UGA Stop UGG Trp | U C A G |
| | C | CUU } CUC } Leu CUA } CUG } | CCU } CCC } Pro CCA } CCG } | CAU } His CAC } CAA } Gln CAG } | CGU } CGC } Arg CGA } CGG } | U C A G |
| | A | AUU } AUC } Ile AUA } AUG Met | ACU } ACC } Thr ACA } ACG } | AAU } Asn AAC } AAA } Lys AAG } | AGU } Ser AGC } AGA } Arg AGG } | U C A G |
| | G | GUU } GUC } Val GUA } GUG } | GCU } GCC } Ala GCA } GCG } | GAU } Asp GAC } GAA } Glu GAG } | GGU } GGC } Gly GGA } GGG } | U C A G |

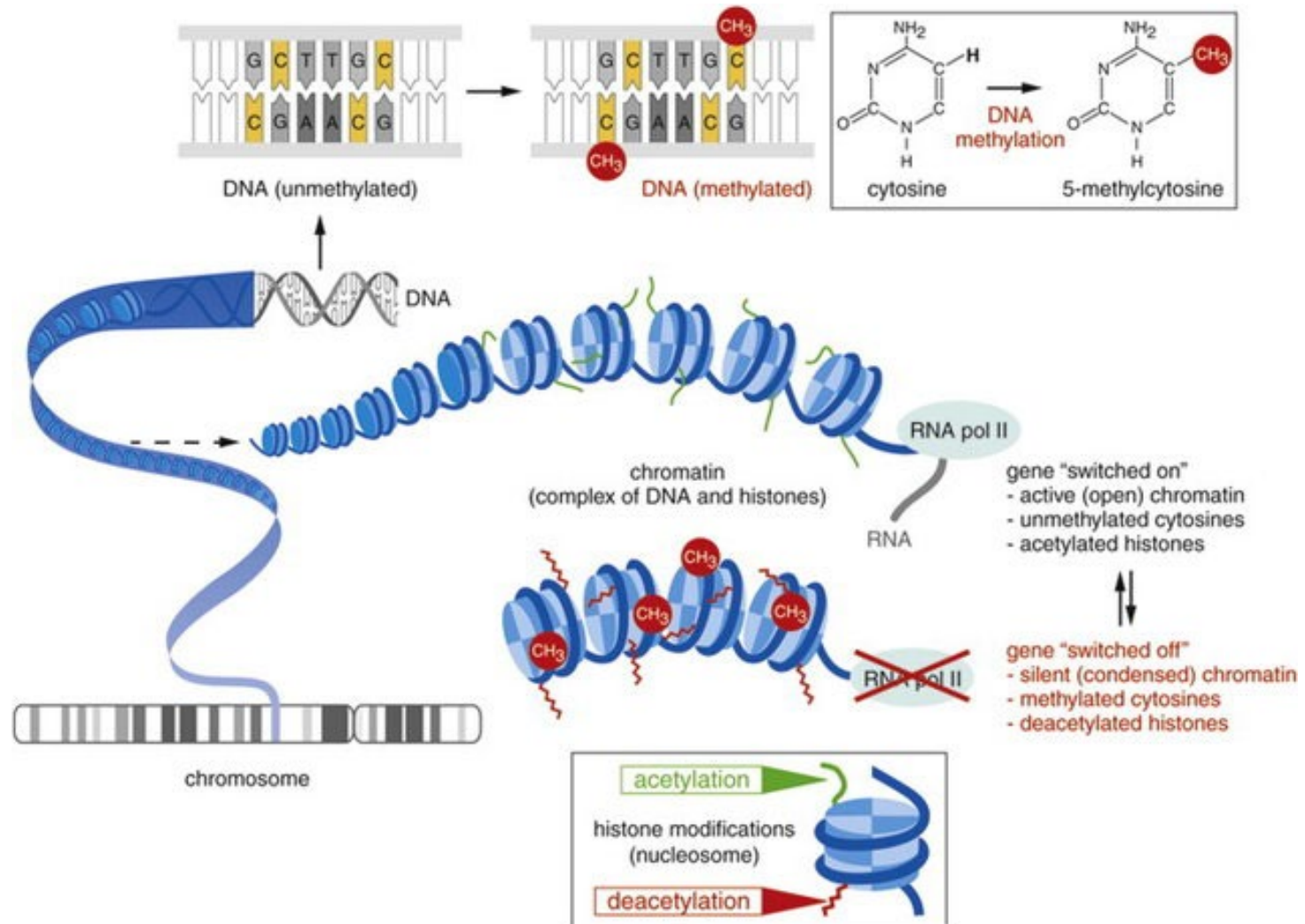
Post Transcription Modification of RNA

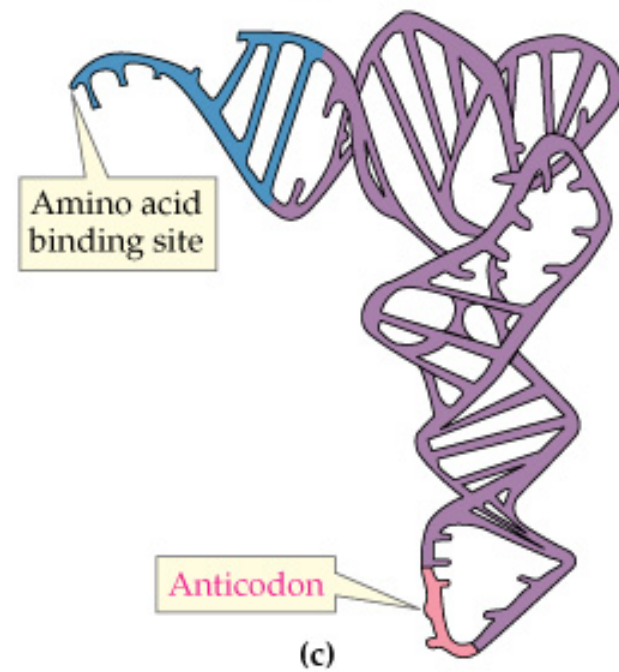
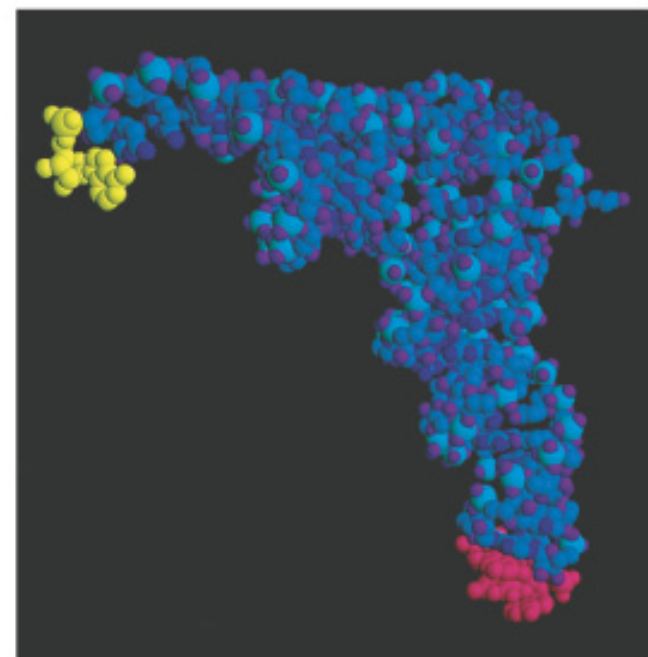
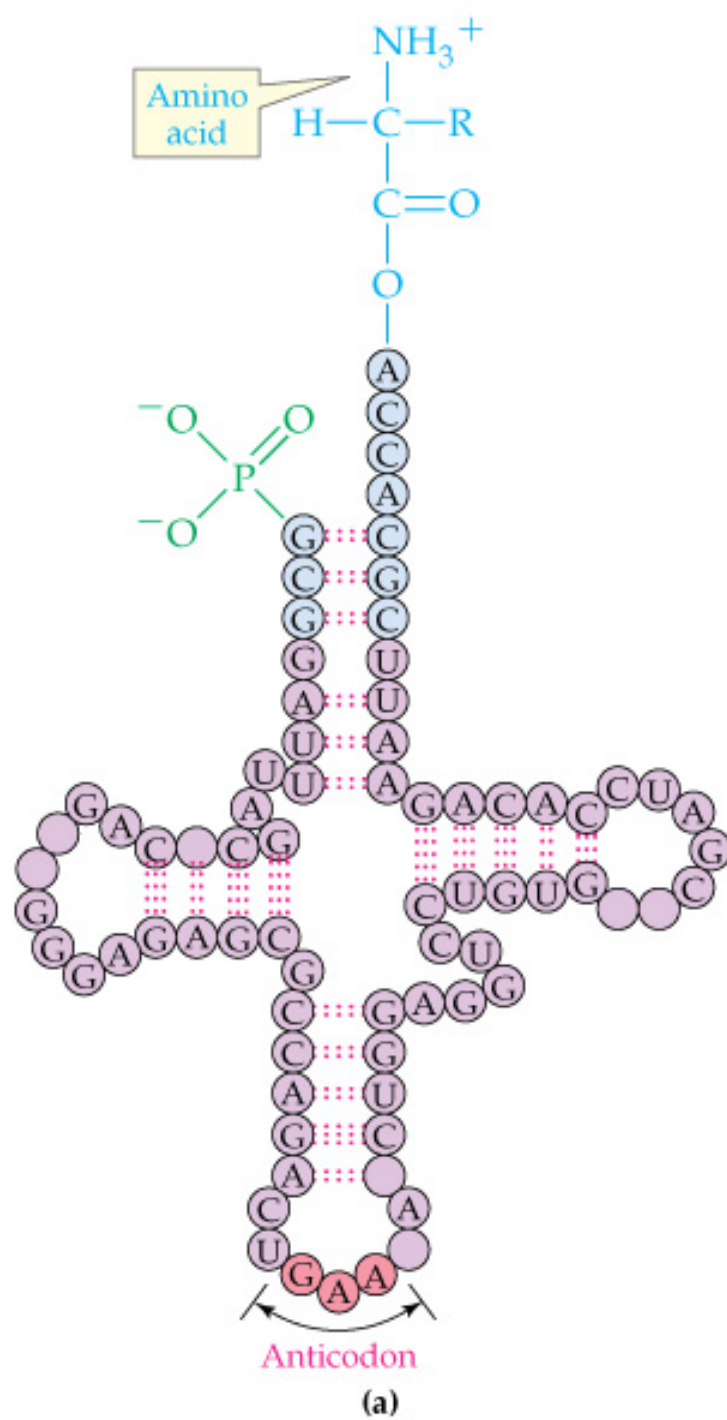
1. RNA capping
2. PolyA tail
3. Splicing



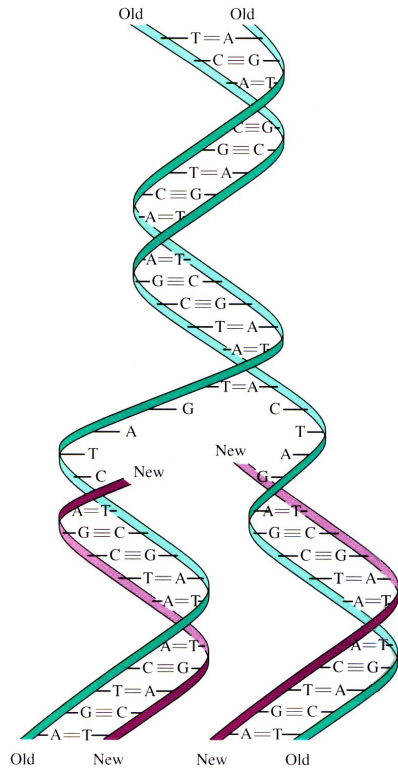


DNA Methylation and Histone Acetylation





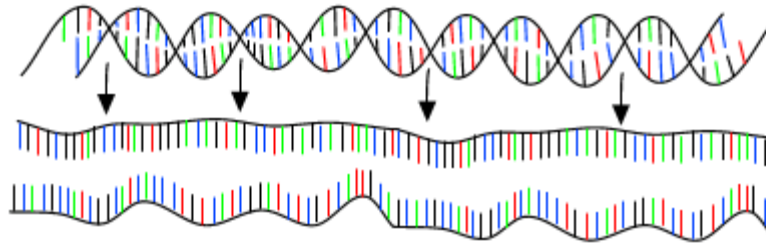
Self-Assembly Process in Nature



5' cap AUGAGAUACCAAGAACCUACCAAGGUAGAGCUUUAGCCCG AAAAAAAAAAAAAA 3'

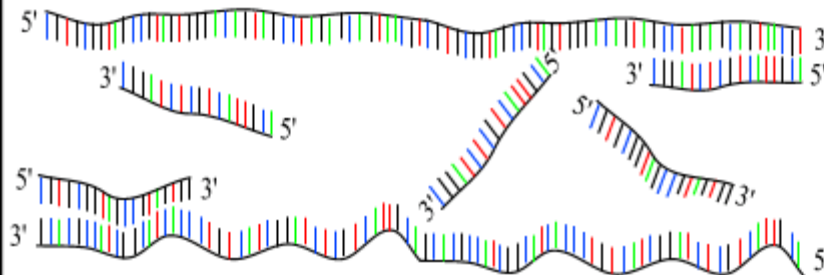
PCR : Polymerase Chain Reaction

30 - 40 cycles of 3 steps :



Step 1 : denaturation

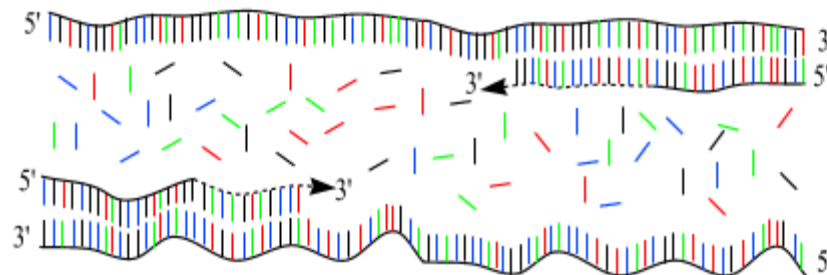
1 minut 94 °C



Step 2 : annealing

45 seconds 54 °C

forward and reverse
primers !!!

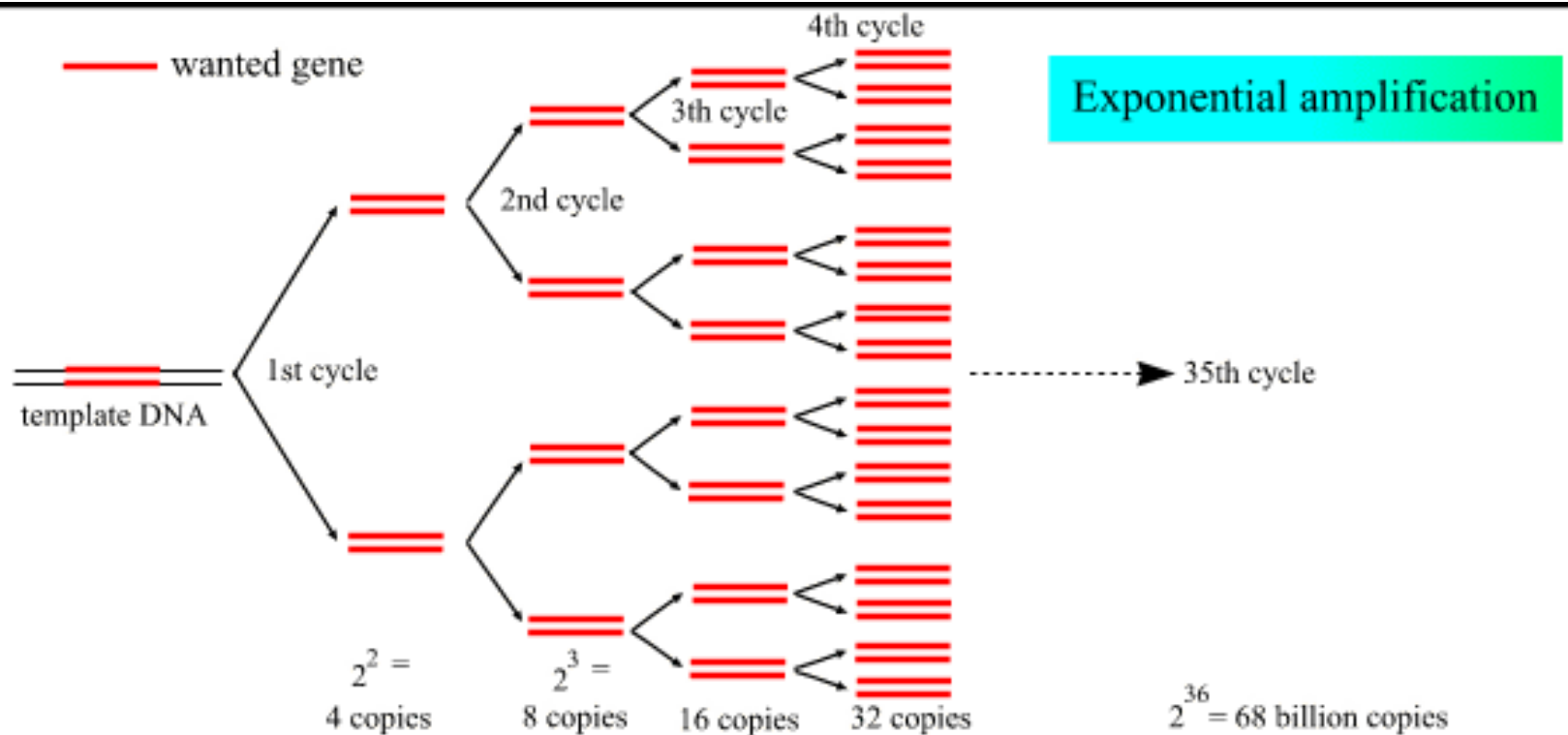


Step 3 : extension

2 minutes 72 °C

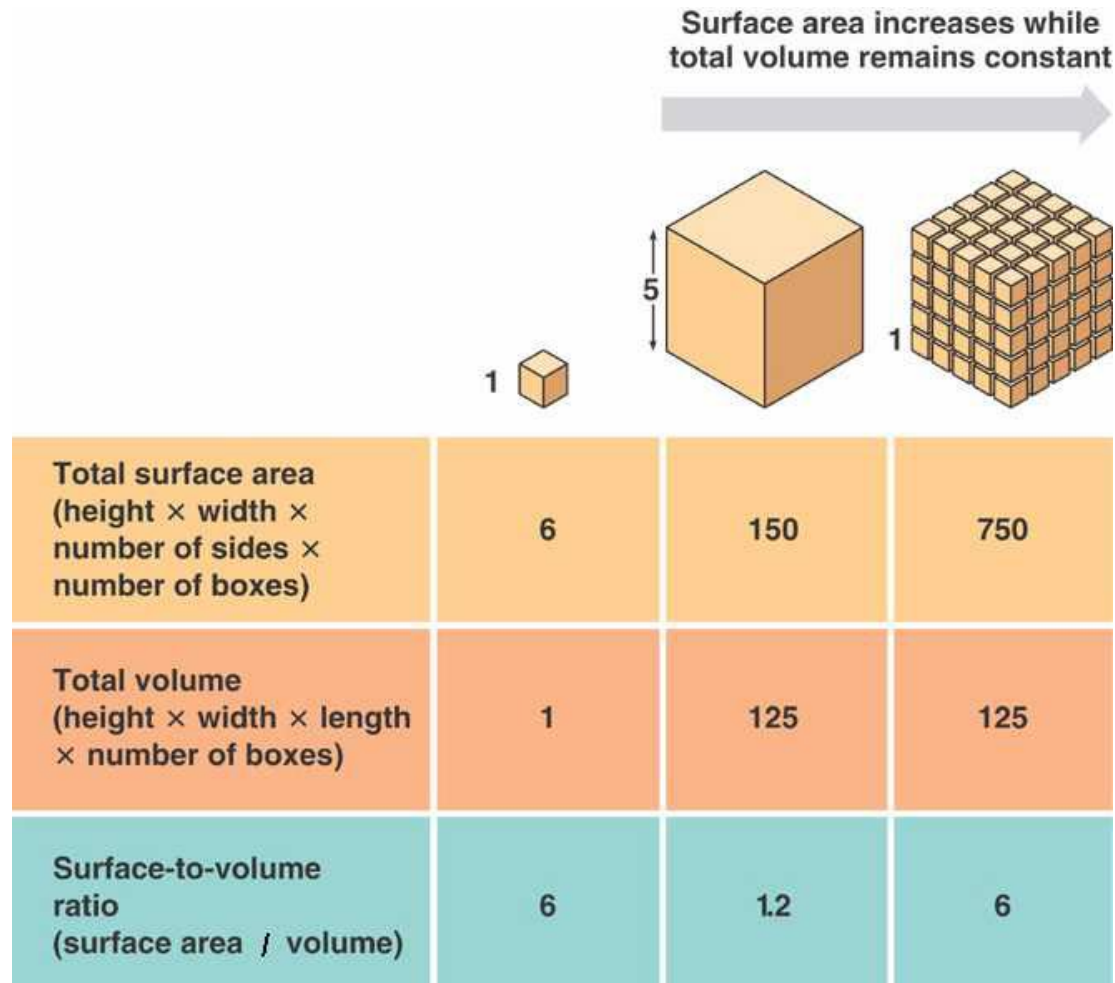
only dNTP's

(Andy Viersraete 1999)



(Andy Vierstraete 1999)

Surface to Volume Ratio



Surface Energy

One face surface energy: γ

27 cube: $27 \times 6 \gamma$

3 x 9 cube line: 114γ

3 x (3x3) square: 90γ

3 x 3 x 3 cube: 54γ

DLVO Theory

$$V_T = V_A + V_R + V_S$$

$$V_A = -A/(12 \pi D^2)$$

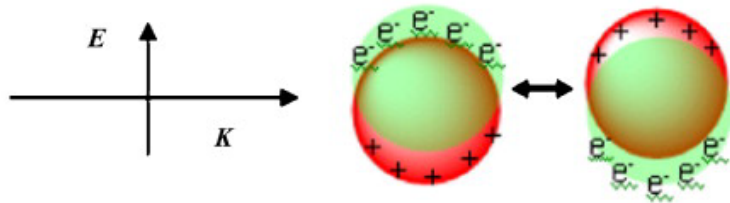
A is the Hamaker constant and D is the particle separation

$$V_R = 2 \pi \epsilon a \xi^2 \exp(-\kappa D)$$

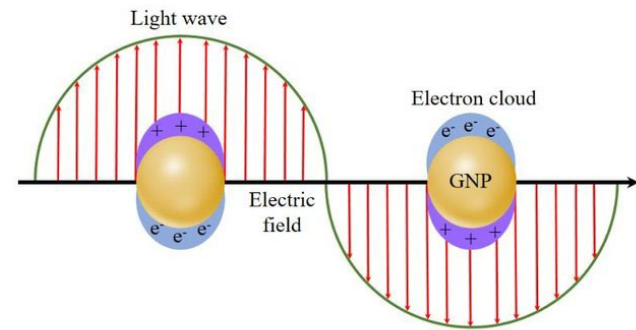
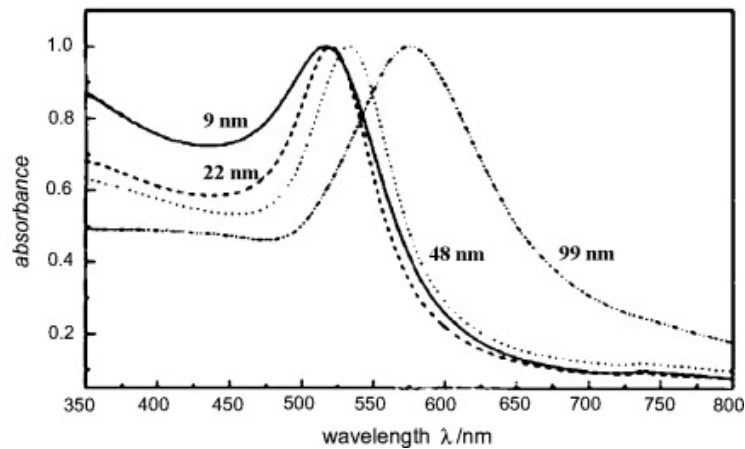
a is the particle radius, π is the solvent permeability,
 κ is a function of the ionic composition and ξ is the zeta potential

Localized Surface Plasmon

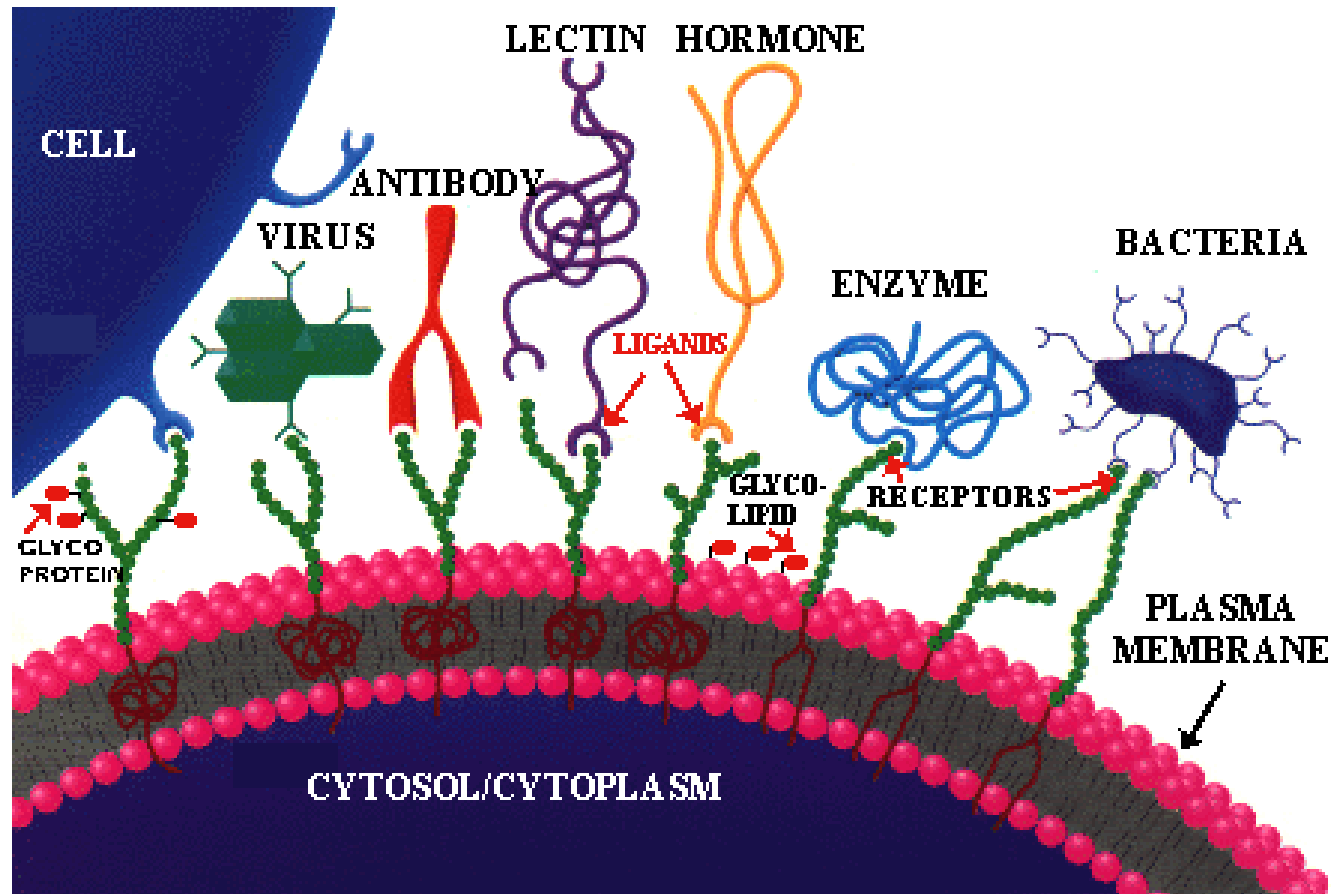
A



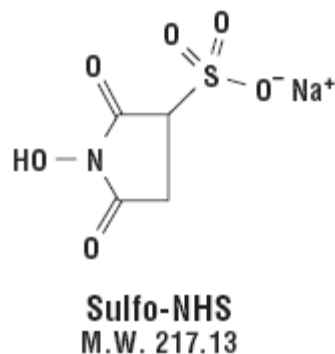
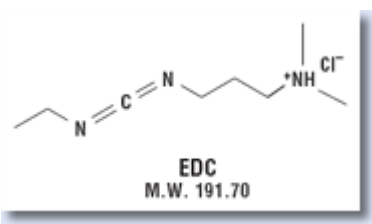
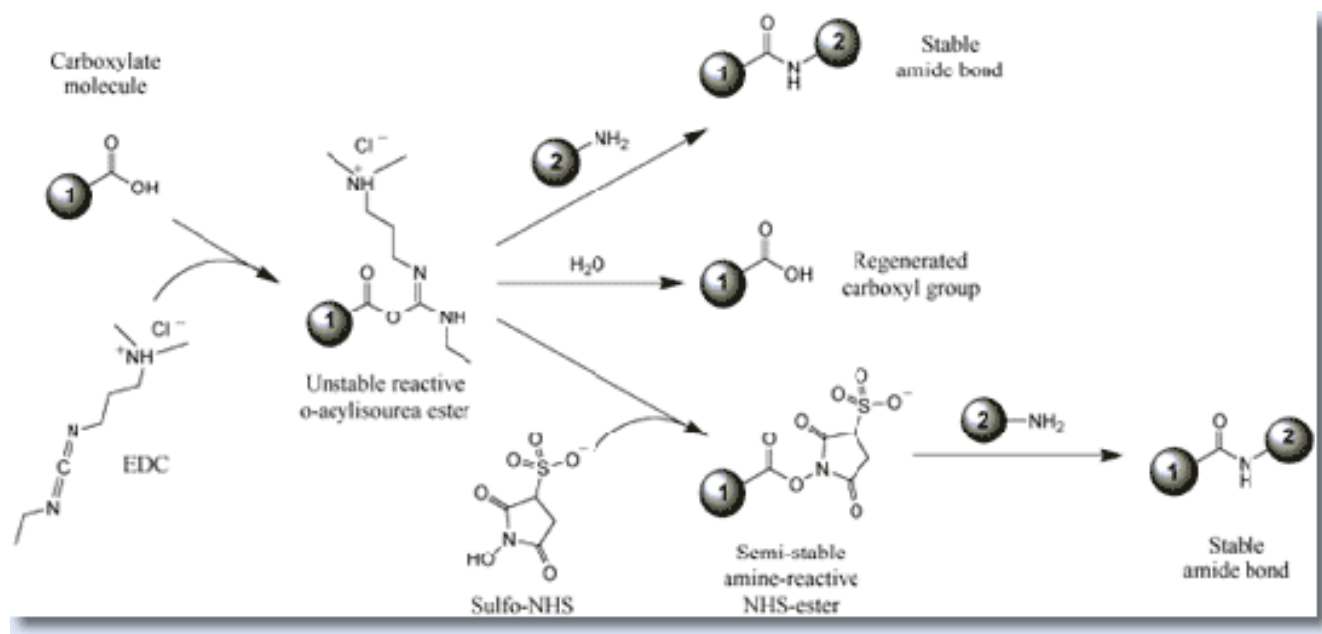
B



Molecular Recognition

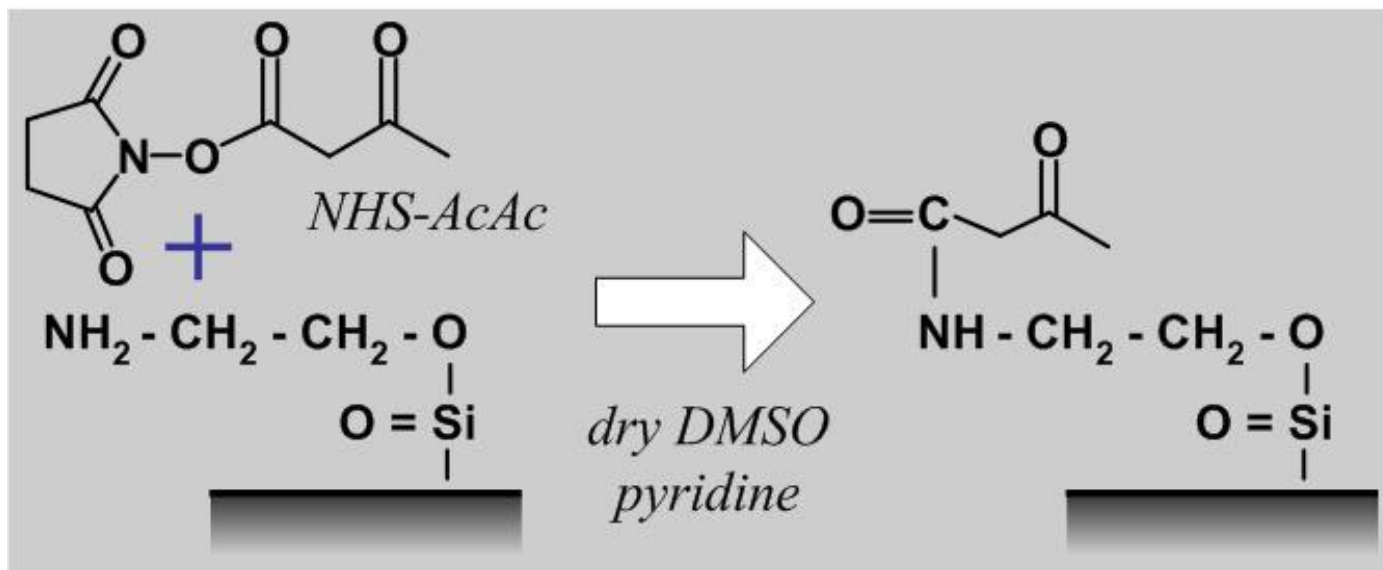


Carboxyl Presenting Surfaces

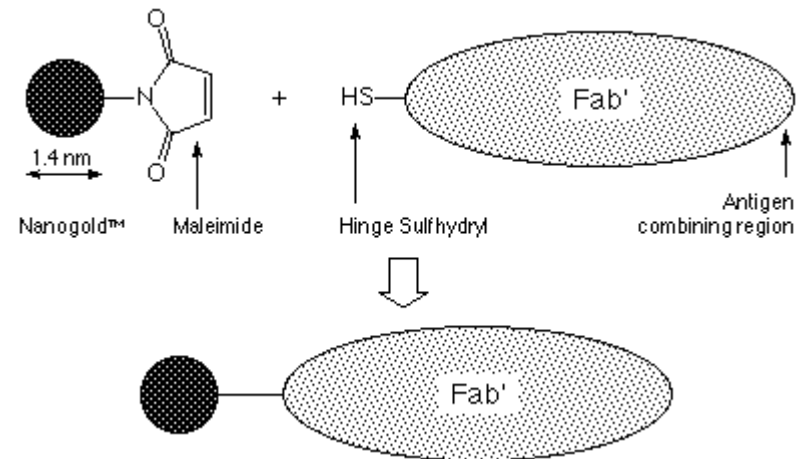
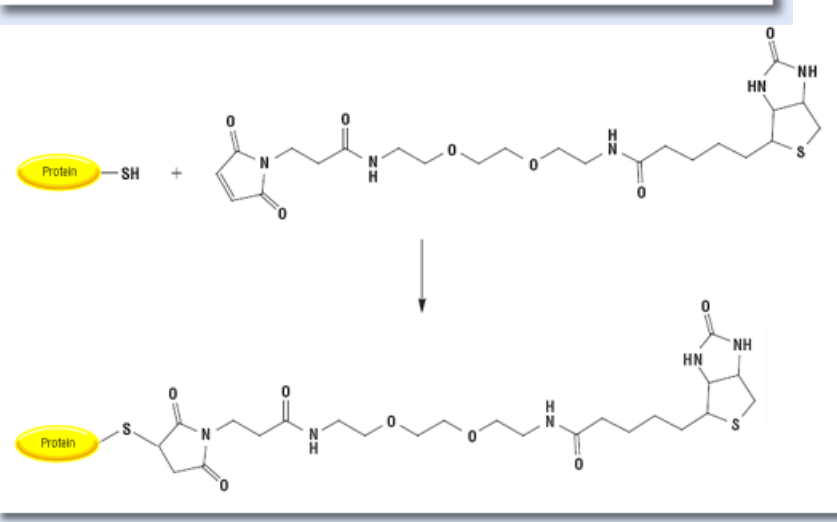
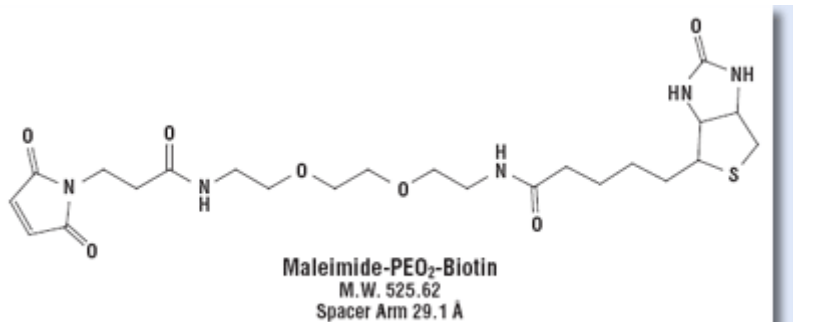
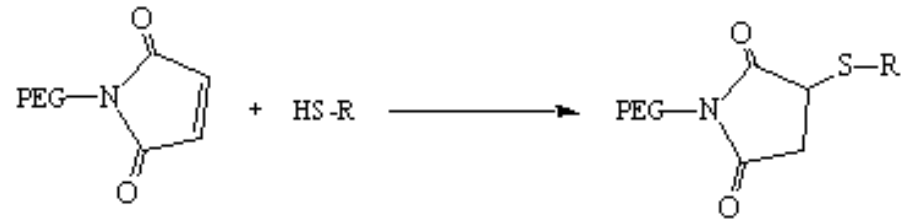


EDC (1-Ethyl-3-[3-dimethylaminopropyl]carbodiimide Hydrochloride)

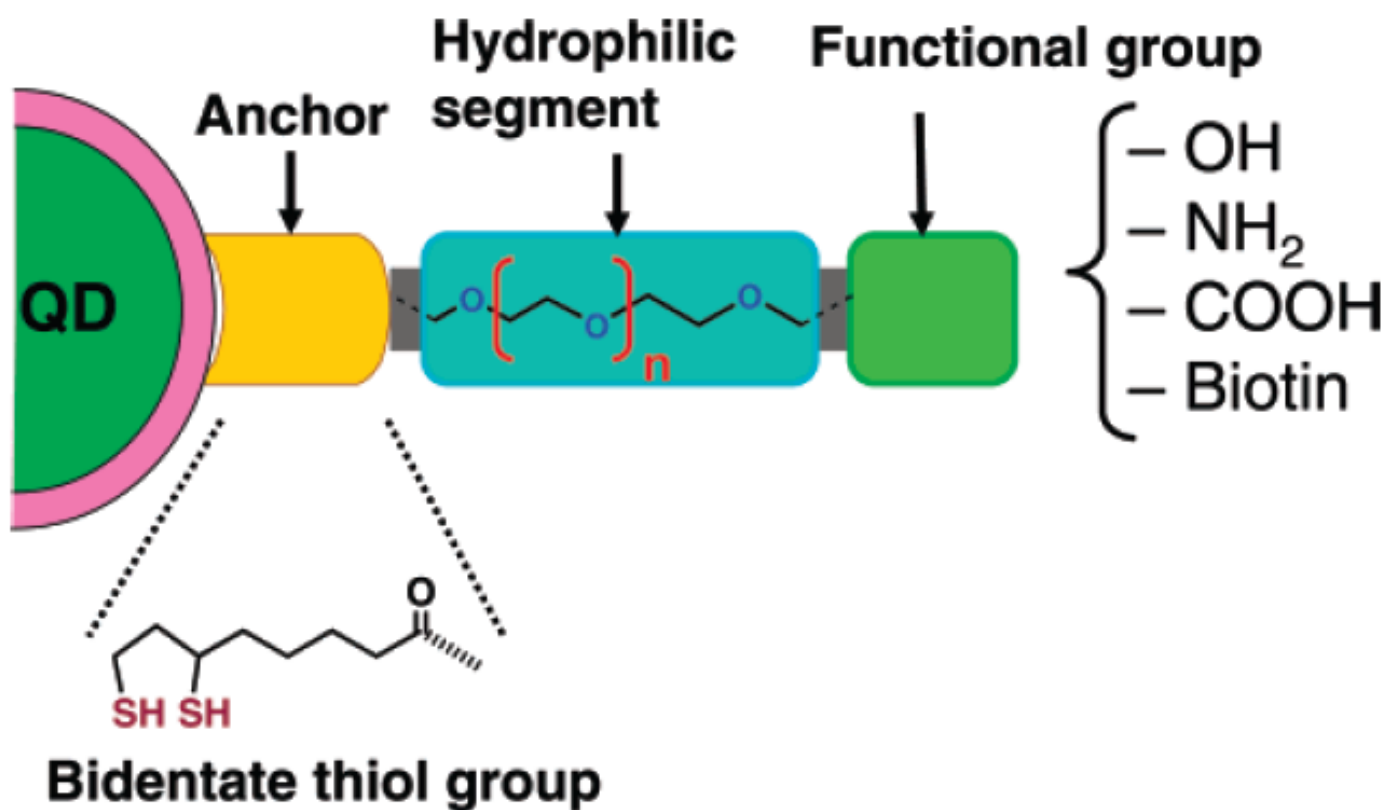
Amine Presenting Surface



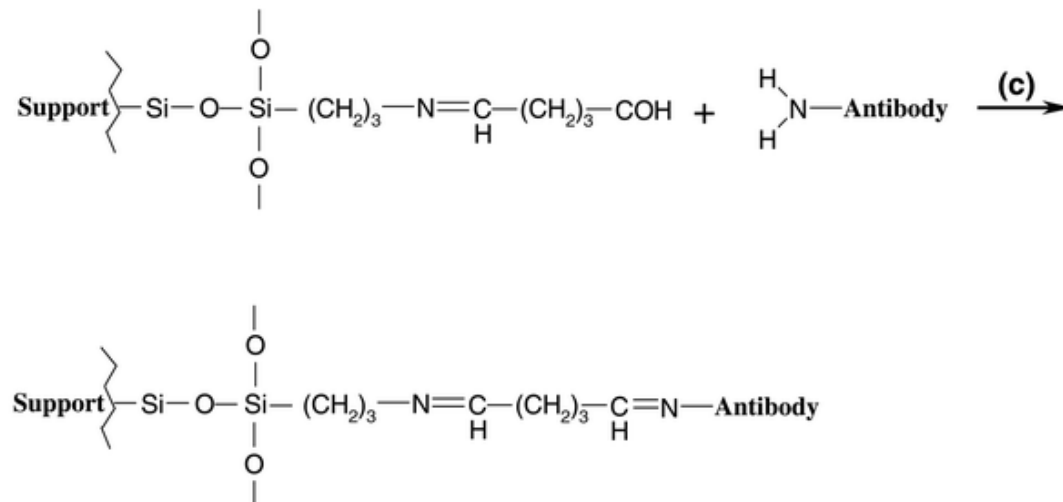
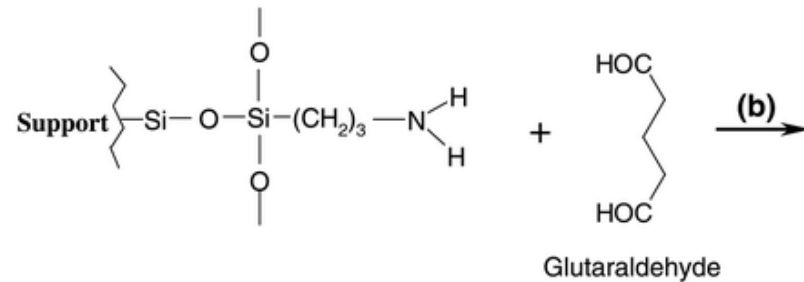
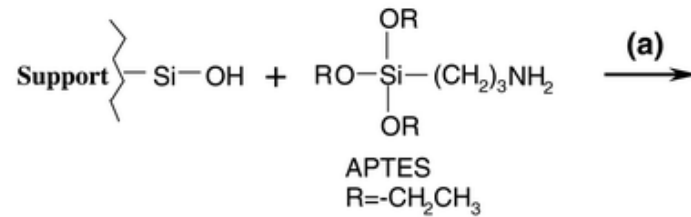
Sulfhydryl Labeling



Scheme 1. Modular Design of Hydrophilic Ligands with Terminal Functional Groups Used in This Study



Silica Modification



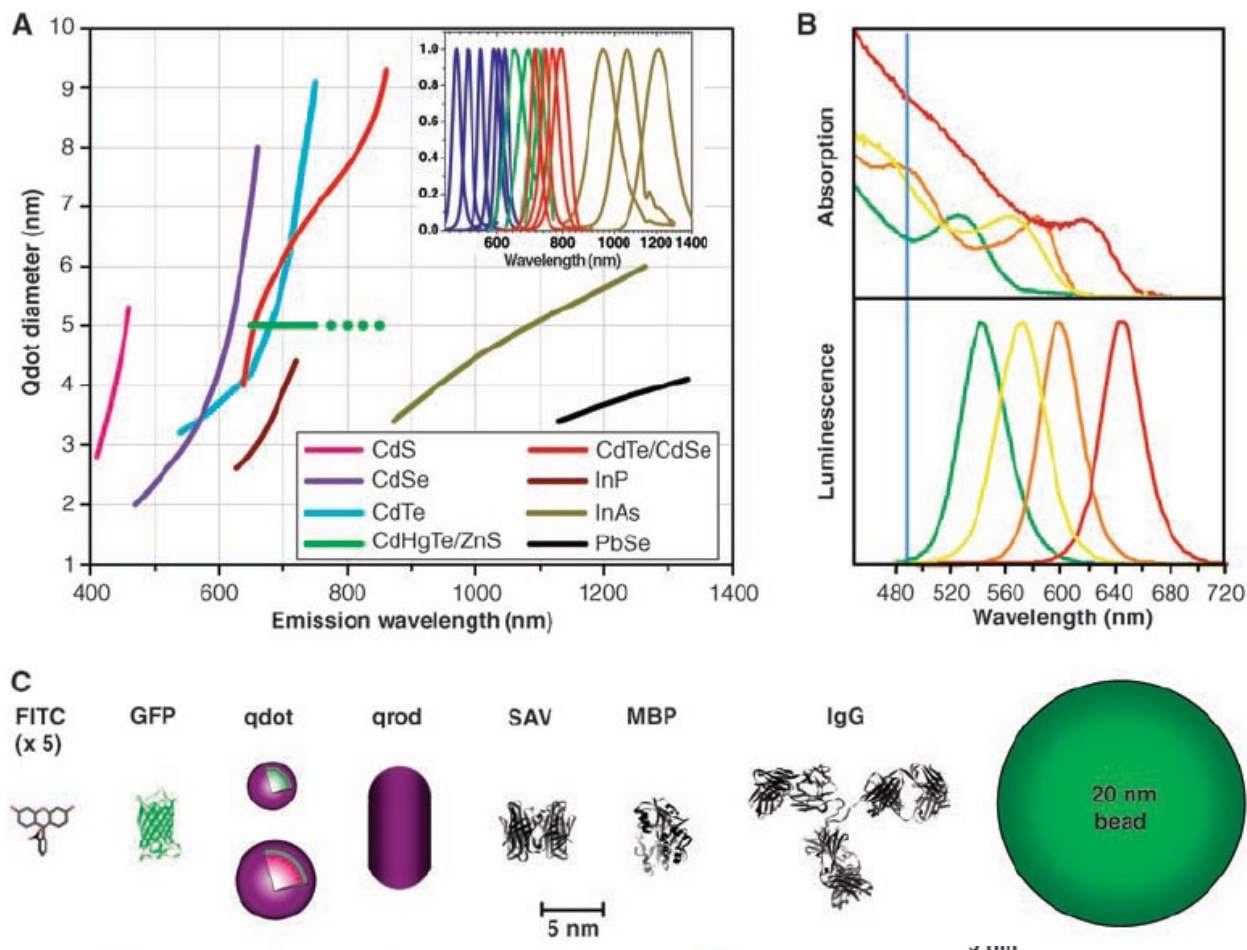


Fig. 1. (A) Emission maxima and sizes of quantum dots of different composition. Quantum dots can be synthesized from various types of semiconductor materials (II-VI: CdS, CdSe, CdTe...; III-V: InP, InAs...; IV-VI: PbSe...) characterized by different bulk band gap energies. The curves represent experimental data from the literature on the dependence of peak emission wavelength on qdot diameter. The range of emission wavelength is 400 to 1350 nm, with size varying from 2 to 9.5 nm (organic passivation/solubilization layer not included). All spectra are typically around 30 to 50 nm (full width at half maximum). Inset: Representative emission spectra for some materials. Data are from (12, 18, 27, 76–82). Data for CdHgTe/ZnS have been extrapolated to the maximum emission wavelength obtained in our group. (B) Absorption (upper curves) and emission (lower curves) spectra of four CdSe/ZnS qdot samples. The blue vertical line indicates the 488-nm line of an argon-ion laser, which can be used to efficiently excite all four types of qdots simultaneously. [Adapted from (28)] (C) Size comparison of qdots and comparable objects. FITC, fluorescein isothiocyanate; GFP, green fluorescent protein; qdot, green (4 nm, top) and red (6.5 nm, bottom) CdSe/ZnS qdot; qrod, rod-shaped qdot (size from Quantum Dot Corp.'s Web site). Three proteins—streptavidin (SAV), maltose binding protein (MBP), and immunoglobulin G (IgG)—have been used for further functionalization of qdots (see text) and add to the final size of the qdot, in conjunction with the solubilization chemistry (Fig. 2).

Colorimetric Detection of DNA

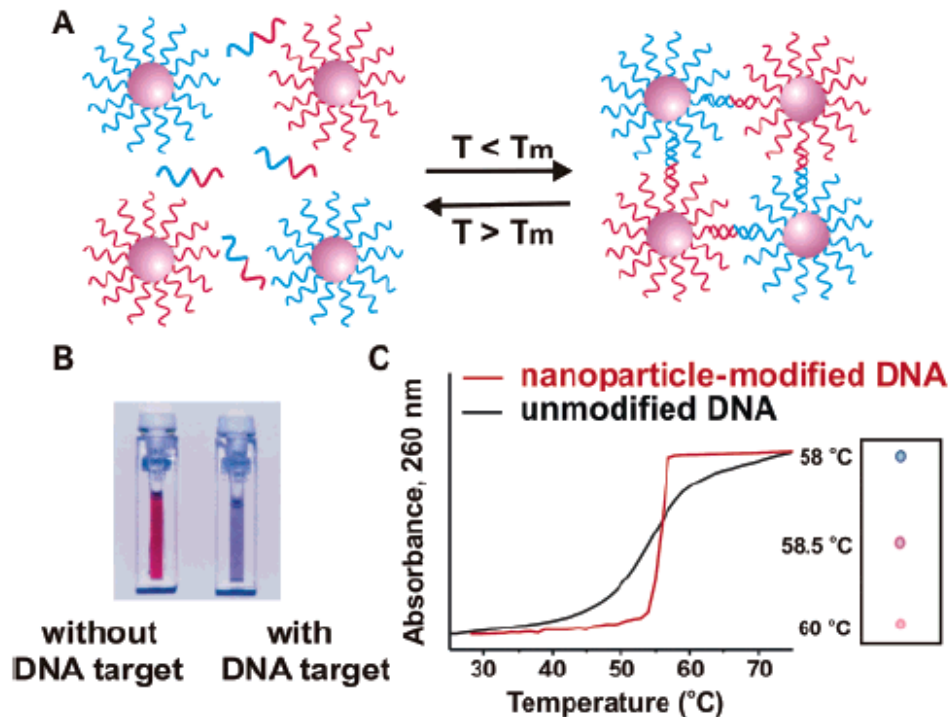
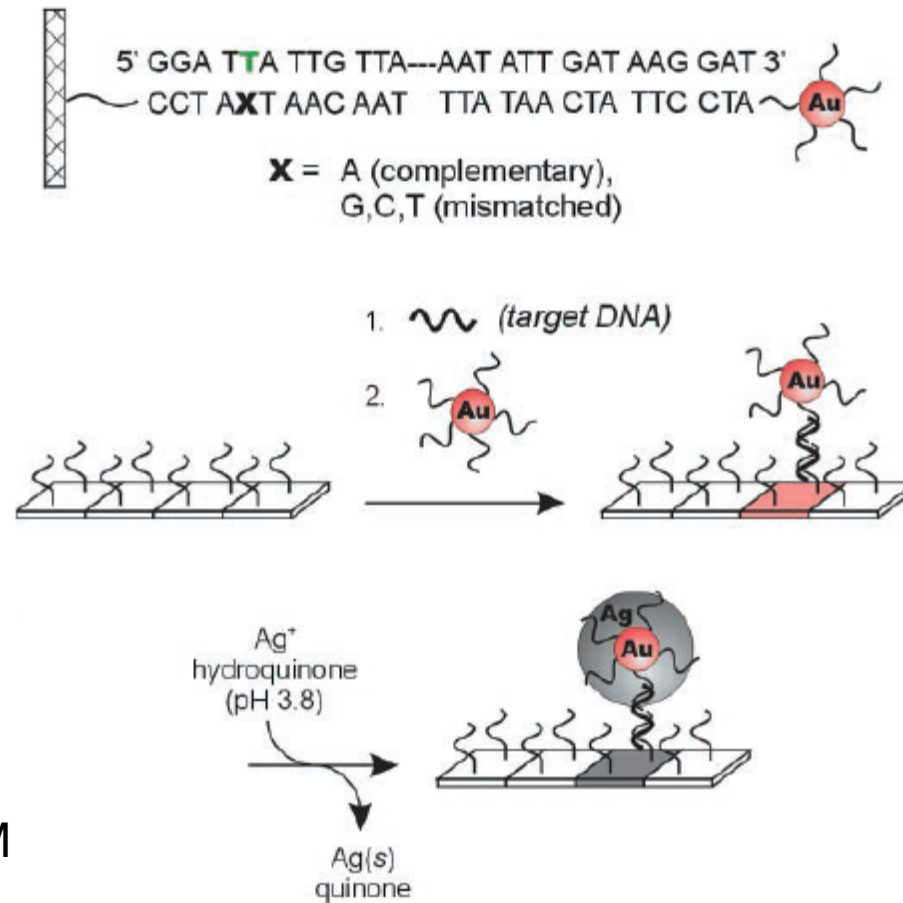


Figure 2. In the presence of complementary target DNA, oligonucleotide-functionalized gold nanoparticles will aggregate (A), resulting in a change of solution color from red to blue (B). The aggregation process can be monitored using UV-vis spectroscopy or simply by spotting the solution on a silica support (C). (Reprinted with permission from *Science* (<http://www.aaas.org>), ref 29. Copyright 1997 American Association for the Advancement of Science.)

Scanometric DNA Array Detection with Nanoparticle Probes

SCIENCE VOL 289 8 SEPTEMBER 2000

T. Andrew Taton,^{1,2} Chad A. Mirkin,^{1,2*} Robert L. Letsinger^{1*}



50 fM => 0.2 fM

Bio-Bar-Code-Based DNA Detection with PCR-like Sensitivity

Jwa-Min Nam, Savka I. Stoeva, and Chad A. Mirkin*

J. AM. CHEM. SOC. 2004, 126, 5932–5933

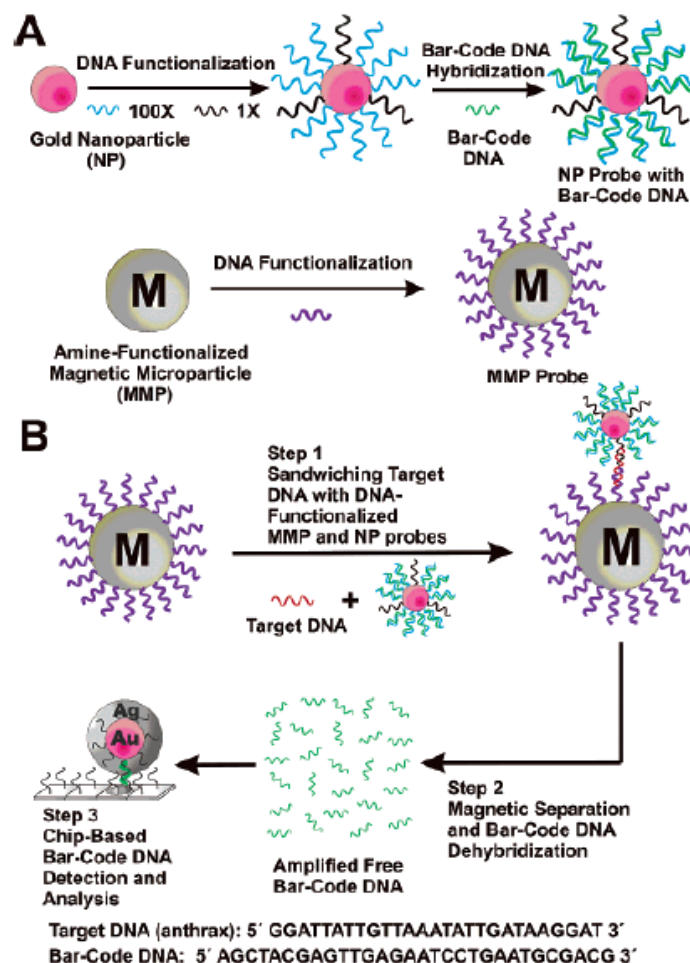


Figure 1. The DNA-BCA assay. (A) Nanoparticle and magnetic micro-particle probe preparation. (B) Nanoparticle-based PCR-less DNA amplification scheme.

Nanoparticle-Based Bio-Bar Codes for the Ultrasensitive Detection of Proteins

26 SEPTEMBER 2003 VOL 301 SCIENCE

Jwa-Min Nam,* C. Shad Thaxton,* Chad A. Mirkin†

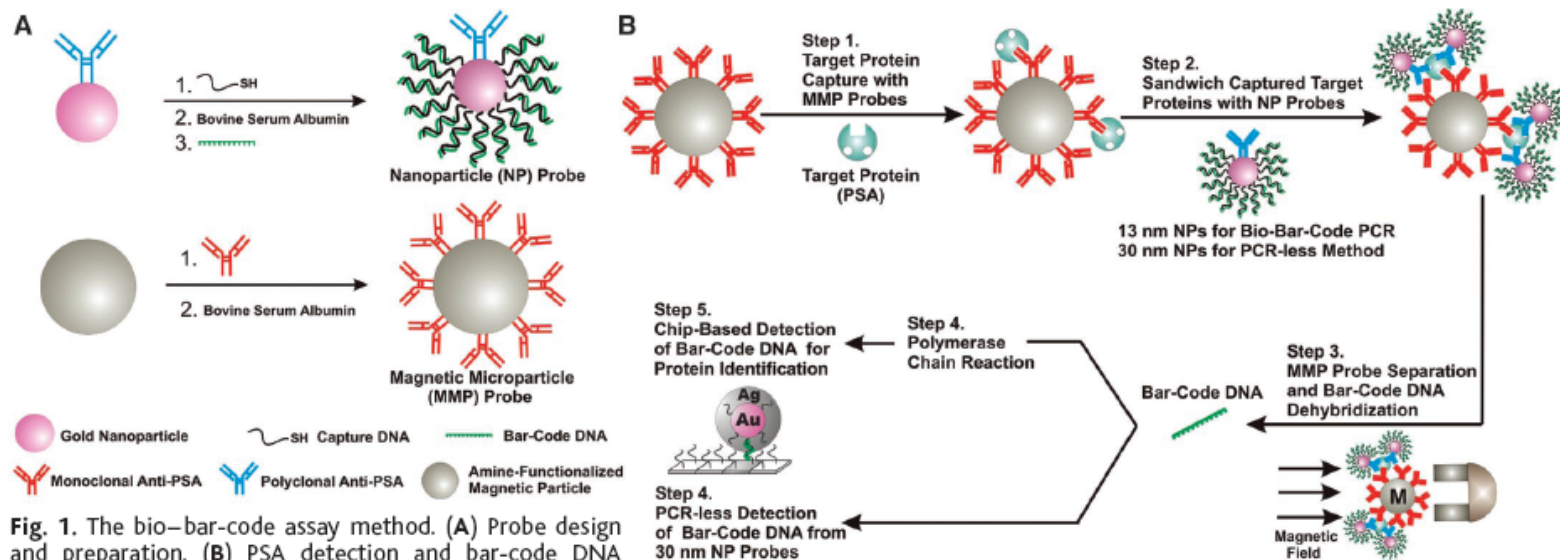
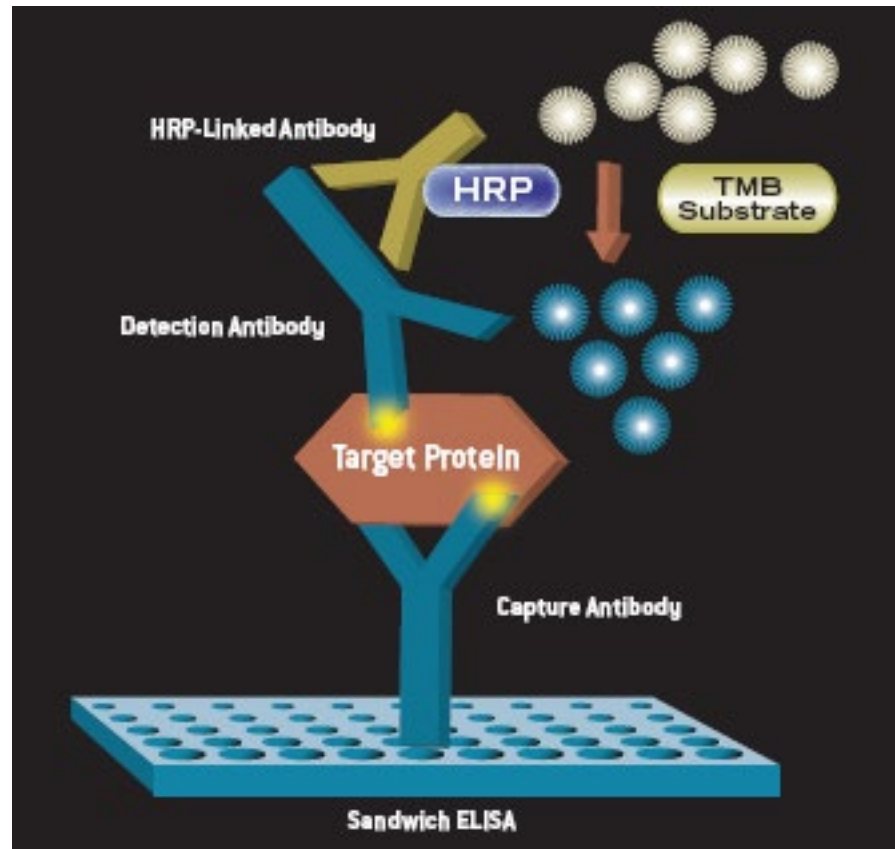


Fig. 1. The bio-bar-code assay method. **(A)** Probe design and preparation. **(B)** PSA detection and bar-code DNA amplification and identification. In a typical PSA-detection experiment, an aqueous dispersion of MMP probes functionalized with mAbs to PSA (50 μ l of 3 mg/ml magnetic probe solution) was mixed with an aqueous solution of free PSA (10 μ l of PSA) and stirred at 37°C for 30 min (Step 1). A 1.5-ml tube containing the assay solution was placed in a BioMag microcentrifuge tube separator (Polysciences, Incorporated, Warrington, PA) at room temperature. After 15 s, the MMP-PSA hybrids were concentrated on the wall of the tube. The supernatant (solution of unbound PSA molecules) was removed, and the MMPs were resuspended in 50 μ l of 0.1 M phosphate-buffered saline (PBS) (repeated twice). The NP probes (for 13-nm NP probes, 50 μ l at 1 nM; for 30-nm NP probes, 50 μ l at 200 pM), functionalized with polyclonal Abs to PSA and hybridized bar-code DNA strands, were then added to the assay solution. The NPs reacted with the PSA immobilized on the MMPs and provided DNA strands for signal amplification and protein identification (Step 2). This solution was vigorously stirred at 37°C for 30 min. The MMPs were then washed with 0.1 M PBS with the magnetic separator to isolate the mag-

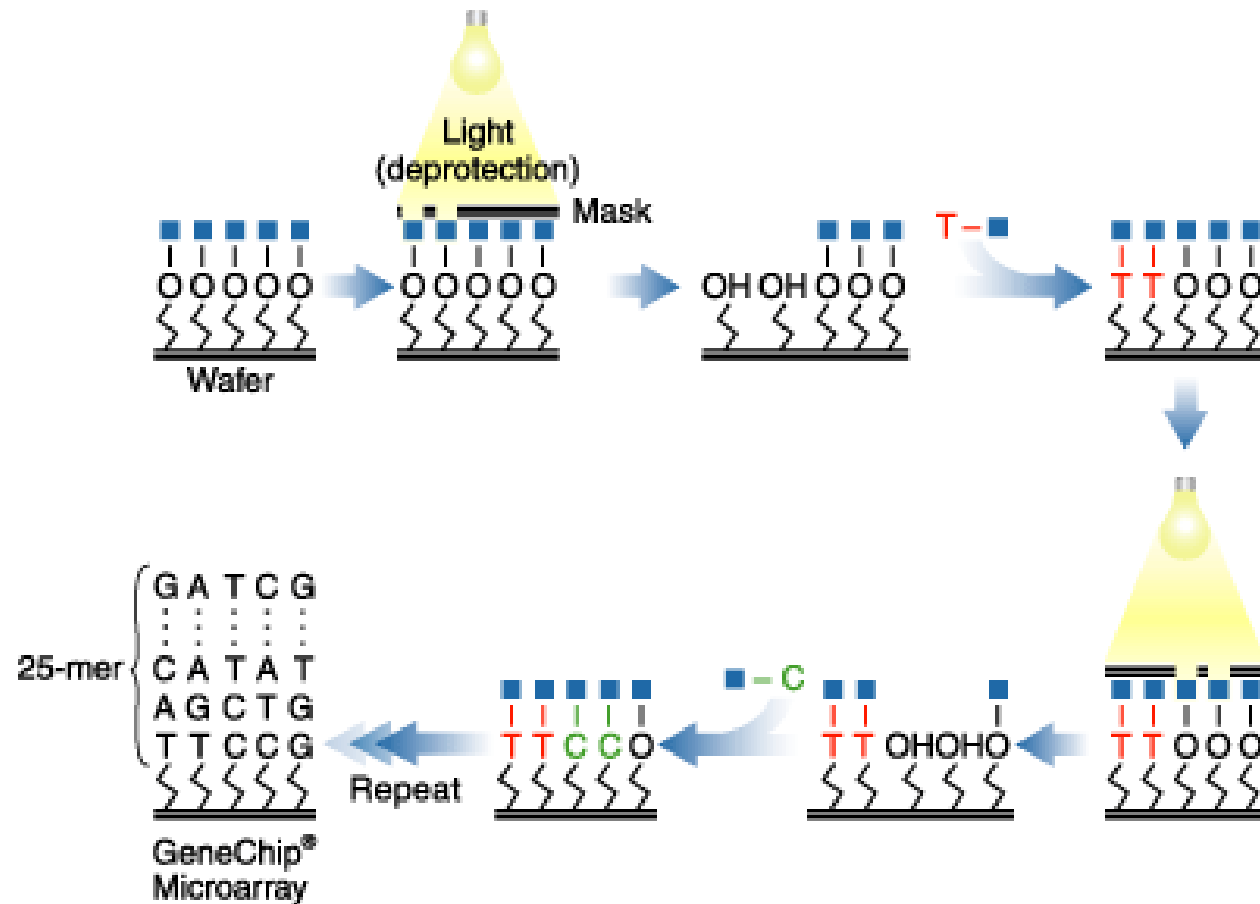
netic particles. This step was repeated four times, each time for 1 min, to remove everything but the MMPs (along with the PSA-bound NP probes). After the final wash step, the MMP probes were resuspended in NANOpure water (50 μ l) for 2 min to dehybridize bar-code DNA strands from the nanoparticle probe surface. Dehybridized bar-code DNA was then easily separated and collected from the probes with the use of the magnetic separator (Step 3). For bar-code DNA amplification (Step 4), isolated bar-code DNA was added to a PCR reaction mixture (20- μ l final volume) containing the appropriate primers, and the solution was then thermally cycled (20). The bar-code DNA amplicon was stained with ethidium bromide and mixed with gel-loading dye (20). Gel electrophoresis or scanometric DNA detection (24) was then performed to determine whether amplification had taken place. Primer amplification was ruled out with appropriate control experiments (20). Notice that the number of bound NP probes for each PSA is unknown and will depend upon target protein concentration.

Enzyme-Linked ImmunoSorbent Assay (ELISA)

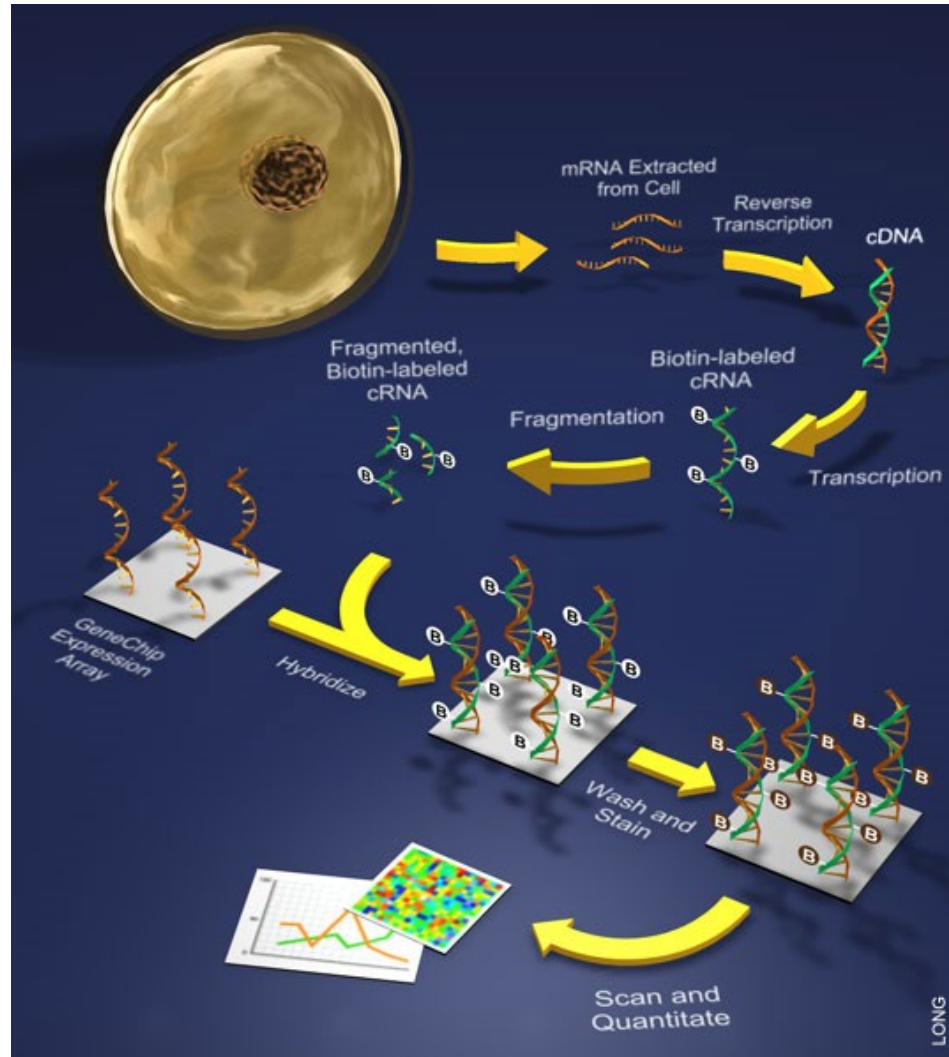


Labeling
BSA/PEG

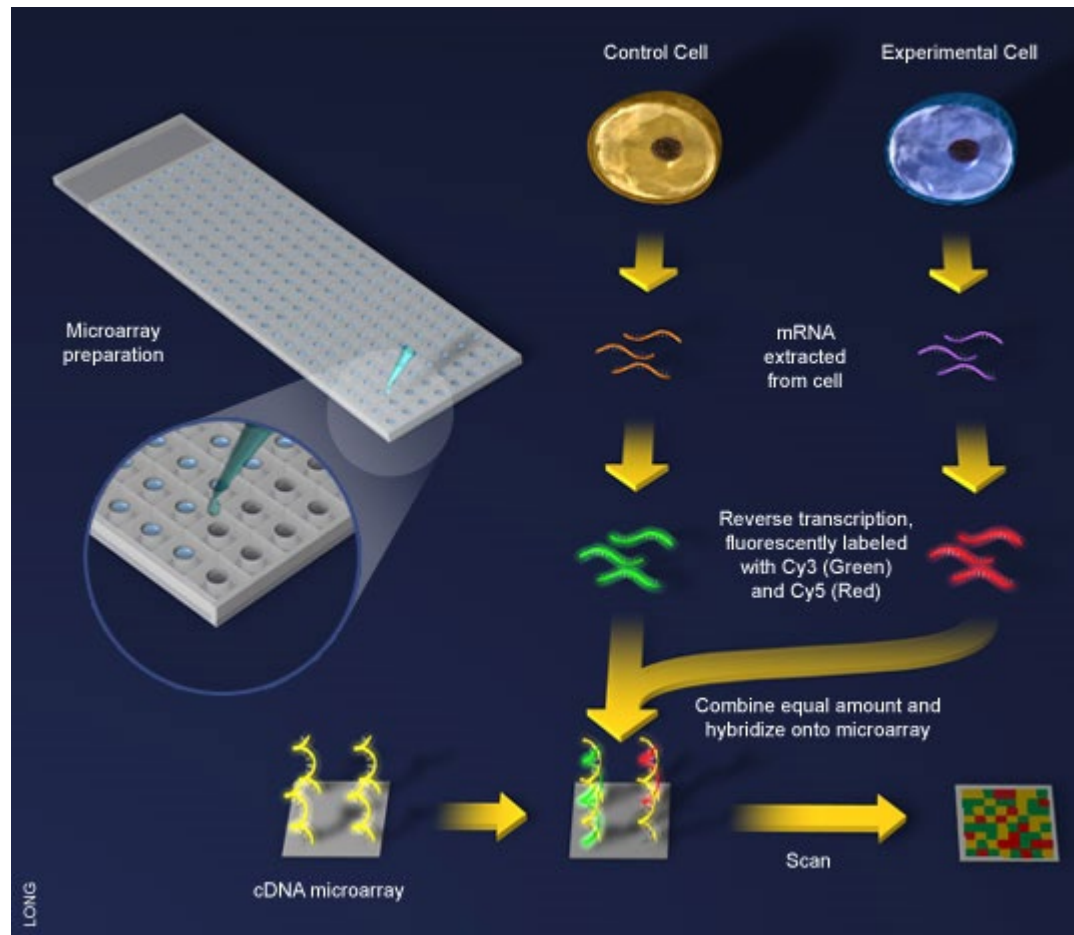
GeneChip



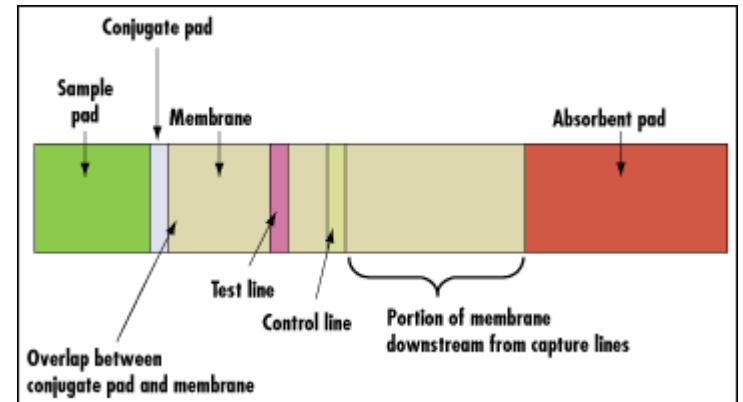
Scheme



cDNA Microarray

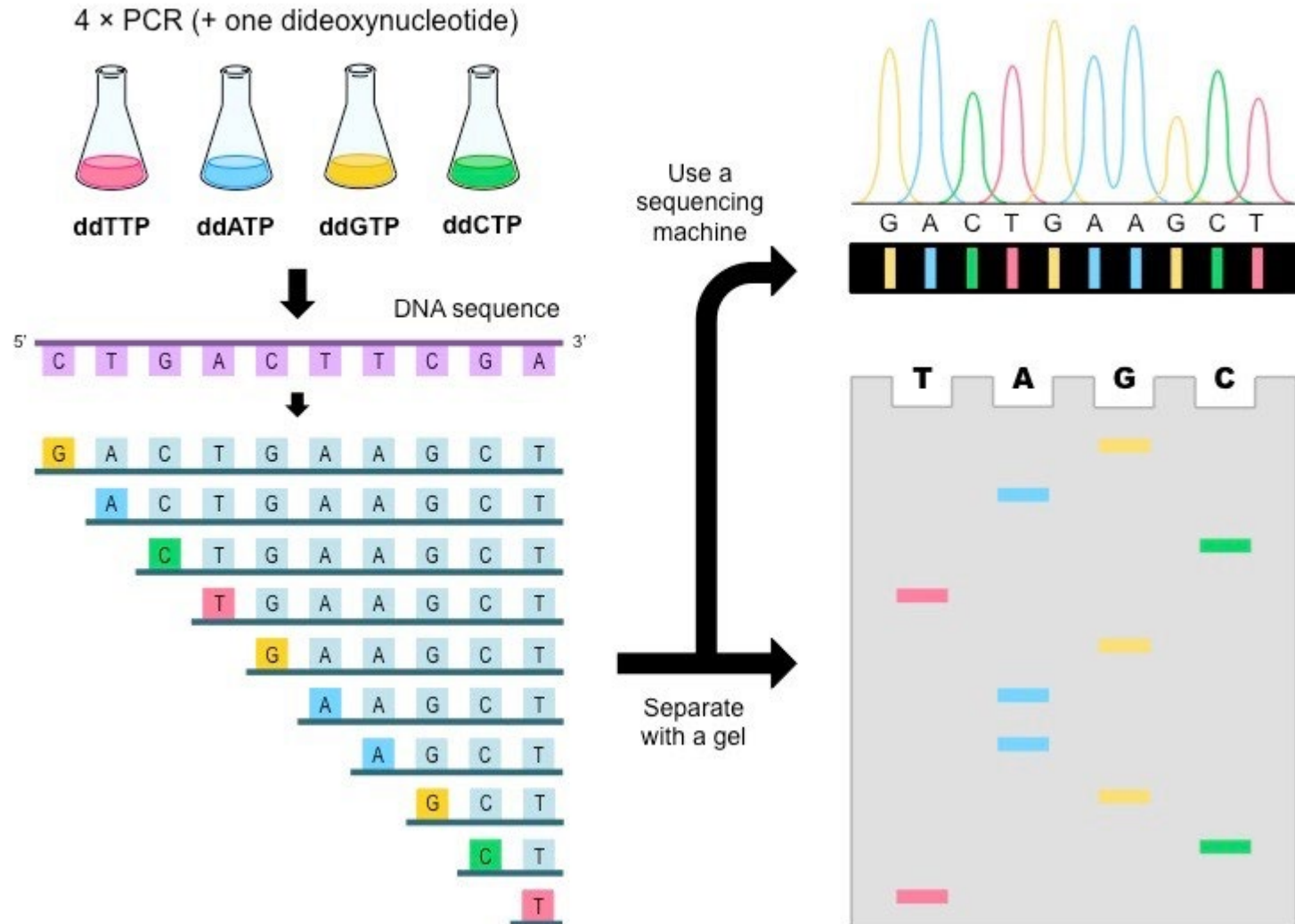


hCG immunoassay

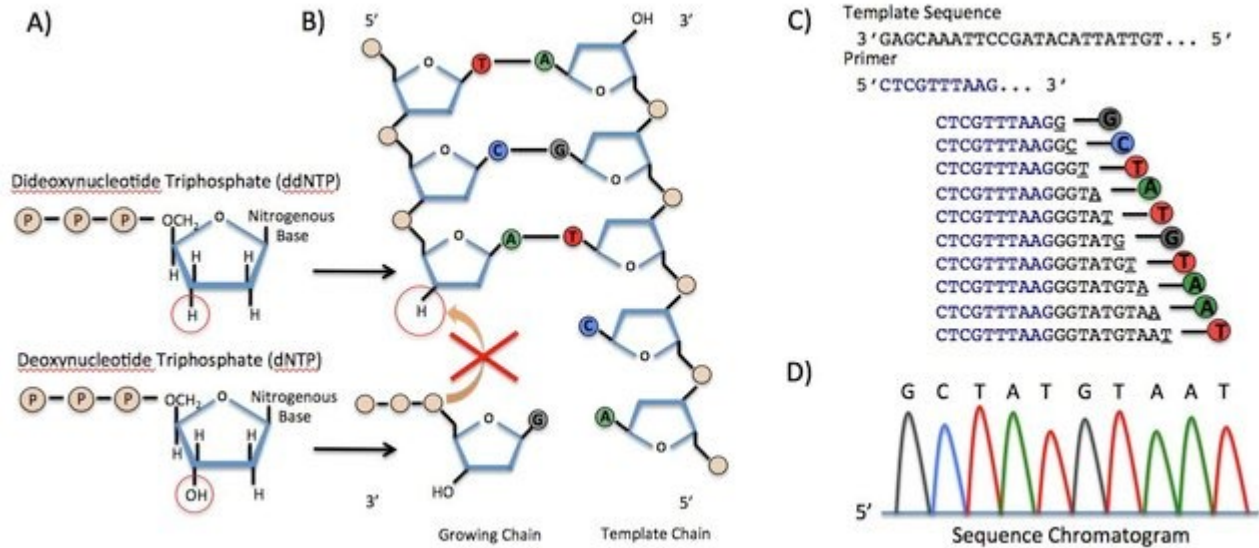


human chorionic gonadotropin (hCG)

DNA Sequencing



Sanger Sequencing



Dye Terminations

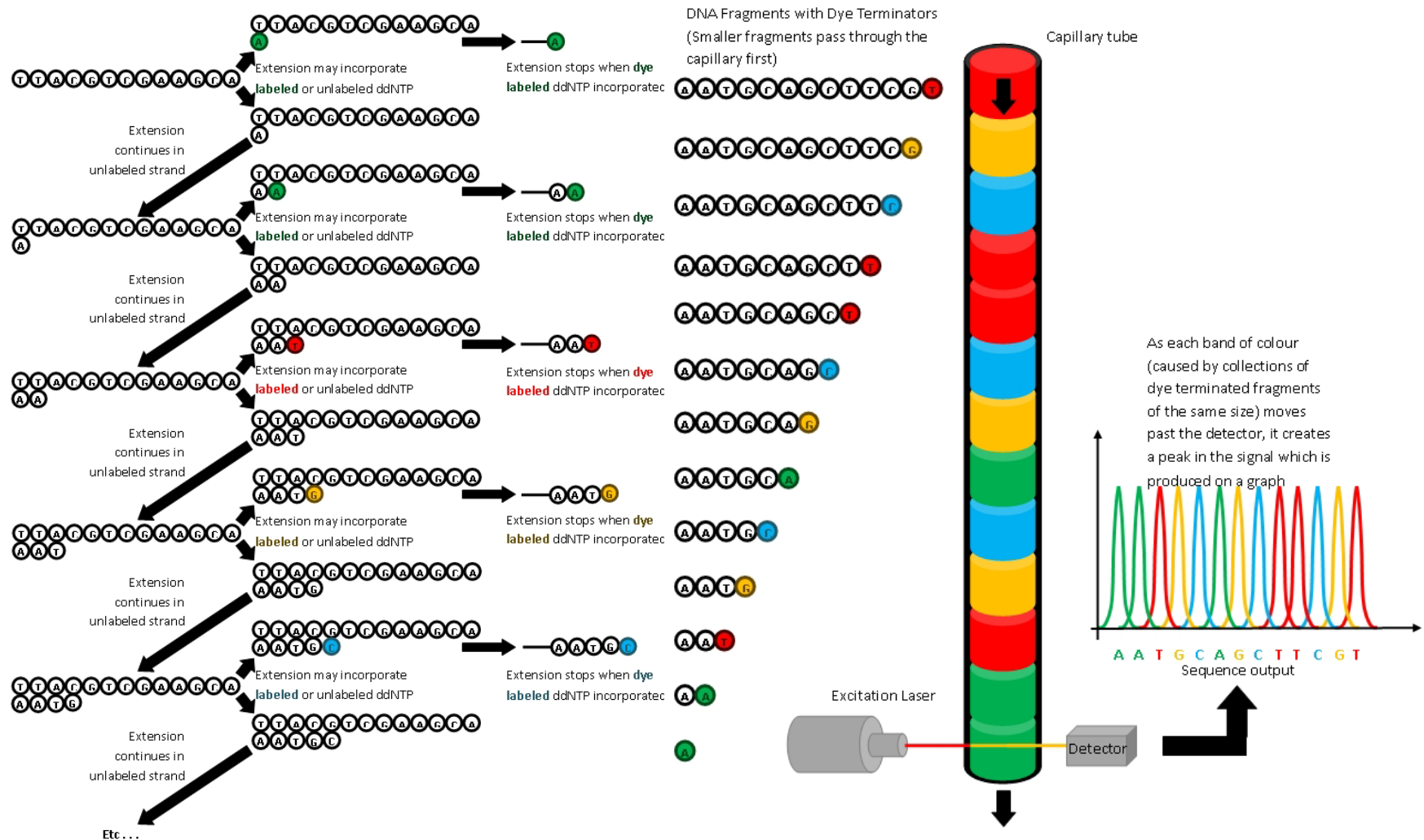


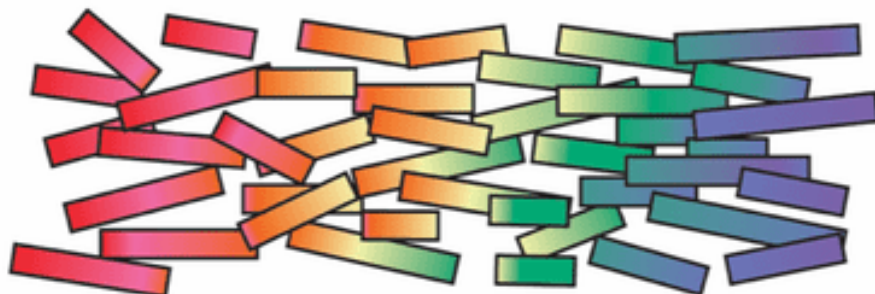
Figure 2: Shotgun Whole-Genome Sequencing



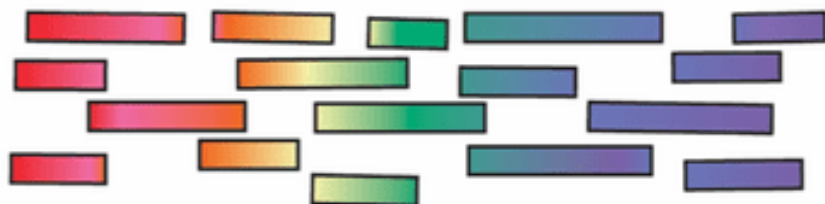
A DNA sample is collected



Many copies of the DNA are made



The copies are broken into many pieces

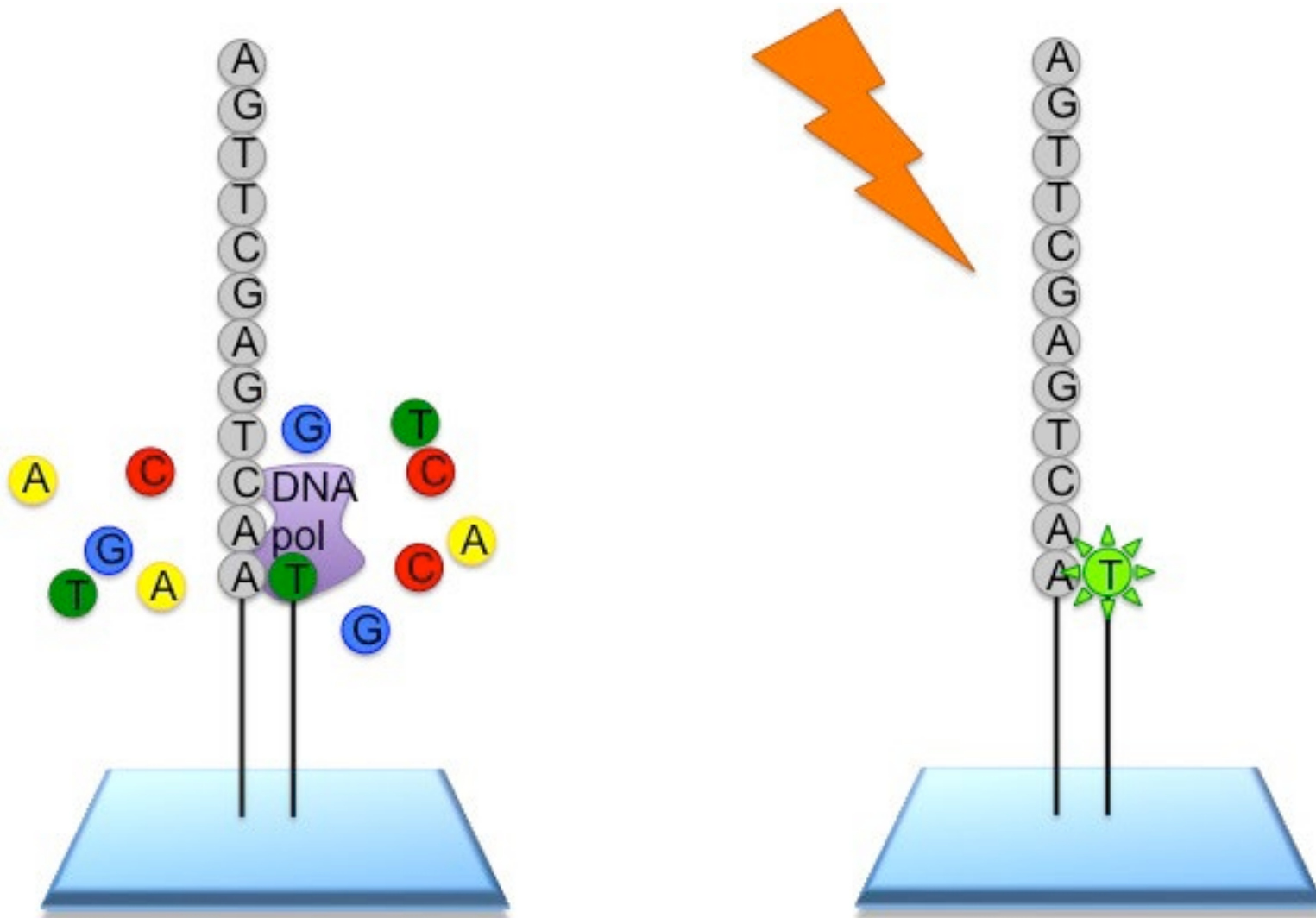


Sequences are arranged in the correct order

...AATGCACTGCGATTCCGATGAAGGGCATTGGC...

The complete genome is assembled

NGS Illumina



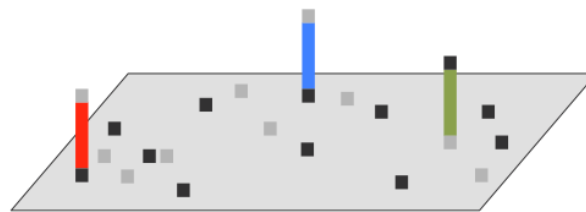
100-150 bp



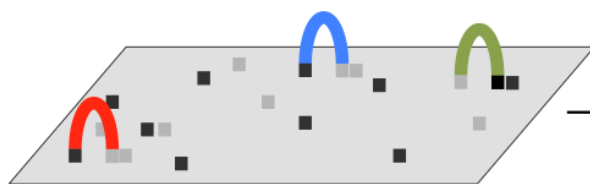
Fragments



Add adaptors



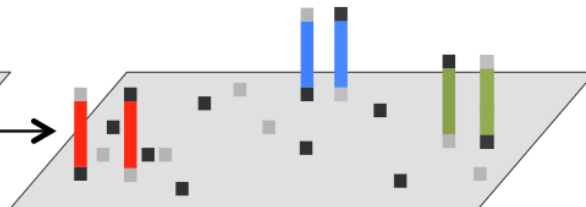
Attach to flowcell



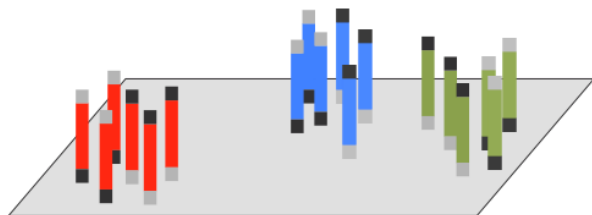
Bind to primer



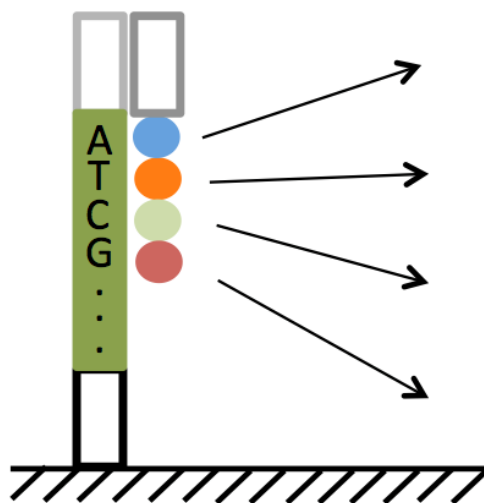
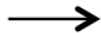
PCR extension



Dissociation



Cluster formation



Sequencing

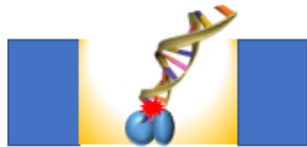


Signal scanning

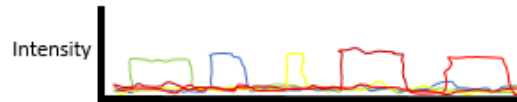
Third Generation Sequencing

PacBio SMRT seq

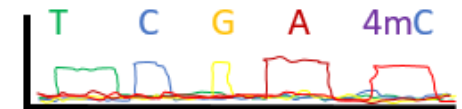
DNA passes thru
polymerase in an
illuminated volume



Raw output is fluorescent signal
of the nucleotide incorporation,
specific to each nucleotide

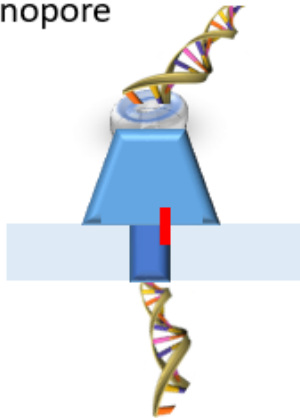


A,C,T,G have known pulse
durations, which are used to
infer methylated nucleotides

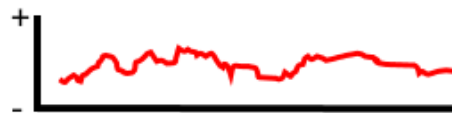


Oxford Nanopore

DNA passes thru
nanopore



Raw output is electrical signal
caused by nucleotide blocking
ion flow in nanopore



Each nucleotide has a specific
electric "signature"

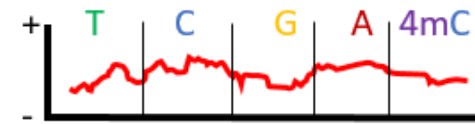
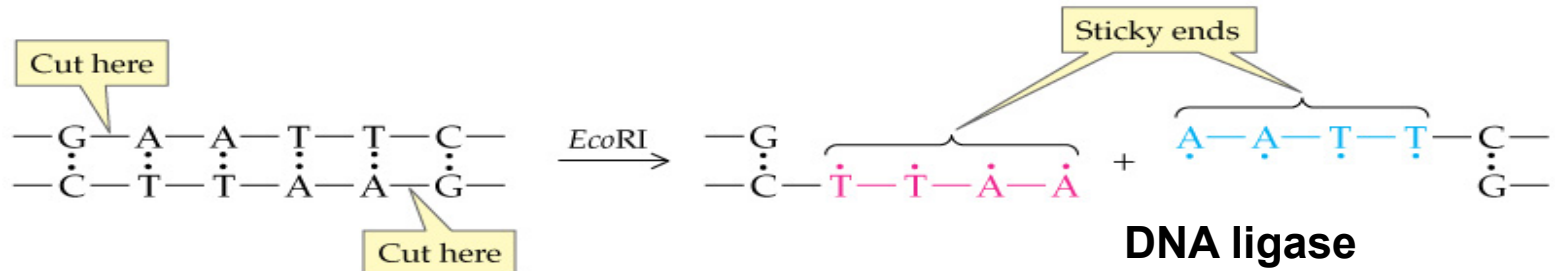


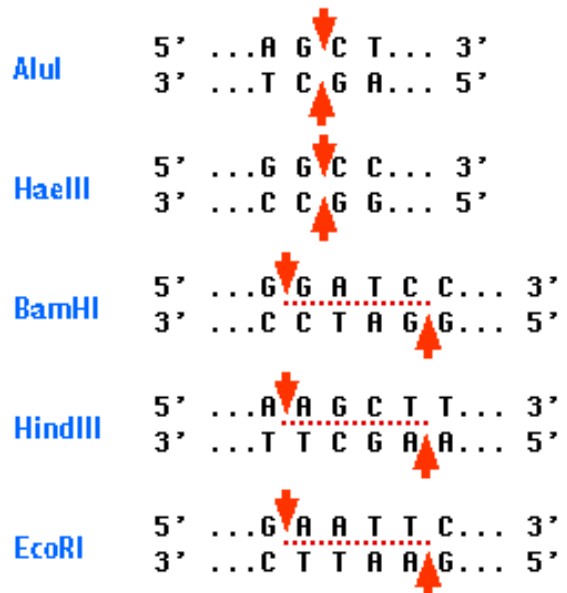
Table 2 Comparison of first-, second-, and third-generation genomic sequencing

| | First generation | Second generation | Third generation |
|----------------------------------|---|---|--------------------------------------|
| Fundamental technology | Size-separation of specifically end-labeled DNA fragments | Wash-and-scan SBS | Single molecule real time sequencing |
| Resolution | Averaged across many copies of the DNA molecule | Averaged across many copies of the DNA molecule | Single DNA molecule |
| Current raw read accuracy | High | High | Lower |
| Current read length | Moderate (800-1000 bp) | Short (generally much shorter than Sanger sequencing) | > 1000 bp |
| Current throughput | Low | High | High |
| Current cost | High cost per base, Low cost per run | Low cost per base, High cost per run | Low cost per base, High cost per run |
| RNA-sequencing method | cDNA sequencing | cDNA sequencing | Direct RNA sequencing |
| Time to result | Hours | Days | < 1 day |
| Sample preparation | Moderately complex, PCR amplification is not required | Complex, PCR amplification is required | Various |
| Data analysis | Routine | Complex (due to large data volumes & short reads) | Complex |
| Primary results | Base calls with quality values | Base calls with quality values | Base calls with quality values |

Adapted from Schadt, et al. Hum Mol Genet 2010¹³

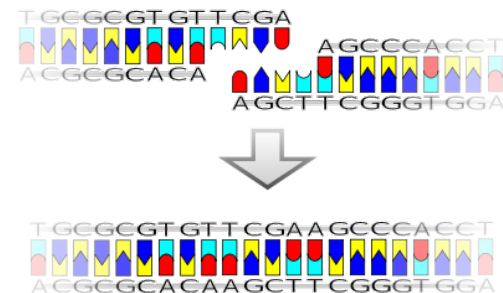


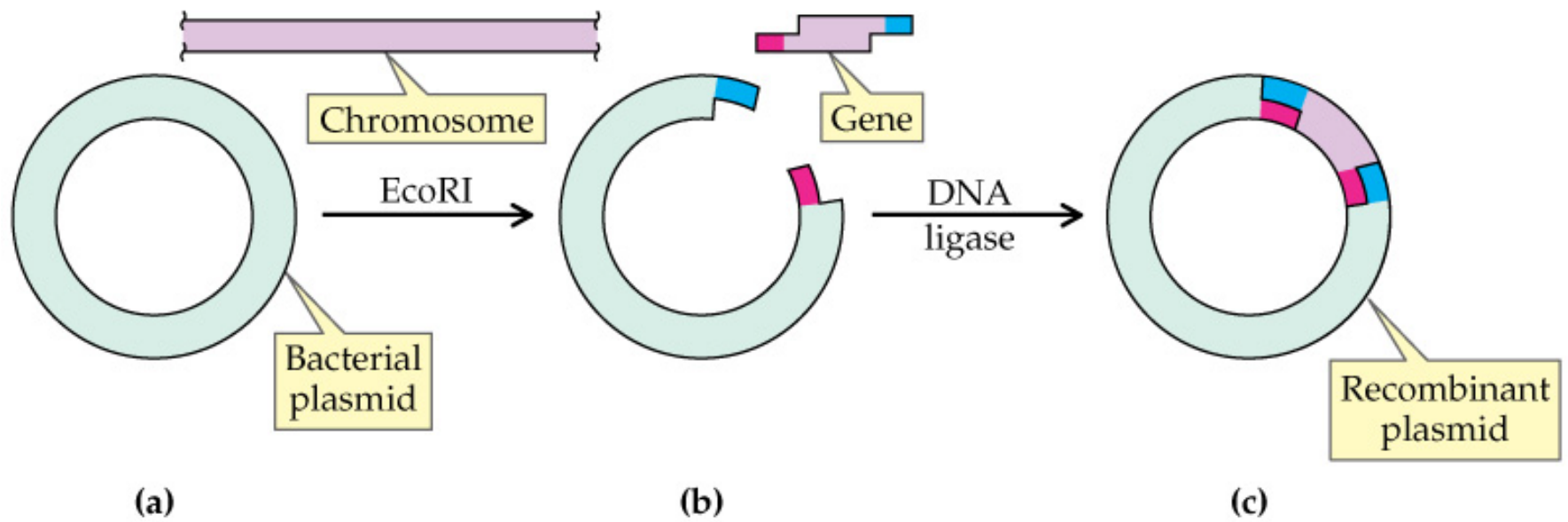
Restriction Enzyme

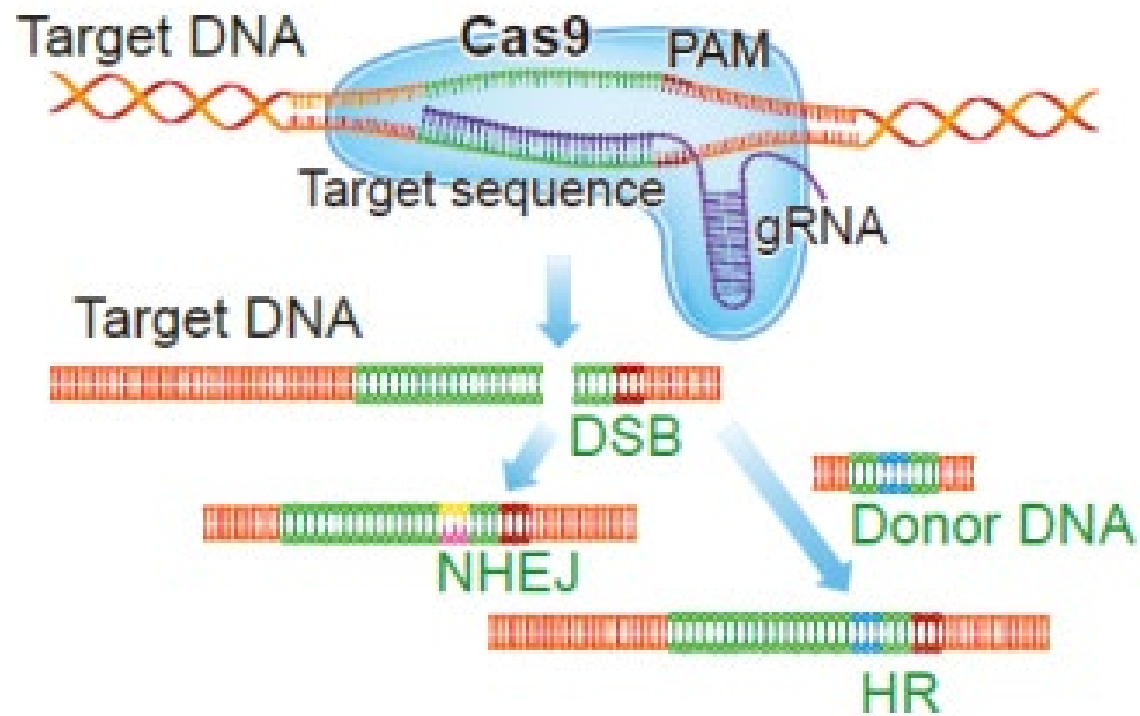


AluI and **HaeIII** produce blunt ends

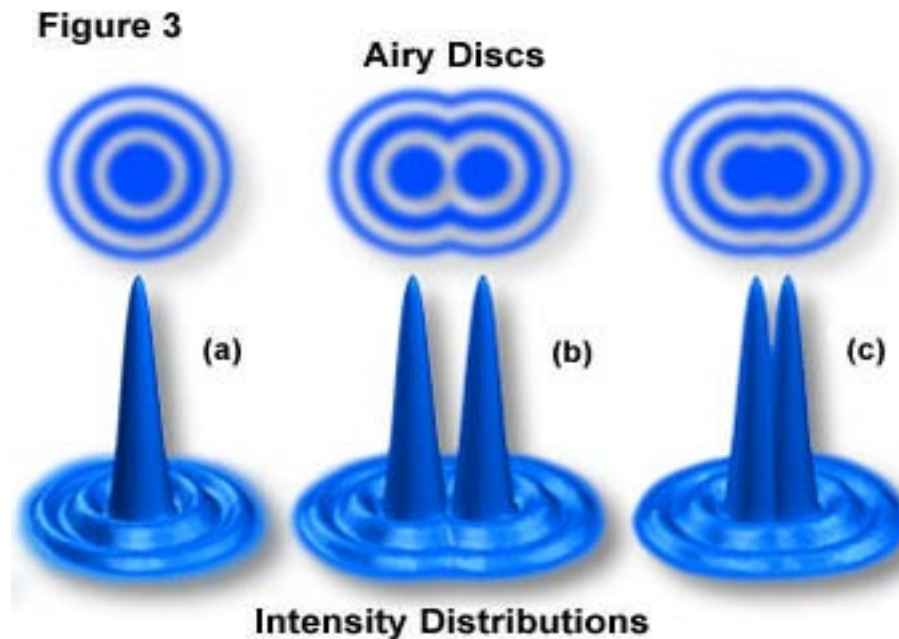
BamHI, **HindIII** and **EcoRI** produce "sticky" ends







Resolution



$$\text{Resolution } (r) = \lambda / (2NA) \quad (1)$$

$$\text{Resolution } (r) = 0.61 \lambda / NA \quad (2)$$

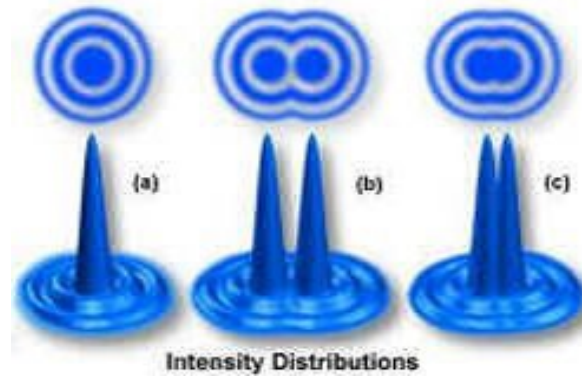
$$\text{Resolution } (r) = 1.22 \lambda / (NA(\text{obj}) + NA(\text{cond})) \quad (3)$$

Diffraction Limit

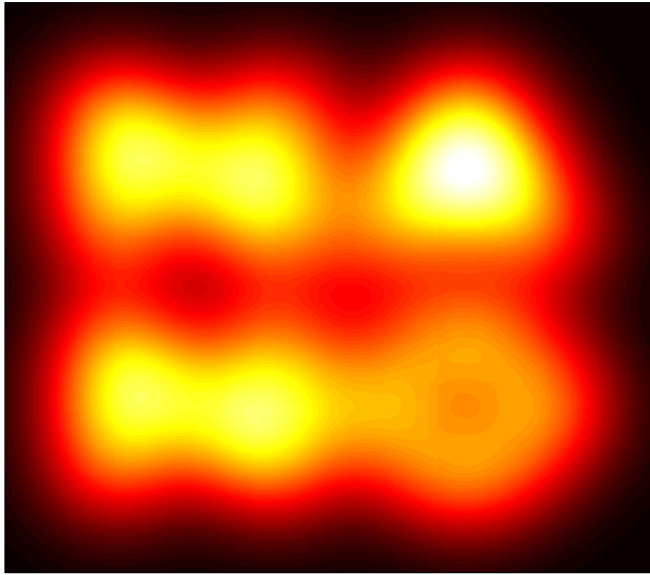


$$d = \lambda / (2n \sin \alpha)$$

$$, k_0 = 2NA / \lambda_{em}$$



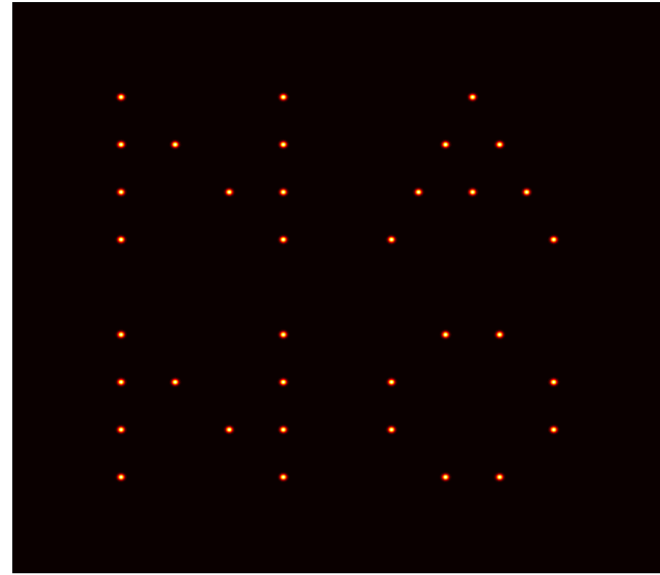
Photoactivation localization microscopy (PALM)



Diffraction-limited system:

Lateral resolution $\Delta xy \approx 0.61 \lambda / \text{N.A.}$
 $\approx 200 \text{ nm}$

Axis resolution $\Delta z \approx 2\lambda / \text{N.A.}^2$
 $\approx 450 \text{ nm}$



Mean-squared position error:

$$\left(\sigma_{x,y}^2\right)_m \approx \frac{s^2 + a^2/12}{N_m} + \frac{4\sqrt{\pi}s^3b_m^2}{aN_m^2}$$

s is the standard deviation of the PSF.

a is the pixel size in the image

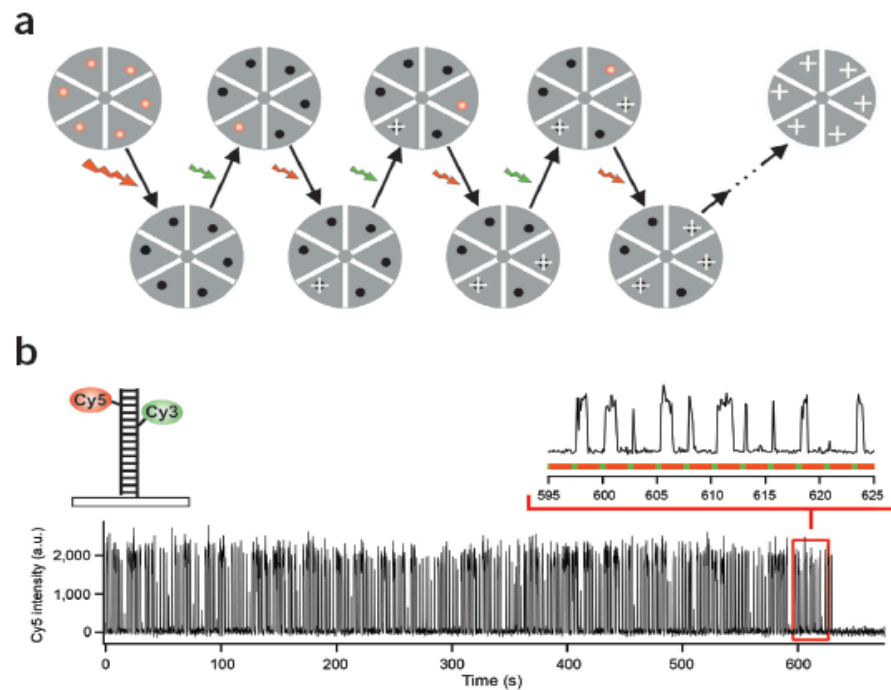
N_m is the total number of photons measured from molecule *m*

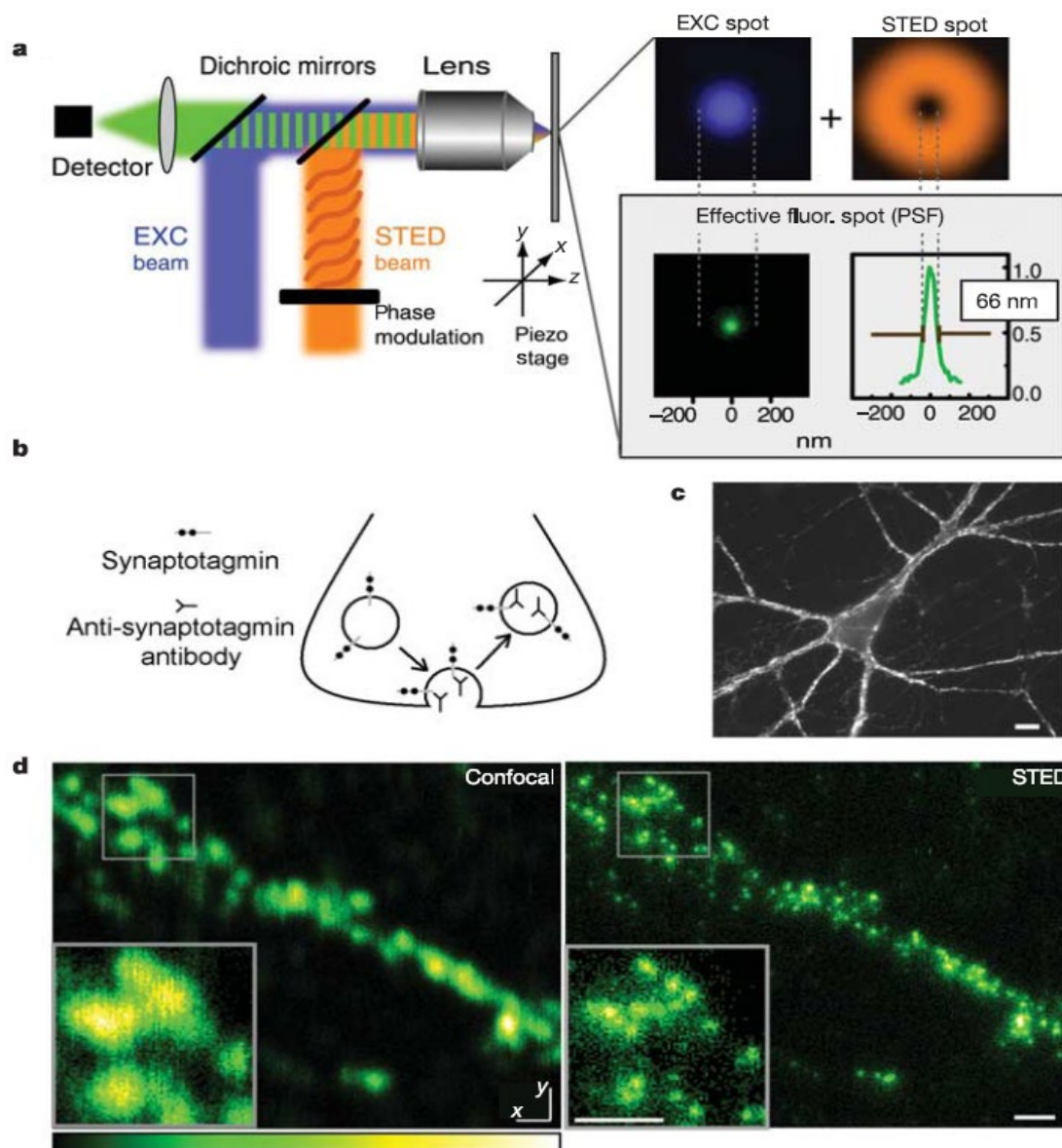
b_m is the number of background photons collected in the fitting window

Sub-diffraction-limit imaging by stochastic optical reconstruction microscopy (STORM)

Michael J Rust^{1,5}, Mark Bates^{2,5} & Xiaowei Zhuang^{1,3,4}

NATURE METHODS





Nonlinear structured-illumination microscopy: Wide-field fluorescence imaging with theoretically unlimited resolution

PNAS 102, September 12, 2005, 14081–14086 • DOI: 10.1073/pnas.0507337102

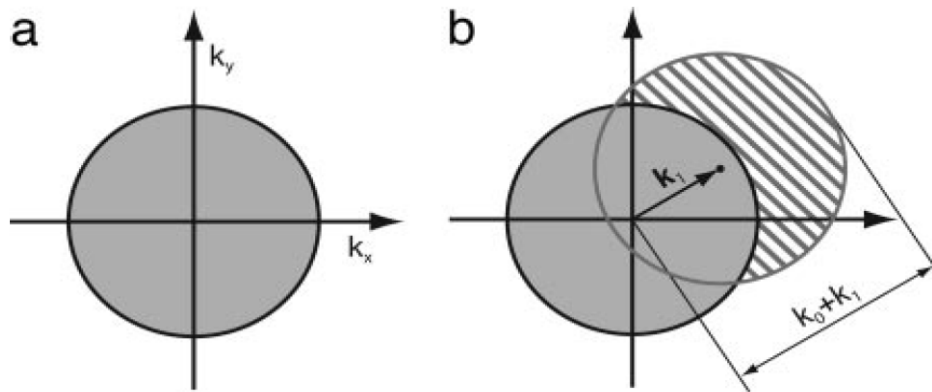
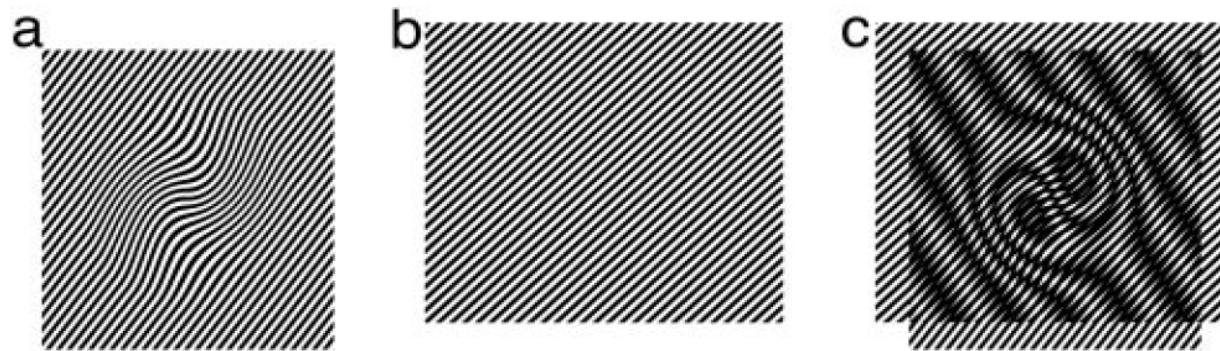


Fig. 2. Structured-illumination concept. (a) The set of sample spatial frequencies that can be observed by the conventional microscope defines a circular observable region of radius k_0 in frequency space. (b) If the excitation light contains a spatial frequency k_1 , a new set of information becomes visible in the form of moiré fringes (hatched circle). This region has the same shape as the normal observable region but is centered at k_1 . The maximum spatial frequency that can be detected (in this direction) is $k_0 + k_1$.